APPLICATION OF SIMPLIFIED OPERATING DEFLECTION SHAPE TECHNIQUE IN MACHINERY VIBRATION ASSESSMENT

MOHD BAKAR BIN MOHD MISHANI

FACULTY OF ENGINEERING
UNIVERSITY OF MALAYA
KUALA LUMPUR

2017

APPLICATION OF SIMPLIFIED OPERATING DEFLECTION SHAPE TECHNIQUE IN MACHINERY VIBRATION ASSESSMENT

MOHD BAKAR BIN MOHD MISHANI

THESIS SUBMITTED IN FULFILMENT OF THE REQUIREMENTS FOR THE DEGREE OF MASTER OF ENGINEERING SCIENCE

FACULTY OF ENGINEERING
UNIVERSITY OF MALAYA
KUALA LUMPUR

2017

For

My Beloved Parents, Wife & Family

UNIVERSITY OF MALAYA

ORIGINAL LITERARY WORK DECLARATION

Name of Candidate : Mohd Bakar Bin Mohd Mishani

I.C/Passport No :

Registration/Matric No : KGA130069

Name of Degree : Master of Engineering Science

Title of Dissertation : Application of Simplified Operating Deflection Shape Technique in Machinery Vibration Assessment

Field of Study : Engineering Design

I do solemnly and sincerely declare that:

(1) I am the sole author/writer of this Work;
(2) This Work is original;
(3) Any use of any work in which copyright exists was done by way of fair dealing and for permitted purposes and any excerpt or extract from, or reference to or reproduction of any copyright work has been disclosed expressly and sufficiently and the title of the Work and its authorship have been acknowledged in this Work;
(4) I do not have any actual knowledge nor do I ought reasonably to know that the making of this work constitutes an infringement of any copyright work;
(5) I hereby assign all and every rights in the copyright to this Work to the University of Malaya ("UM"), who henceforth shall be owner of the copyright in this Work and that any reproduction or use in any form or by any means whatsoever is prohibited without the written consent of UM having been first had and obtained;
(6) I am fully aware that if in the course of making this Work I have infringed any copyright whether intentionally or otherwise, I may be subject to legal action or any other action as may be determined by UM.

Candidate's Signature: Date:

Subscribed and solemnly declared before,

Witness's Signature: Date:

Name:

Designation:

UNIVERSITI MALAYA

PERAKUAN KEASLIAN PENULISAN

Nama : Mohd Bakar Bin Mohd Mishani

No. K.P/Pasport

No. Pendaftaran/Matrik : KGA130069

Nama Ijazah : Ijazah Sarjana Sains Kejuruteraan

Tajuk Disertasi : Pemantauan ke atas Getaran Mesin Menggunakan Kaedah Operasi Bentuk Pesongan yang Dipermudahkan

Bidang Penyelidikan : Kejuruteraan Rekabentuk

Saya dengan sesungguhnya dan sebenarnya mengaku bahawa:

(1) Saya adalah satu-satunya pengarang/penulis Hasil Kerja ini;
(2) Hasil Kerja ini adalah asli;
(3) Apa-apa penggunaan mana-mana hasil kerja yang mengandungi hakcipta telah dilakukan secara urusan yang wajar dan bagi maksud yang dibenarkan dan apa-apa petikan, ekstrak, rujukan atau pengeluaran semula daripada atau kepada mana-mana hasil kerja yang mengandungi hakcipta telah dinyatakan dengan sejelasnya dan secukupnya dan satu pengiktirafan tajuk hasil kerja tersebut dan pengarang/penulisnya telah dilakukan di dalam Hasil Kerja ini;
(4) Saya tidak mempunyai apa-apa pengetahuan sebenar atau patut semunasabahnya tahu bahawa penghasilan Hasil Kerja ini melanggar suatu hakcipta hasil kerja yang lain;
(5) Saya dengan ini menyerahkan kesemua dan tiap-tiap hak yang terkandung di dalam hakcipta Hasil Kerja ini kepada Universiti Malaya ("UM") yang seterusnya mula dari sekarang adalah tuan punya kepada hakcipta di dalam Hasil Kerja ini dan apa-apa pengeluaran semula atau penggunaan dalam apa jua bentuk atau dengan apa juga cara sekalipun adalah dilarang tanpa terlebih dahulu mendapat kebenaran bertulis dari UM;
(6) Saya sedar sepenuhnya sekiranya dalam masa penghasilan Hasil Kerja ini saya telah melanggar suatu hakcipta hasil kerja yang lain sama ada dengan niat atau sebaliknya, saya boleh dikenakan tindakan undang-undang atau apa-apa tindakan lain sebagaimanayang diputuskan oleh UM.

Tandatangan Calon: Tarikh:

Diperbuat dan sesungguhnya diakui di hadapan,

Tandatangan Saksi: Tarikh:

Nama:

Jawatan:

ABSTRACT

Machines are designed to help and improve human daily work load. The availability of machines make daily work can be performed faster, easier, safer and in a large scale. It is natural for any operated machines to produce vibration due to its moving part. Some of this vibration can be acceptable and some are harmful to human body if exposed to this machinery vibration for a long period. Because of this, it is crucial to investigate and assess machinery vibration to determine the machines condition and its minimal exposure to human body. Researchers have put an effort to develop an advanced method to perform this machinery vibration assessment. Current machinery vibration assessment requires highly skilled and trained personnel to be able to perform the vibration data analysis. Therefore, a simplified technique through the application of operating deflection shape (ODS) analysis is proposed to reduce the time required for performing vibration data acquisition and analysis. This study was divided into 2 main parts which are assessment on rotating machinery and assessment on reciprocating machinery. The first part of this study is to test the effectiveness of the simplified technique in a laboratory condition before being applied in real industrial case studies. The second part is to test the application on reciprocating motion of an air compressor before being applied on bio-fuel powered diesel engine to determine optimum bio-fuel blend. The results on rotating machinery vibration assessment show vibration data acquisition is more efficient and time saving by using tri-axis accelerometer and relative phase technique. Furthermore, analysis and machinery fault can be identified effectively and faster through visualising the machine motion using a simplified ODS technique. This simplified technique is seen as practical approach to be proposed and integrated into conventional machinery vibration assessment. Meanwhile, the results on diesel engine vibration assessment show optimum bio-fuel blend can be determined faster and

easier by using the proposed technique which consists of time domain analysis, frequency domain analysis and motion visualisation analysis / ODS analysis. The time domain and frequency domain analysis is first performed to minimise the effect of external vibration source due to torque before studying the performance of bio-fuel blends in a single-cylinder 4-stroke diesel engine. It is observed that bio-fuel powered engine at full speed with the lowest engine torque is more suitable to be used in identifying optimum fuel blend with minimal engine vibration. Bio-fuel blend B20 has the minimal vibration in overall RMS acceleration at full speed compared to other bio-fuel blends.

ABSTRAK

Mesin direkabentuk bagi membantu meringankan kerja harian. Dengan wujudnya mesin-mesin ini, kerja-kerja harian dapat dilaksanakan dengan pantas, mudah, selamat dan dalam skala yang besar. Adalah menjadi kebiasaan bagi sesuatu mesin yang beroperasi untuk menghasilkan getaran daripada bahagian mesin yang bergerak. Sesetengah getaran ini adalah selamat manakala sesetengah getaran boleh mendatangkan kemudaratan kepada tubuh manusia sekiranya terdedah kepada getaran yang tinggi bagi tempoh yang lama. Oleh kerana itu, kajian keatas penialain getaran mesin serta kesannya keatas tubuh manusia adalah penting. Para penyelidik telah berusaha dalam membangunkan kaedah termaju dalam penilaian getaran mesin. Pada masa kini, penilaian getaran mesin memerlukan kepakaran yang tinggi dan tenaga terlatih bagi melaksanakan analisis keatas getaran mesin. Oleh kerana itu, kaedah yang lebih mudah melalui aplikasi analisis ODS di perkenalkan bagi menjimatkan masa dalam memperoleh dan menganalisis data getaran. Ujikaji ini dibahagikan kepada 2 bahagian utama iaitu penilaian keatas mesin berputar dan penilaian keatas mesin maju mundur. Bahagian pertama adalah mengkaji keberkesanan teknik ini di dalam makmal sebelum menggunakannya keatas mesin industri. Bahagian kedua adalah mengkaji aplikasi teknik ini keatas gerakan maju mundur pemampat udara sebelum digunakan keatas enjin diesel bagi menentukan campuran minyak bio yang terbaik berdasarkan getaran enjin yang paling rendah. Hasil ujikaji ini keatas penilaian getaran mesin berputar menunjukkan pengumpulan data getaran dapat dilakukan dengan lebih berkesan dan menjimatkan masa dengan menggunakan “tri-axis accelerometer” dan juga data perbandingan fasa. Malah analisis keatas masalah mesin juga dapat dilaksanakan dengan lebih berkesan dan pantas melalui pemerhatian gerakan mesin menggunakan kaedah ODS mudah ini. Kaedah yang lebih mudah ini dilihat sebagai

pendekatan munasabah dan harus diterapkan dalam kaedah penilaian getaran mesin yang sedia ada. Manakala, hasil ujikaji keatas enjin diesel menunjukkan campuran minyak bio terbaik dapat diperolehi dengan lebih pantas dan mudah melalui kaedah yang dicadangkan yang merangkumi analisis domain masa, analisis domain kekerapan dan analisis pemantauan gerakan mesin atau analisis ODS. Terlebih dahulu, analisis ruang masa dan analsis ruang kekerapan dijalankan bagi megurangkan kesan getaran luaran akibat daya kilasan sebelum mengkaji kesan campuran minyak bio keatas enjin diesel 4-kitaran-1-silinder. Hasil ujikaji menunjukkan ujikaji pada kelajuan enjin 2400rpm dengan daya kilasan yang rendah lebih sesuai dalam menentukan campuran minyak bio terbaik dengan getaran enjin yang paling rendah. Analisis getaran menunjukkan campuran minyak bio B20 adalah yang terbaik dan menghasilkan getaran enjin yang lebih rendah berbanding campuran minyak bio yang lain.

ACKNOWLEDGEMENTS

In The Name of ALLAH, the Most Gracious the Most Merciful

All praise is to ALLAH, the Sustainers of the worlds; and blessings and peace be upon our leader and chief, Muhammad S.A.W., upon his Companions, and upon those who followed them with sincerity until the Day of Judgment.

I would like to express my appreciation and thanks to my Supervisor, Ir. Dr. Alex Ong Zhi Chao and Co-Supervisor, Prof. Zubaidah Ismail and Assoc. Prof. Chong Wen Tong for contributing their invaluable knowledge, experience and advices throughout the project.

Dr. Khoo Shin Yee, Prof. Abdul Ghaffar Abdul Rahman and Dr. Ong Hwai Chyuan; thanks for sharing the experience and advices in analysis and discussions on vibration and bio-fuel field.

Fellows; Soon Roon Sheng, Yap Huey Tyng, Mahmudur Rahman, Lim Hong Cheet, Tam Jun Hui, Ken Chin Wei & Natalina Damanik thanks for all the help directly and indirectly in my dissertation project.

Mr. Syed Mahathir and Mr. Eng Hoe Cheng thanks for all the time, space, consideration and exposure in real industries.

Special thanks for Doa's and moral support from my parents; Mohd Mishani & Wanita, in-laws; Mohamed Sail & Ismunah and family members; Fadhilah, Ridhwan, Akhmal, Burhanuddin and Iskandar.

Lastly, to my wife; Maizatul Zalela and kids; Afifah and Adam Muhammad… thanks for the love, care and patience throughout this project.

TABLE OF CONTENTS

LIST OF FIGURES

LIST OF TABLES

LIST OF SYMBOLS AND ABBREVIATIONS

CBM	:	Condition Based Monitoring
CI	:	Calophyllum Inophyllum
IC	:	Internal Combustion
RPM	:	Rotation Per Minute (Running Speed)
RMS	:	Root Mean Square
ODS	:	Operating Deflection Shapes
BPFO	:	Ball Pass Frequency of Outer Race
BPFI	:	Ball Pass Frequency of Inner Race
GMF	:	Gear Mesh Frequency
DOF	:	Degree of Freedom
x_{pr}	:	Damped Steady State Response of r^{th} Mode
Q	:	Force Vector on the Applied Structure
T	:	Denote the Transpose Vector
$\emptyset_r$	:	Vectors of the Modal Deformation of r^{th} Mode
ω_{or}	:	r^{th} Natural Frequency of the Structure
$\boldsymbol{\omega}$	:	Frequency of the Applied Force
ξ_r	:	Damping of the r^{th} Mode
N_b	:	Number of Ball Bearing
B_d	:	Ball of Bearing Diameter
P_d	:	Pitch of Bearing Diameter
θ	:	Contact Angle of Self-aligning Bearing

LIST OF APPENDICES

CHAPTER 1: INTRODUCTION

1.1 General Overview

Machines are designed to help and improve human daily work load. The availability of machines make daily work can be performed faster, easier, safer and in a large scale. It is natural for any operated machines to produce vibration due to its moving part. Some of this vibration can be acceptable and some are harmful to human body if exposed to this machinery vibration for a long period. Furthermore, the level of this vibration can be an indicator in assessing the machines condition. Because of this, it is crucial to investigate and assess machinery vibration to determine the machines condition and its minimal exposure to human body. Researchers have put an effort to develop an advanced method to perform this machinery vibration assessment. Current machinery vibration assessment requires highly skilled and trained personnel to be able to perform the vibration data analysis. The common practice that utilises absolute phase data acquisition through tachometer is not the best practice since it requires a machine to be shut down and will interrupt the operational performance. This study aims to enhance the current practice of machinery vibration assessment through an easier, faster and simplified technique by visualising the machinery motion using the developed technique.

1.2 Research Objectives

There are 4 main objectives for conducting this research;

- To develop a machinery vibration assessment system based on machinery motion visualisation using virtual instrumentation.
- To investigate the effectiveness of the proposed technique in identifying different machinery faults during routine machinery vibration assessment and machinery fault diagnostic on rotating machinery.
- To investigate the effectiveness of the proposed technique in identifying reciprocating motion in reciprocating machinery.
- To apply the proposed technique in reciprocating machine vibration assessment, i.e. bio-fuel powered diesel engine.

1.3 Research Scope and Flow

There are 2 main parts of this research which is rotating machinery and reciprocating machinery and will be discussed separately in Chapter 2, Chapter 3 and Chapter 4. For the first part, laboratory testing was conducted to study the motion of rotating machinery. The proposed technique provides new alternative with an easier, faster and simplified technique for detecting machinery failure compared to current practice of machinery condition assessment. Some of the machinery failures tested in the lab was rotor imbalance, misalignment, structural looseness, rotor eccentricity, gear fault and bearing fault. Furthermore, the effectiveness of this technique was investigated and applied on industrial machinery. Rotor imbalance and misalignment were identified as the primary machinery failures which cause secondary machinery failure such as rotor eccentricity, gear fault, bearing fault and etc. Therefore, the detection of rotor imbalance and misalignment were being focused for the real industry case study. Data interpretation can be made in shorter time by visualising the machine motion which can show the data of all measurement point concurrently of a machine. Compared to the conventional machinery condition assessment, the proposed technique is seen as a better approach in terms of time saving for data acquisition and analysis. Furthermore, an effective interpretation can be ensured with the acquired relative phase data and visualisation of the machine motion. The proposed technique introduces a more simplified approach using frequency domain ODS technique. The integration of the proposed technique will eventually enhance current practice of machinery condition assessment by reducing time required for performing vibration acquisition and analysis. Furthermore, advance specialised knowledge, highly skilled and experienced personnel is unnecessary to apply this technique into machinery condition assessment. With a more effective assessment, machine faults can be identified and detected earlier thus giving ample planning time for machine maintenance. It would avoid sudden machine failures and shut down and this may possibly reduce the downtime cost.

The effectiveness of simplified ODS technique in machine vibration assessment was further investigated in the second part by studying the motion of reciprocating machinery. The proposed technique was tested on an air compressor in the lab. The result from the air compressor test was used as the baseline to show reciprocating motion using the simplified ODS technique therefore, the effectiveness of the proposed technique was further studied in the final test on bio-fuel diesel engine testing. The testing on a bio-fuel powered diesel engine was conducted to study the effect of bio-fuel blend on reciprocating diesel engine vibration using the simplified ODS technique. This study focuses on ‘second generation’ bio-fuel (non-edible feedstock) which do not compete directly with arable land to be sustainable bio-fuel i.e. Calophyllum Inophyllum (CI). The performance of this non-edible bio-fuel and its blends as an alternative fuel is investigated and compared by using vibration as the engine parameter.

The proposed technique could identify the fuel blends with the minimal vibration of the diesel engine as the replacement fuel in comparison to the conventional diesel fuel. Furthermore, vibration source can be identified and separated in determining the optimum bio-fuel which is purely affected by the bio-fuel combustion. The flow of the conducted research is shown in Figure 1.1.

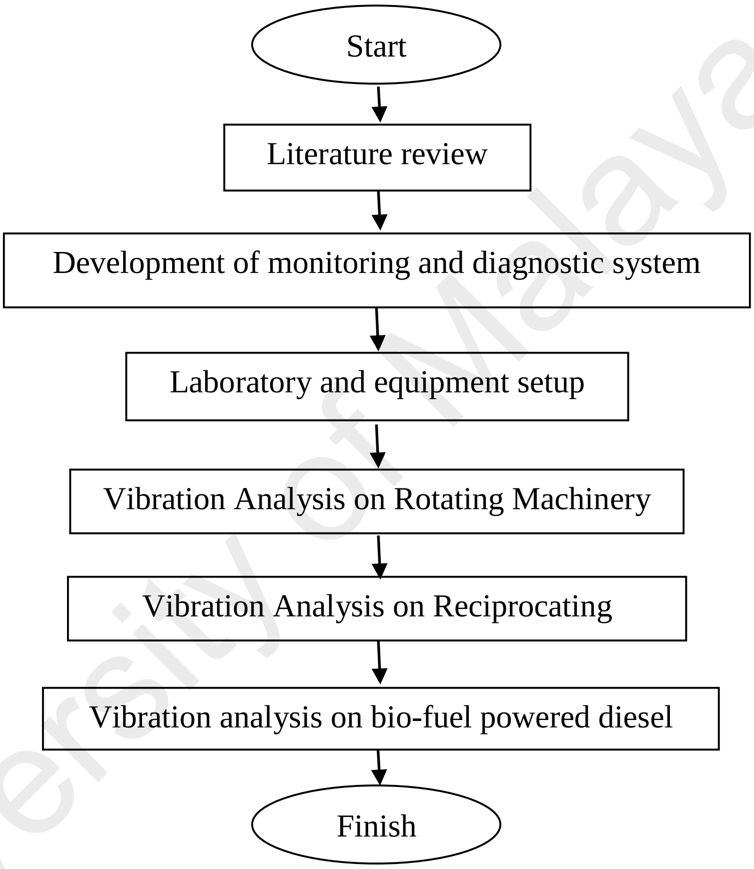

Figure 1.1: Research flow chart

CHAPTER 2: RESEARCH BACKGROUND

2.1 Literature Review

Vibration is defined as a movement in rotational, swinging or linear direction. Most machines in operation produce certain amount of vibration affecting the associated components and systems including pipelines and pipe systems. The systems are of great importance in many industries such as water supply, oil and gas, and nuclear power generating. Structural reliability of a systems such as beams structures (Fayyadh et al., 2011; Z. Ismail et al., 2008; Z. Ismail, Abdul Razak, et al., 2006; Z. Ismail, Tan, et al., 2006; Z Ismail, 2012; Z Ismail et al., 2001, 2011; Zubaidah Ismail & Ong, 2012; Zubaidah Ismail, Kuan, et al., 2014; Razak et al., 2001), frame structures (Mazinani et al., 2014; Monajemi et al., 2012, 2013) and bridges (Z Ismail et al., 2012) can be affected by vibration and has to be continually inspected. (Liu & Kleiner, 2013) reviewed the state-of-the-art of inspection techniques and technologies towards condition assessment of water distribution and transmission mains. Several approaches of fault diagnosis of structural systems have been studied (Zubaidah Ismail, 2012; Khoo et al., 2014; Rahman, Chao, et al., 2011; Rahman, Ong, et al., 2011). Research works were also conducted on machinery fault diagnosis (Bakar et al., 2013; Saghafinia et al., 2012; J. Wang & Hu, 2006). After a continuous run, a machine and its associated systems will have their downtime due to the fatigue and malfunction of its critical parts. Failure of the systems has to be avoided since it can have disastrous effects, leading to injuries and fatalities as well as substantial cost to industry and the environment (Zubaidah Ismail & Karim, 2013; Zubaidah Ismail et al., 2013; Zubaidah Ismail, Doostdar, et al., 2012; Zubaidah Ismail, Kong, et al., 2014; Zubaidah Ismail, Ramli, et al., 2012). Therefore, it is very crucial to perform maintenance activity to ensure the continuation of the machine operation and preventing from machinery failure that may cause injuries, fatalities and disastrous effect on the environment.

2.1.1 Current Practice of Machinery Vibration Assessment

Maintenance activity is very crucial in industrial area such as water supply, power generating and oil and gas. The reliability of the maintenance activity ensures continuous production of the industry. Any interruption such as machinery failure and shut down due to minor or major accident must be reduced or avoided.

2.1.1.1 Rotating Machinery Vibration Assessment

General machinery maintenance can be categorised into three which are breakdown maintenance, scheduled (preventive) maintenance, and predictive maintenance also known as condition-based monitoring (CBM). Oil and gas industry and power generation plant are two sectors that comprehensively conducting CBM assessment on maintaining machinery reliability. For example, from the author previous experience working in a Malaysia onshore petrochemical plant, the CBM assessment program is performed on monthly basis. Approximately around 200 rotating machinery need to be monitored every month. For more critical machinery, the routine CBM assessment is performed twice a month, and some machines are installed with permanent sensors for continuous online CBM assessment. The rest few hundred machines which are identified as uncritical are monitored under offline CBM assessment once a month. The current health of a machine can be determined by measuring the machines vibration and comparing the measurement to its baseline value. CBM assessment program can predict developing problems before failure and damage can occur by trending and analysing the machinery vibration. The most desirable way to maintain machinery condition is by performing the inspection while machine under operation. Early detection of minor defects and machine failure characteristic can be identified while the machine runs and it will not affect the operation performance (Mobley, 2002). This shows the importance of CBM assessment program especially in oil and gas industry and power generation plant to ensure continuous operation with less interruption.

Despite the advantages, conventional CBM assessment program is still relying on using single axis accelerometer for vibration data acquisition and using a tachometer as a mean of gathering the phase data. To get an absolute phase using a tachometer, a machine needs to be shut down and re-run again. This conventional practice is seen as time consuming and can be unsuccessful due to lack of skilled and experienced manpower. Currently, CBM assessment program involves expensive and complicated instruments and software and it requires competent personnel to perform machinery fault detection and analyse the output (Scheffer & Girdhar, 2004). Most portable vibration instruments available in oil and gas industry and power generation plant are incorporated with single channel which are suitable for analysis of a machine that operates at steady speed. Another type of vibration instruments are incorporated with a second channel but limited to input from a tachometer. This second channel is not used for capturing vibration data. Besides, current CBM assessment only interprets the vibration signal obtained by examining every single spectrum. The spectrum consists of certain frequencies which match with certain machine parts (such as bearing, gear and impeller) or certain machine fault (such as imbalance and misalignment). Phase measurement is another additional data that was not carried out regularly in current CBM assessment. Only when machinery fault occurs, phase measurement will be considered for detail vibration analysis. However, absolute phase using tachometer only works when a reflector is already attached on the shaft. To do this, a machine needs to be shut down and re-run again. Without it, personnel can only rely on spectrum data and it makes fault diagnostic becomes more difficult. This has eventually increased the time needed for data collection and analysis. Other common analyses which use the phase data are Bode plot and Nyquist plot analyses. However, both analyses are more suitable for transient testing where the machine speed either ramped-up or coasted-down. Furthermore, a permanent tachometer or key-phasor is necessary to conduct both Bode plot and Nyquist plot analyses. Rather than using a tachometer, the proposed technique uses two accelerometers to provide the relative phase. Any machine without permanent tachometer or key-phasor can be monitored without interrupting machine operation.

Another example of conventional machinery vibration assessment is to detect blade passing problem. (Abdelrhman et al., 2012) conducted a research on vibration monitoring as a diagnostic tool for the turbine blade faults. Methods used in this research include analysis of blade passing frequencies and extraction of dynamic signals from the measured vibration response. These include frequency analysis, wavelet analysis, neural networks, fuzzy logic and model based analysis. There are a lot of parameters that need to be monitored for the diagnosis of blade passing problem. Therefore, it is necessary to detect a blade passing problem faster and easier through a more simplified approach.

Vibration and acoustic measurement methods can also be used for the defects detection in rolling element bearings. Vibration data can be obtained through parameters such as Root Mean Square (RMS) level, crest factor, probability density and kurtosis. Vibration in the frequency domain can detect the defect location. However, the direct vibration spectrum from defective bearing may not indicate the defect at early stage. Thus, the high-frequency resonance technique (HFRT) and wavelet transform method were introduced to overcome this problem (Tandon & Choudhury, 1999). The detection of this rolling element bearing failure can be performed easier and faster with the support from the simplified machinery motion visualisation assessment.

The primary problem in oil and gas industry and power generation plants around the world is rotor imbalance and misalignment. They cause a lot of problems that lead to other secondary damage (Boyce, 2012; Buscarello, 1985; Mobley, 1999). As a result, parts of a machine will suffer, bearings will wear out, foundations will crack, and machines will have a shorter live. Both these problems are the main factors that contribute to other machine parts failure. Therefore, it is crucial to be able to detect these primary machinery problems accurately, faster and easier.

2.1.1.2 Reciprocating Machinery Vibration Assessment

Several studies and industrial applications have shown the effectiveness of CBM in maintaining the lifetime of rotating machinery (Al-Badour et al., 2011; Carnero, 2006; Chen et al., 1995; Edwards et al., 1998; Elbhbah & Sinha, 2013; Fu et al., 2004; Hameed et al., 2009; Hashemian, 2011; Huang et al., 2005; A K S Jardine et al., 1999; Andrew K S Jardine et al., 2006; Pan et al., 2012; Sheng et al., 2011; Tsang, 1995; Velarde-Suárez et al., 2006). However, the implementation of CBM to the internal combustion (IC) engine is not as effective as those for other rotating machineries. The difficulties in implementing the CBM to monitor IC engine is due to the complexity of the vibration signals involved. Unlike other rotating machineries, the vibration of IC engines may come from complex problems, such as injection pump malfunctions, injector clogging, excessive clearances of cylinders, and burn out of valves, which do not have any specific vibration characteristic corresponding to each problem. Therefore, the vibration of the combustion engine must be evaluated. Previous studies have shown alternatives for evaluating the vibration of IC engines (Zunmin Geng et al., 2003). However, skilled and experienced personnel in vibration are required to analyse and understand vibration data (e.g., Wigner-Ville Distribution). Sound and vibration resulting from engine combustion directly affect users. One of the drawbacks of diesel fuels is loud noise and strong vibration, which can lead to harmful physical effects. Noise is most observable among engines with high compression ratios and fast-rising combustion pressure (Selim, 2001). The pressure rise rate decreases with the increasing of the engine running speed. Thus, the combustion noise also decreases as the engine speed increases due to the reduction in the maximum rate of heat release. Therefore, it is important to evaluate the vibration of the IC engine, to be able to determine the minimal vibration produced by the IC engine. Meanwhile, other studies had considered other parameters, such as cylinder pressure, acoustic signal, injection parameter, pistons slap, and knock detection, to be compared with IC engine vibration for fault diagnosis.

The variation of the injection parameters such as injection number and timings, mean injection pressure and fuel quantity can affect the IC engine vibration. Preliminary analysis of differences in the cylinder pressure and vibration signals with and without injection was analysed by Fourier and time-frequency analysis (Carlucci et al., 2006). This research showed that it is possible to use engine block vibration as a parameter to diagnose the combustion modifications. Therefore, it can improve the engine operation by reducing costs of maintenance using cheaper diagnosis system, if compared to the use of pressure sensor.

Cooling water temperature can also affect the engine vibration. The effects were investigated in a research by conducting a spectrum analysis (Griffiths & Skorecki, 1964). It was shown that reducing cooling water temperature will increase the mean vibration frequencies from 500 Hz to 2000 Hz. This effect is considered adequate to require a temperature control when organising investigations about the effect of other engine variables on vibration to make sure that the factor of cooling water temperature will not contaminate the actual results. Therefore, the cooling water temperature should be controlled carefully to prevent the engine vibration.

Piston slap is one of the major factors of the IC engine cylinder block vibration. Piston slap is a general impact phenomenon which occurs in reciprocating engine and it will affect the transverse vibration which is perpendicular to the crankshaft. An investigation from theoretical modelling to experimental verification was conducted by (Z. Geng & Chen, 2005). As a result, an effective approach for the engine dynamic behaviour simulation and monitoring during working condition was discovered. The nonlinear model was used to model the response of vibration induced by shock. The shock induced responses and its correlation with created impact were evaluated using numerical integration. The non-linear dynamic model developed is suitable to show the mutually dependent correlations of inner-cylinder excitations, wall structural properties of piston-cylinder and vibration response.

Piston-to-cylinder friction is also a factor to produce the torsional vibration of a reciprocating engine. From (Guzzomi et al., 2007), it was shown that the geometry produces piston-to-cylinder friction and the piston side force to be interdependent. The piston friction is dominated by ring friction produced by static ring tension which applying a distributed force against the cylinder wall and dynamic friction produced by piston side force when the piston is moving up or down the cylinder. It is shown that piston friction between the cylinder and piston can also affect an engine's effective inertia function. Thus, it can affect non-linear behaviour of the IC engines.

A simple method for low intensity knock detection which occurred in spark ignition engines was created based on the modelling of the cylinder block vibration signal by auto regressive moving average (ARMA) parametric mode (Ettefagh et al., 2008). One of the estimated moving average parameters is sensitive to knock, thus it is possible to detect the knock even in very initial stages by monitoring this parameter. It is possible to detect knock by simple hardware with low sampling frequency which can help to reduce the computation time, hardware complexity and cost. Through this research, a simple and cost-effective method was performed by combining the tachometer and acceleration signals with high accuracy.

Investigations on the noise created by engine vibration caused by knocking inside cylinder were performed by (Ghobadian et al., 1992). The noise data of a small single-cylinder direct injection diesel engine was measured in a stationery condition. Some aspects such as the transmitted noise from engine, the pressure inside cylinder, the fuel line pressure and the acceleration signals were measured and analysed in the time domain and frequency domain for different engine running speed. The results obtained were higher compared with multi-cylinder diesel engine due to its robust structure.

Investigations on the effect of vibration on the power tiller operator with the diesel engine were conducted by (Taghizadeh et al., 2010). The experiment was conducted for different cases under different engine running speed at several positions which are the chassis, handle, driver arm and chest. The results showed that the higher the engine running speed, the higher the RMS of acceleration values. It was observed that dominance of vibration in each locations and axes is same with the piston stroke number or engine revolution.

Vibration analysis on diesel engine can also be performed by using software simulation only. In the research by (Bhansali & Shirgire, 2014), finite element software, i.e., ANSYS was used to analysed the vibration in diesel engine cylinder liner. Firstly, the system was modelled using ANSYS software to create a needed geometry for simulations. Vibration analysis was performed for 2 dimensional (2-D) and 3 dimensional (3-D) models along with different direction for different materials and nodes. Thus, it is proven that vibration levels during engine operating conditions can be predicted in a better and easier way by using the ANSYS software.

Faults in the diesel engines valves are another factor that may cause the increasing of vibrations. A fault diagnosis method was developed by (C. Wang et al., 2008) to process the Wigner-Ville distributions (WVD) of signals by time-frequency methods. The results were then showed in grey images and the probabilistic neural networks (PNN) are used to categorise the time-frequency images to recognise the states after the images are normalised. Lastly, the experimental results in diesel valve train proved the diagnosis method is acceptable.

In general, all the mentioned research works on reciprocating machinery vibration assessment involves complicated technique thus requires highly skilled and trained personnel to analyse the vibration data. Therefore, it is considered as a potential area to test the effectiveness of the proposed technique which is more simplified for performing reciprocating machinery vibration assessment. In this research the testing for reciprocating machinery is performed on a diesel engine powered by bio-fuel. Recent increasing attention by researchers on the bio-fuel production has led to the needs of evaluating the performance of the engine together with the engine vibration assessment.

2.1.2 Background on Bio-Fuel Powered Diesel Engine

Bio-fuel is an alternative fuel extracted from fat tissues and vegetable oils. Bio-fuel is made up of saturated and unsaturated long-chain fatty acid alkyl esters (Fazal et al., 2011). It can be used in combustion engines by using a suitable portion of bio-fuel to be mixed with diesel fuel. The advantages of bio-fuel have been proven by previous studies (Sadeghinezhad et al., 2013, 2014) Exhaust from bio-fuel combustion produces less pollution as compared with that from diesel fuel (H. C. Ong et al., 2011; Hwai Chyuan Ong et al., 2014; Sadeghinezhad et al., 2013, 2014; Silitonga et al., 2013). A critical issue was raised regarding the disagreement on food versus fuel for edible oil sources. Hence, researchers have paid attention into finding the most efficient bio-fuel from non-edible feed-stocks (Maleki et al., 2013; H. C. Ong et al., 2013; Salaheldeen et al., 2014; Silitonga et al., 2013). Various non-edible plants have been tested and considered suitable for producing bio-fuel. Some of the identified non-edible plants are Jatropha curcas, Calophyllum inophyllum, Ceiba pentandra, Hevea brasiliensis, Rice bran, Nicotiana tabacum, Sapindus mukorossi, Cerbera odollam etc. Various feed-stocks for bio-fuel are being studied to avoid global dependence on certain sources, which might eventually cause high demand low supply. Generally, most of non-edible feed-stocks are high in acid content (H. C. Ong et al., 2013). Methods for reducing acid content need to be identified and tested before any non-edible feed-stocks can be proposed. Furthermore, the properties of non-edible feed-stocks should be within acceptable ranges that comply with ASTM D6751 and EN 12412 standards (Atabani et al., 2013). Some of the known advantages of non-edible bio-fuel are its portability, availability, renewability, high heat content, low sulfur content, low aromatic content, and biodegradability. A previous study (Maleki et al., 2013) found that non-edible bio-fuel can be an alternative to existing fossil fuels..

An example of a non-edible plant that can be produced as bio-fuel is *Calophyllum inophyllum* (CI). A previous study (Dweck & Meadows, 2002) investigated the origin of CI and its application in medicine and consumers products. CI plant is commonly available around Indonesia and Malaysia. In different parts of the world, CI is used as medicine, soap, lamp oil, hair grease and cosmetic. The production of CI bio-fuel through the process of degumming, esterification, neutralisation and transesterification had been studied (Hwai Chyuan Ong et al., 2014). Reportedly, CI bio-fuels can improve engine performance and fuel uptake, as well as reduce carbon monoxide emission and smoke opacity. Aside from all of the tests and characteristics mentioned, a vibration test to evaluate the engine vibration using CI bio-fuel has not been conducted.

The growing interest in the production of a suitable alternative bio-fuel blend necessitates the evaluation of IC engine vibration. (Taghizadeh-Alisaraei et al., 2012) conducted a study on the bio-fuel and its effect on the engine vibration. In this research, edible bio-fuel used is produced from vegetable oils which are soybean and canola, animal fats, and waste oil based on AST MD 6751-09 standard. The diesel engine used in this experiment is a single differential MF399 tractor engine and biodiesel fuel blends prepared are B5, B10, B15, B20, B30, B40, B50, pure biodiesel B100, and pure diesel. 3 high accurate accelerometers with specifications of CTC AC102-1A were used to acquire the vibration signals. In this study, the vibration analysis performed is shown in the time domain signal and the frequency domain signal. The time domain signals were obtained in vertical (z), lateral (y) and longitudinal (x) axes. Vibrations of engine before the services and after the services were also studied in cold weather. The complete combustion cycles can be observed clearly in the filtered time domain signal. The signal was processed through a high pass filter for a more resolution of combustion. For the comparison of engine vibration at different engine running speeds and different fuel blends, the RMS of acceleration for each axis was measured at different conditions of experiments. The results showed that the engine vibrations depend on its service and maintenance too. Engine vibration can be reduced by replacing the air filter and engine lubrication oil. Besides that, the results showed that the dominant frequency is in accordance with piston strokes in all engine speeds. Most of the vibrations rising are between 1800 and 2000 rpm. This study proved that bio-fuel blends have significant effect on the vibration. It showed that B40 and B20 have the lowest vibration.

Meanwhile, other research works on vibration analysis of 2 types of non-edible bio-fuels which are Jatropha Methyl Ester (JME) and Mahua Methyl Ester (MME) in diesel engine were conducted. The studies focused in evaluating the performance of JME and MME by evaluating the combustion properties as well as engine vibration and noise.

JME heated to 60°C is the most effective preheated temperature in the view of the engine performance, combustion performance as well as vibration aspects (Reddy & Rao, n.d.). A trail was made to evaluate the feasibility for the possible replacement and it was concluded that MME is suitable for replacement (Kiran Sastry et al., 2005). However, the vibration analysis of other type of bio-fuel and its blends in diesel engine should also be done in order to study the performances of other bio-fuel.

The investigations on the performance of diesel engine from the aspect of emission analysis using Jatropha oil was conducted in previous research. Overall results proved that Jatropha oil can be a good source for transesterification. There is high exhaust when only the diesel is used but the exhaust gas is much less when the blends are used. This proves that different blend of bio-fuel is good to use in the engine without any engine modifications. This is good as it can limit the emission of toxic gases. Jatropha bio-fuel produced is analysed for the use as fuel according to ASTM standards (Bassyouni et al., 2012).

(Sastry et al., 2012) studied the performance, emission and vibration of diesel engine using fish oil biodiesel (FME) blends. Performance parameters such as engine torque, fuel consumption and brake thermal efficiency are measured for pure diesel and different FME blending. Besides that, CO, NO_x and smoke emissions are studied. The results showed that diesel fuel generates higher vibratory trend than FME. Therefore, FME blends can be recommended to be implemented to run the engine without necessarily to change the basic design of the engine.

Bio-fuel powered diesel engine is similar to other IC engine where it produces high noise and vibration. Researchers have investigated the vibration of bio-fuel powered diesel engine on different aspects. Most of the studies have analysed the performance of bio-fuel powered diesel engine by determining the engine power or torque, brake thermal efficiency, brake-specific fuel consumption or energy consumption. There are limited research works which consider vibration analysis as one of the engine performance parameter.

(Fazal et al., 2011) stated that engine performance with bio-fuel blend depends more on the combustion, air turbulence, air-fuel mixture quality, injector pressure, actual start of combustion and others which cause the results to be different for each engine. Moreover, the results may change depending on quality of bio-fuel and engine operating parameters such as running speed and load. This research showed that bio-fuel from different origins provide better lubricating characteristic compared to diesel fuel but bio-fuel loses its lubricating characteristic due to its oxidative nature in long term. Besides that, it shows that bio-fuel can improve combustion. Bio-fuel allows acceptable engine performance and it can be further improved if its viscosity can be reduced. This research also showed that high concentration of oxygen in bio-fuel improves lubricating characteristic and reduces emissions. However, both oxygen and alcohol will enhance the corrosion. The advantages of bio-fuel include higher cetane number, flash point and oxygen, sulphur-free, better lubricating characteristic and less emission.

Another study (How et al., 2014) used palm oil for engine vibration testing . The testing was done on one engine speed, 2,000 rpm, i.e., maximum torque with different injection pressure. The optimum bio-fuel blend was determined through the overall RMS vibration value. The technique was simple but no in-depth studies were conducted on the effect of vibration caused by combustion of bio-fuel blend itself. Overall vibration in RMS could consist of vibration components due to combustion as well as other external vibration sources. The overall vibration may possibly be contaminated by these external vibration sources, which could limit the effectiveness of identifying the optimum fuel blend in engine vibration. Torque is one of the external vibration sources that could contribute to the overall vibration of an engine. According to Figure 6 in (Taghizadeh-Alisaraei et al., 2012), maximum torque must be observed at low engine speed, whereas minimal torque is required at full speed. Therefore, these two speeds are used to study the effect of torque as the external factor in overall engine vibration. The cause of external vibration source, such as torque should be eliminated before determining the optimum bio-fuel blend in engine vibration. To achieve this, an advanced vibration analysis through time domain and frequency domain analysis is required to identify the major effect of bio-fuel combustion on the engine vibration. Together with the support of the proposed simplified technique, the optimum bio-fuel blend based on the minimal engine vibration can be identified easier and faster.

2.1.3 Visualisation of Machinery Motion Technique

Conventionally, primary rotating machinery problems which are rotor imbalance and misalignment can be detected by analysing vibration spectrum. However, researchers found that analysis by depending only to vibration spectra does not provide the best information for detecting machinery rotor imbalance and misalignment. There are some cases where misalignment, rotor imbalance and even structural looseness are producing the same vibration characteristic, which may lead to false data interpretation and diagnosis (Buscarello, 1985; Ferrando Chacon et al., 2014; Ganeriwala.S et al., 1999; Pennacchi et al., 2012; Verma et al., 2013). Research works and studies have been carried out to find better method to accurately identify the primary machinery part failure. Other alternatives such as using current signal and Operating Deflection Shapes (ODS) analysis were proposed to detect rotor imbalance and misalignment (Ferrando Chacon et al., 2014; Ganeriwala et al., 2008, 2009; Gong & Qiao, 2012; Saleem & Diwakar, 2012; Verma et al., 2013).

The introduced rotating machinery motion visualisation can be performed through the ODS analysis technique. ODS is a measurement technique of determining the motion of a machine while it is in operation. The actual motion is too fast and the amplitude is too small to be visualised by our naked eyes. The motion of a machine in actual condition at certain vibration frequency component can be obtained from ODS analysis and helps a personnel to determine the cause of the motion using some digital signal processing technique (Heaton & Hewitt, 2006; Hermans & Van Der Auweraer, 1999; Pascual et al., 1999; Reilly, 2011; B. Schwarz & Richardson, 2004; B. J. Schwarz & Richardson, 1999). Two parameters which is vibration value and phase data are required to perform the ODS. Phase data is the position of a vibration measurement point on a machine relative to a reference measurement point of the same machine. The combination of these two parameters will enable the visualisation of machinery rotating motion. The ODS can be performed in two methods using time domain ODS and frequency domain ODS.

Time domain ODS analysis requires "*n*" sets of accelerometers and a minimum *n*-channel data acquisition system, where "*n*" equals to the number of required degree of freedom for the structure to be analysed. The time waveform of all signals is simultaneously recorded. Assigning each waveform to a particular freedom node in a structure and scanning through all the time traces synchronously will generate the ODS of the structure. For example, four units of accelerometer are required to show the ODS motion of a structure. All the accelerometers were mounted firmly at the measurement points and vibration signals were acquired simultaneously. This method is ideal for analysing signals that are not steady-state, such as the transient response (McHargue & Richardson, 1993). However, the equipment cost escalates with the increase in the number of accelerometers. Hence, time domain ODS which requires a lot of channels and accelerometers for data acquisition is not practical for CBM assessment program.

A more practical approach for applying the ODS analysis technique into the CBM program is by using the frequency domain ODS. Frequency domain ODS utilises the Frequency Response Function (FRF) measurements to determine the actual deflection of a structure or a system. FRF is a measurement of the vibration amplitude and phase output as a function of frequency instead of function of time used in time domain ODS. Instead of using actual phase from a tachometer, relative phase is considered as more practical approach. This can be done by using 2 accelerometers to measure vibration signal, one of the accelerometers remains fixed while the other unit is moved throughout the selected points on the structure (Abdul Rahman et al., 2013; McHargue & Richardson, 1993). The frequency domain ODS method can be implemented by using tri-axis accelerometers to capture the vibration data with respect to the fixed accelerometer. The relation of the amplitude and phase was calculated for each of the roving accelerometer locations with respect to the fixed accelerometer. In the frequency domain, a cursor need to be put at a specific frequency component before the visualisation of the ODS motion can be observed. So far, no research had been reported by implementing the frequency domain ODS analysis technique into CBM program or vibration assessment on a rotating machinery.

The same simplified ODS technique used for rotating machinery vibration assessment is used to assessed the vibration on the reciprocating machinery. So far, no research had been reported on diesel engine vibration assessment using ODS technique. ODS can also show reciprocating motion and could possibly detect any machinery fault. Since diesel engines commonly produce high vibration that may be harmful if exposed for a long time of period. The purpose of using this simplified technique is to identify the minimal vibration from the diesel engine caused by the bio-fuel combustion. Furthermore, the external source of vibration can be differentiated and separated through advanced vibration analysis which involves time domain analysis and frequency domain analysis.

2.2 ODS Theory

ODS provides practical information for understanding and analysing the dynamic behaviour of machine, component or whole structure. ODS analysis is an easy method used for visualisation of the pattern of vibration for a machine or structure under actual operating conditions. Measurements are done at different points on the structure which is known as degrees of freedom (DOFs) and the pattern of vibration can be shown in many ways including animated geometry model. ODS represents the deflection of a structure subjected to a particular excitation frequency and thus depends on the applied forces or loads. The forced vibration response of a linear structure for a general system in original coordinates can be written as Equation (2.1),

$$M\ddot{X} + C\dot{X} + SX = Q \tag{2.1}$$

where $C = aM + bS$ (2.2)

Expanding Equation (2.1),

$$\begin{bmatrix} M_{11} & M_{12} & \dots & M_{1n} \\ M_{21} & M_{22} & \dots & M_{2n} \\ \dots & \dots & \dots & \dots \\ M_{n1} & M_{n2} & \dots & M_{nn} \end{bmatrix} \begin{bmatrix} \ddot{x}_1 \\ \ddot{x}_2 \\ \dots \\ \ddot{x}_n \end{bmatrix} + \begin{bmatrix} C_{11} & C_{12} & \dots & C_{1n} \\ C_{21} & C_{22} & \dots & C_{2n} \\ \dots & \dots & \dots & \dots \\ C_{n1} & C_{n2} & \dots & C_{nn} \end{bmatrix} \begin{bmatrix} \dot{x}_1 \\ \dot{x}_2 \\ \dots \\ \dot{x}_n \end{bmatrix} +$$

$$\begin{bmatrix} K_{11} & K_{12} & \dots & K_{1n} \\ K_{21} & K_{22} & \dots & K_{2n} \\ \dots & \dots & \dots & \dots \\ K_{n1} & K_{n2} & \dots & K_{nn} \end{bmatrix} \begin{bmatrix} x_1 \\ x_2 \\ \dots \\ x_n \end{bmatrix} = \begin{bmatrix} Q_1 \\ Q_2 \\ \dots \\ Q_n \end{bmatrix} \tag{2.3}$$

Thus in principal coordinates, it can be written as Equation (2.4),

$$M_P\ddot{X}_P + C_P\dot{X}_P + S_PX_P = Q_P \tag{2.4}$$

Where $C_P = X_M^T C X_M = aM_P + bS_P$ (2.5)

Expanding Equation (2.4),

$$\begin{bmatrix} M_{P1} & 0 & \dots & 0 \\ 0 & M_{P2} & \dots & 0 \\ \dots & \dots & \dots & \dots \\ 0 & 0 & \dots & M_{Pn} \end{bmatrix} \begin{bmatrix} \ddot{x}_{P1} \\ \ddot{x}_{P2} \\ \dots \\ \ddot{x}_{Pn} \end{bmatrix} + \begin{bmatrix} C_{P1} & 0 & \dots & 0 \\ 0 & C_{P2} & \dots & 0 \\ \dots & \dots & \dots & \dots \\ 0 & 0 & \dots & C_{Pn} \end{bmatrix} \begin{bmatrix} \dot{x}_{P1} \\ \dot{x}_{P2} \\ \dots \\ \dot{x}_{Pn} \end{bmatrix} +$$

$$\begin{bmatrix} K_{P1} & 0 & \dots & 0 \\ 0 & K_{P2} & \dots & 0 \\ \dots & \dots & \dots & \dots \\ 0 & 0 & \dots & K_{Pn} \end{bmatrix} \begin{bmatrix} x_{P1} \\ x_{P2} \\ \dots \\ x_{Pn} \end{bmatrix} = \begin{bmatrix} q_{P1} \\ q_{P2} \\ \dots \\ q_{pn} \end{bmatrix} \quad (2.6)$$

The equations are diagonalised and then uncoupled into n modal sets of single degree of freedom (SDOF) system.

When modal matrix is normalised with respect to M, the damping matrix in normal coordinates will become,

$$C_P = \emptyset^T C \emptyset = al + b\omega_o^2 \quad (2.7)$$

Equation of motion in normal coordinates is,

$$\ddot{X}_P + C_P \dot{X}_P + S_P X_P = Q_P \quad (2.8)$$

Substitute Equation (2.7) into (2.8), equation of motion for mode r is,

$$\ddot{x}_{pr} + (a + b\omega_{or}^2)\dot{x}_{pr} + \omega_{or}^2 x_{pr} = q_{pr} \quad (2.9)$$

where $r = 1,2,3, \dots \dots n$

To make this expression analogous to that for 1-degree system,

$$C_P = 2\sigma_r = a + b\omega_o^2 \quad (2.10)$$

where C_P is defined as modal damping constant for r[th] mode, σ_r is modal decay rate.

From the Equation (2.9), equation of motion is,

$$\ddot{x}_{pr} + (a + b\omega_{or}^2)\dot{x}_{pr} + \omega_{or}^2 x_{pr} = q_{pr} \tag{2.11}$$

If the system is subjected to a harmonic excitation force defined by $Q = Pcos\omega t$, the transformation of the action equations of motion to normal coordinates produces the typical modal equation

$$\ddot{x}_{pr} + (a + b\omega_{or}^2)\dot{x}_{pr} + \omega_{or}^2 x_{pr} = q_{pr}cos\omega t \tag{2.12}$$

Damped steady-state response of rth mode is

$$x_{pr} = \frac{q_{pr}e^{i\omega t}}{\omega_{or}^2 - \omega^2 + 2\sigma_r \omega i} \tag{2.13}$$

Where $\sigma_r = \xi_r \omega_{or}$ (2.14)

Equation (2.13) can be expressed in terms of magnitude and phase,

$$x_{pr} = q_{pr}\beta_r \cos(\omega t - \theta_r) \tag{2.15}$$

Where the magnification factor β_r is,

$$\beta_r = \frac{1}{\sqrt{(\omega_{or}^2 - \omega^2)^2 + (2\sigma_r \omega)^2}} \tag{2.16}$$

And the phase angle θ_r is,

$$\theta_r = tan^{-1}\left(\frac{2\sigma_r \omega}{\omega_{or}^2 - \omega^2}\right) \tag{2.17}$$

Back transformation to obtain the contribution of the considered mode

$$X(\omega) = \sum_{r=1}^{n} \emptyset_r x_{pr} = Q(\omega) \sum_{r=1}^{n} \frac{\emptyset_r^T \emptyset_r}{(\omega_{or}^2 - \omega^2) + (2\xi_r \omega_{or} \omega) i} \tag{2.18}$$

where X is the displacement vector of the structure

x_{pr} is the damped steady-state response of rth mode

$\emptyset_r$ is the vectors of the modal deformation of rth mode

Q is the force vector applied on the structure

T denotes the transposed vector

ω_{or} is the rth natural frequency of the structure

ω is the frequency of the applied force

ξ_r is the damping of the rth mode

The Equation (2.18) represents the ODS of the system subject to a harmonic excitation (Abdul Rahman et al., 2013; McHargue & Richardson, 1993; B. J. Schwarz & Richardson, 1999).

The process to obtain the FRF and $Z(\omega)$ from the FFT analyser and the estimation of FRF are discussed. The correlation function inspects the relationships between signals at 2 points in time. If the signal is a sine wave with a period τ, then there will be an good correlation as the responses are the same.

The auto-correlation of output signal at first point is given by Equation (2.19)

$$R_{xx}(\tau) = E[x(t)x(t+\tau)] \tag{2.19}$$

where it is defined as the product of $x(t)$ and $x(t+\tau)$

Similarly, the auto-correlation of the output signal at second point is,

$$R_{yy}(\tau) = E[y(t)y(t+\tau)] \tag{2.20}$$

Determination of correlation between 2 signals, the cross-correlation is stated as,

$$R_{xy}(\tau) = E[x(t)y(t+\tau)] \tag{2.21}$$

Cross-correlation is useful to evaluate whether a vibration at one point of structure is being influenced by vibrations at the other point.

The Fourier Transform of the auto-correlation function is called Auto Power Spectrum which can be used to extract the magnitude of the point is given by Equation (2.22) and (2.23),

$$S_{xx}(\omega) = \int_{-\infty}^{\infty} R_{xx}(\tau)e^{-i\omega\tau}d\tau \tag{2.22}$$

$$S_{yy}(\omega) = \int_{-\infty}^{\infty} R_{yy}(\tau)e^{-i\omega\tau}d\tau \tag{2.23}$$

The Fourier Transform of the cross-correlation function is called Cross Power Spectrum which can be used to extract the phase relative to the other point is given by Equation (2.24),

$$S_{xy}(\omega) = \int_{-\infty}^{\infty} R_{xy}(\tau)e^{-i\omega\tau}d\tau \tag{2.24}$$

CHAPTER 3: METHODOLOGY

3.1 Development of Machinery Vibration Assessment System

In order to develop the simplified ODS technique, an icon based software DASYLab® was used. The DASYLab® software can solve complex measurement, control, and simulation tasks interactively on the screen. The software does not require programming but provides an icon based module (Zloto et al., 2012). Each module has different function and can be positioned and connected in the worksheet as shown in Figure 3.1 The task is determined by the connection and configuration of the modules. A display module was used to show the processed signal result in the layout. Furthermore, the DASYLab® software supports standard measurement and control boards and interfaces such as National Instrument (NI) signal conditioner which was used for communication and data acquisition.

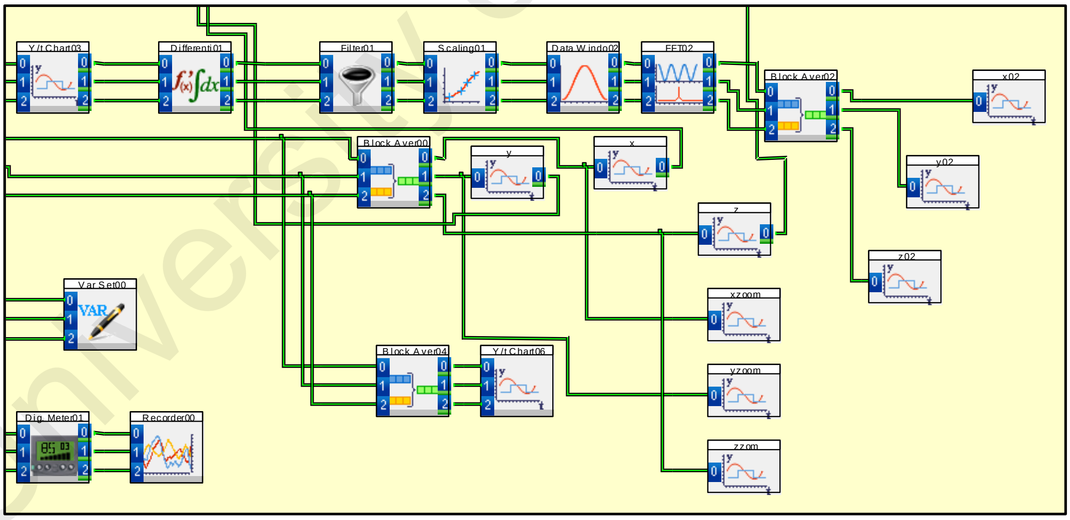

Figure 3.1: Example of DASYLab® Module Connected in the Worksheet

The DASYLab® software provides Switch module which was used to create different buttons with different functions. The Switch module generates up to 16 signals for each activated data channel. The one shot switch type was mostly used with different functions based on the assigned action to the module output. Meanwhile, the

Start/Stop and Pause/Continue switch type were used for stopping or restarting measurement and interrupting or continuing measurement respectively. The usage of these buttons provides a more user friendly method for both data acquisition and analysis.

The acquired acceleration raw data was integrated using the Action Controlled Integration module to present the data in velocity and integrated twice to present the data in displacement. The integrated overall data was also presented in RMS using the Statistical Values module. The RMS value specifies the mean square of the selected sample. Better comparison and analysis can be performed using the RMS value rather than other statistical value i.e. maximum, minimum, mean, standard deviation and variance (Scheffer & Girdhar, 2004). The DASYLab® saves the value to be processed as variable number in Global Variable.

The acquired signal was further processed using the Fast Fourier Transform (FFT) module. The FFT module transforms the vibration signals from the time domain into the frequency domain. Under the FFT module is the Cross Spectrum of Two Real Signals type. This module type was used to calculate the cross spectrum for data channel pairs. The module calculates the complex FFT of two real inputs and multiplies the calculated spectrum of the first input with conjugated complex spectrum of the second input. The module assigned the real part at the first output and the imaginary part at the second output. The time different between the two signals determines the relative phase value. This relative phase value was used together with the vibration amplitude to show the simplified ODS motion.

Analysis of the processed data can be performed using the time domain analysis and frequency domain analysis. Both methods were presented using the Y/t-Chart module before and after FFT module respectively. To present the simplified ODS, the Generator module was used to read the value from the saved Global Variable. The signal value was presented in Sinusoidal signal form to get the cyclic motion of the simplified ODS. The X/Y-Chart module was used to display the data channels pair wise as X and Y curves. The value pairs were interpreted as coordinates. The first channel specifies the X-values and the second channel specifies the Y-values. DASYLab® displays Y over X and connects the individual data with a line, which produces a closed curve.

3.2 Instrumentation Setup

Vibration data was obtained using a calibrated commercial single-axis accelerometer and a tri-axial accelerometer. The accelerometer with the specifications of Wilcoxon 786C (sensitivity, 100 mV/g; measurement range, 80 g peak; source voltage, 18–30 volts; frequency response, 1–9,000 Hz) was used as reference for the phase value. The tri-axial accelerometer with the specifications of IMI 604B31 (sensitivity, 100 mV/g; measurement range, 50 g; source voltage, 18–28 volts; frequency response, 0.5–5000 Hz) was used as a roving point to acquire the vibration signals and phase value corresponding to the reference accelerometer. Both accelerometers were mounted on the engine using a magnet. The accelerometers were connected to National Instruments NI 9234 signal conditioner to transfer the vibration signal to the laptop as shown in Figure 3.2. The DASYLab® software was used for the acquisition of vibration data and signal processing.

The Frequency Response Function (FRF) of all channels were performed simultaneously, and the ODS analysis conducted at specific frequencies were observed. The single-axis accelerometer was used to be used for the determination of reference input signal, triggering and synchronisation, and measurement of phase. Meanwhile, the tri-axial accelerometer was used to capture vibration signals in three orthogonal directions identified as x-axis (axial), y-axis (horizontal), and z-axis (vertical), simultaneously for all measurement points. The roving accelerometer test was performed to observe multiple points instead of using multiple accelerometers simultaneously.

Conventional vibration analysis on rotating machinery evaluates the vibration in terms of velocity with measurement unit mm/s. The vibration data in velocity was attained by single integration of the raw acceleration data using the DASYLab® software. Meanwhile, vibration analysis on reciprocating machinery was evaluated in terms of acceleration with measurement unit m/s^2 which is the raw data from the accelerometer.

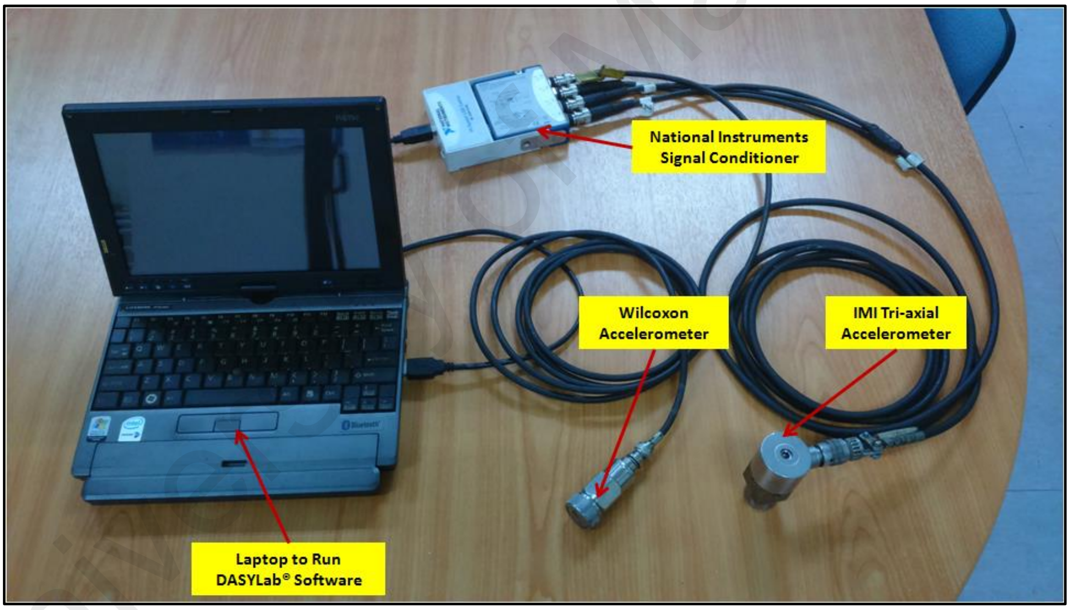

Figure 3.2: Instrumentation arrangement

3.3 Rotating Machinery Setup

The experimental testing of machinery visualisation of rotating machinery motion was performed in the lab. After showing the effectiveness in lab condition, the technique was applied in industrial machinery to prove its effectiveness further in real industrial application.

3.3.1 Laboratory Setup

Laboratory rotor kit was fabricated to create the source of vibration as in Figure 3.3. The rotor kit consists of a variable speed motor, balancing disc, roller bearing, and rubber type coupling. Two measurement points are on the motor side (drive end and non-drive end) and another two measurement points are on each roller bearing where point 1 is driver Non-Drive End (NDE), point 2 is driver Drive End (DE), point 3 is driven DE and point 4 is driven NDE. This laboratory kit setup is used to simulate both rotor imbalance and misalignment fault.

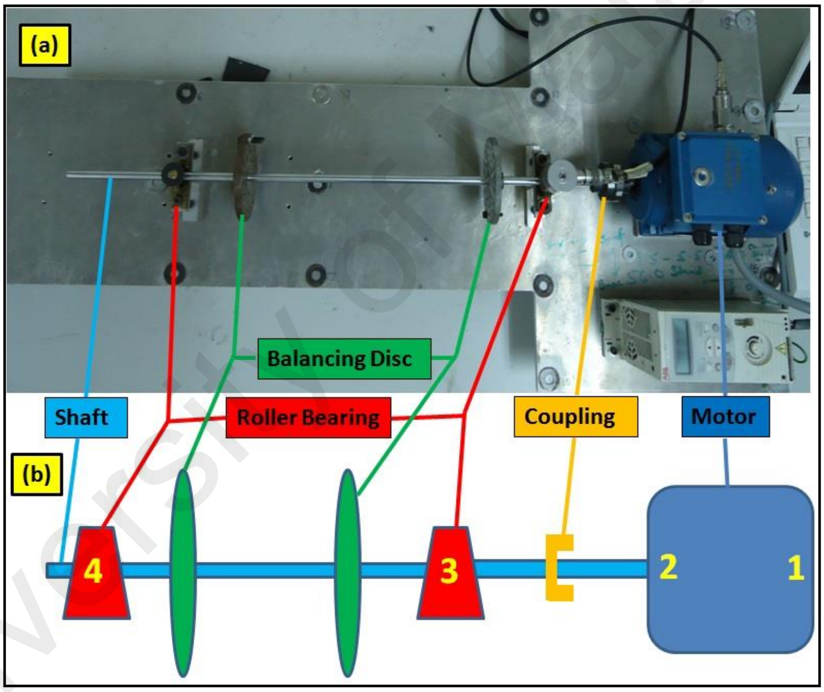

Figure 3.3: Laboratory rotor kit setup

3.3.1.1 Testing of Rotor Imbalance Detection

There are 2 types of rotor imbalance faults which are static imbalance and dynamic imbalance. Using the simplified ODS technique, rotor imbalance can be detected and differentiate easier, faster and more accurate compared to conventional method. Additional mass was added on the balancing disc to simulate the static imbalance and dynamic imbalance as shown in Figure 3.4. The effectiveness of this simplified ODS technique could be validated from the result of differentiating this rotor imbalance fault.

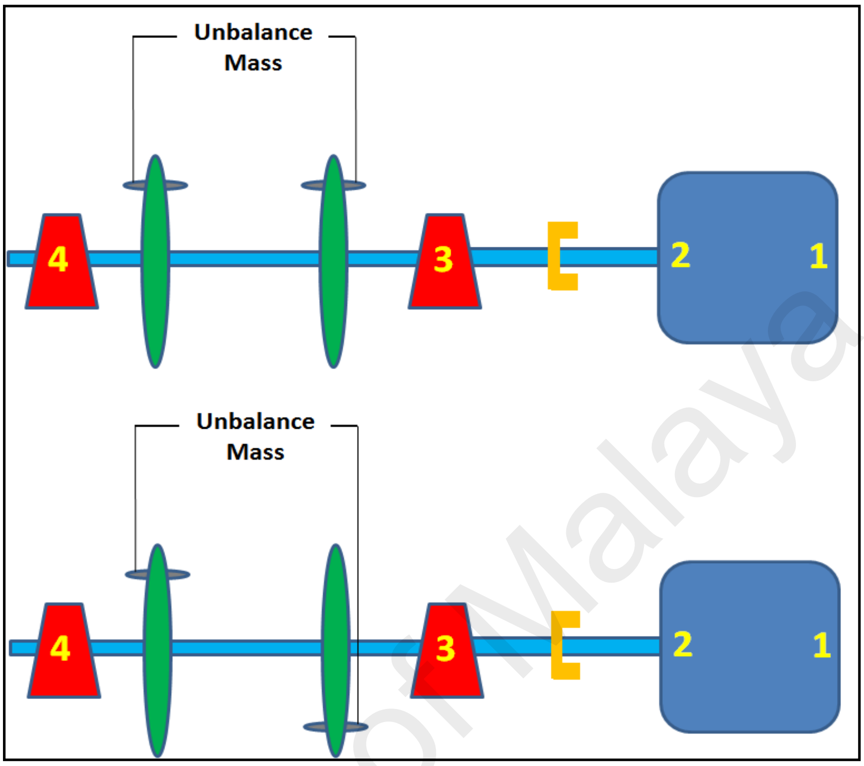

Figure 3.4: Laboratory imbalance fault testing

3.3.1.2 Testing of Misalignment Detection

The effectiveness of the simplified ODS technique was further tested in detecting misalignment fault. There are 2 types of misalignment which is parallel misalignment and angular misalignment. The coupling was misaligned horizontally to get the parallel and angular misalignment behaviour as shown in Figure 3.5. The effectiveness of this simplified ODS technique could be validated from the result of differentiating and detecting the misalignment fault easier, faster and more accurate compared to convention method.

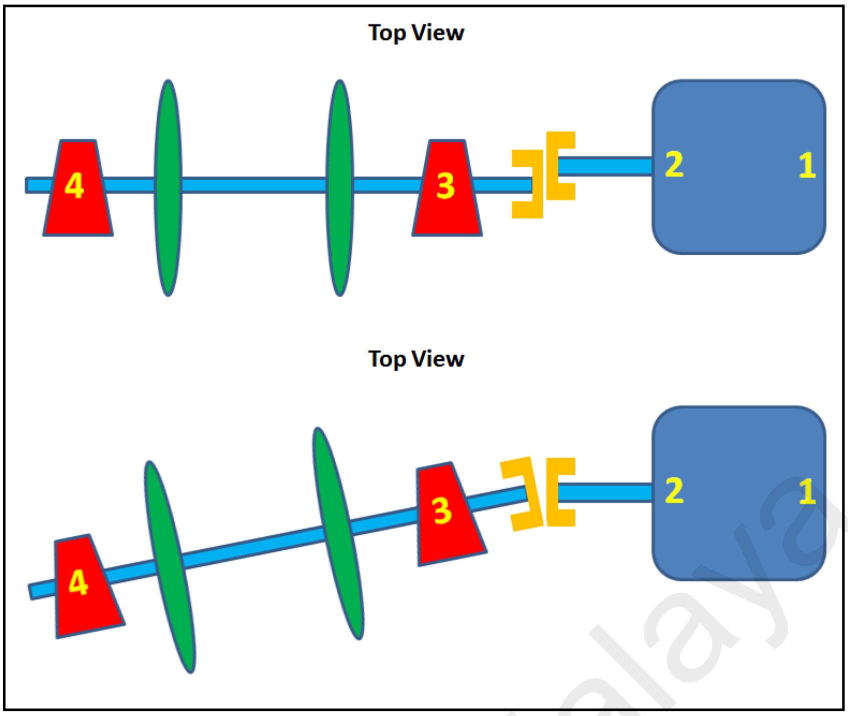

Figure 3.5: Laboratory misalignment fault testing

3.3.1.3 Testing of Support Looseness Detection

The next experimental testing focused on the motor side. This test requires at least 8 measurement points rather than 4 measurement points. 4 points were identified on the motor support and another 4 points on the base as shown in Figure 3.6. The ODS motion of this testing is different from the previous test. The ODS motion was generated as a cubic shape movement. The result from this testing supports the importance and application of relative phase together with vibration data as the best tools to diagnose machinery fault such as rotor imbalance, misalignment and support looseness.

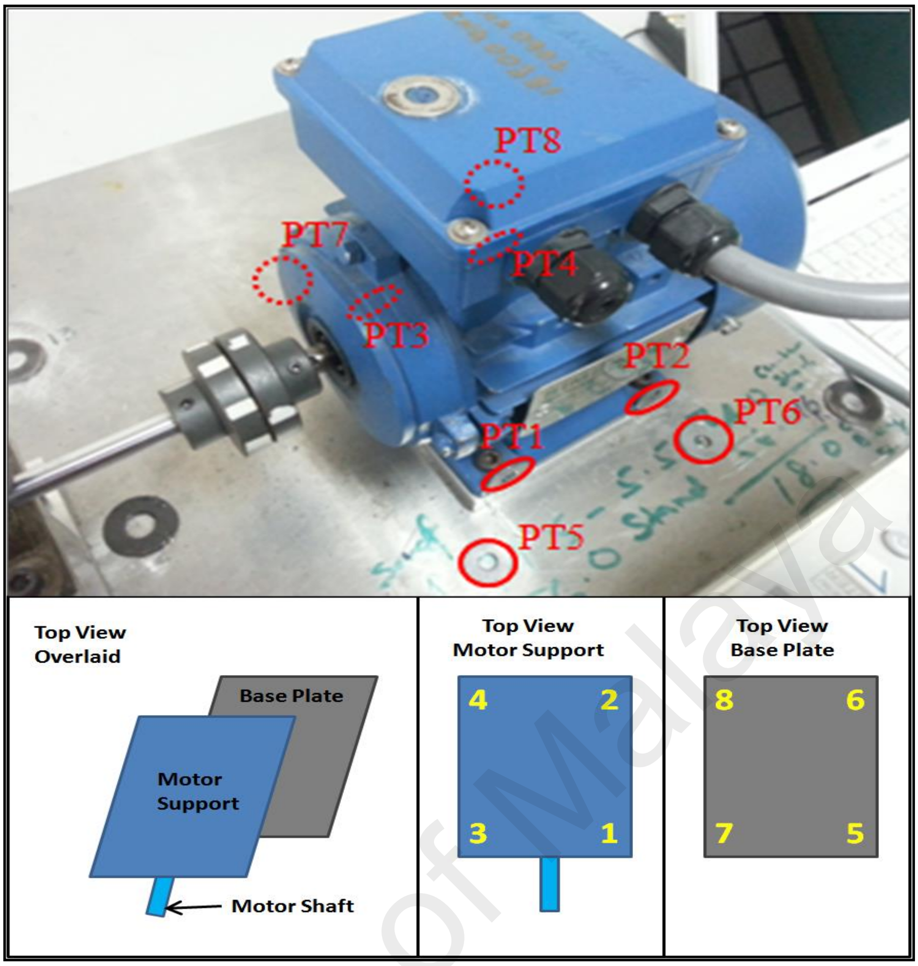

Figure 3.6: Motor support looseness testing

3.3.1.4 Testing of Bearing Fault Detection

Conventionally, this bearing fault detection was identified by capturing the impact cause by the defect bearing. Relative phase data is not necessary while performing bearing fault detection. However, for the purpose to further investigate the application of the simplified ODS technique, both vibration and relative phase data were used in this testing.

The test focused on a ball bearing with two types of fault that may occur on a bearing. Damage on the outer race of a ball bearing generates an impact at ball pass frequency outer race (BPFO) component. While damage on the inner race of a ball bearing generates an impact at ball pass frequency inner race (BPFI) component. Both

BPFO and BPFI are represented in frequency parameter, i.e., Hz. These two components can be found in the frequency domain of vibration spectrum. The outer race of the ball bearing was punched to leave a mark which will create the bearing fault at BPFO component. While the inner race of the ball bearing was drilled to leave a mark which will create the bearing fault at BPFI component. Figure 3.7(a) and Figure 3.7(b) show clear marks on the faulty bearing.

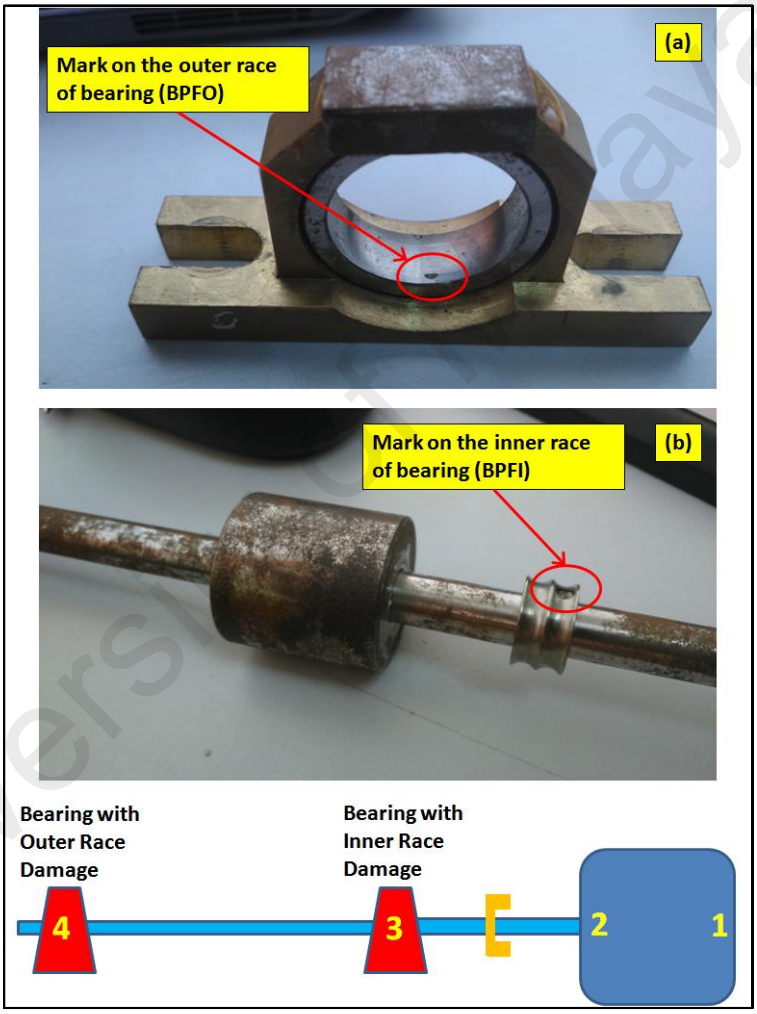

Figure 3.7: Bearing fault testing with (a) Outer race damage (b) Inner race damage

3.3.1.5 Testing of Gear Fault Detection

Same as bearing fault detection, relative phase data is not necessary while performing conventional gear fault detection which was identified by capturing the impact cause by the defect bearing and defect gear. However, for the purpose to further investigate the application of the simplified ODS technique, both vibration and relative phase data were used in this testing.

Testing of gear fault detection focused on a common spur type gear. Two pinions on a same shaft were used with one pinion in good condition and the other one was the damaged pinion. One gear which is on a different shaft is used to be shifted either on the good pinion gear or damage pinion gear. When gear is in contact with the pinion gear, a gear mesh frequency (GMF) component is generated. This GMF component is represented in the frequency domain vibration spectrum with the unit of Hz. Figure 3.8(a) and Figure 3.8(b) show the arrangement for the gear fault testing.

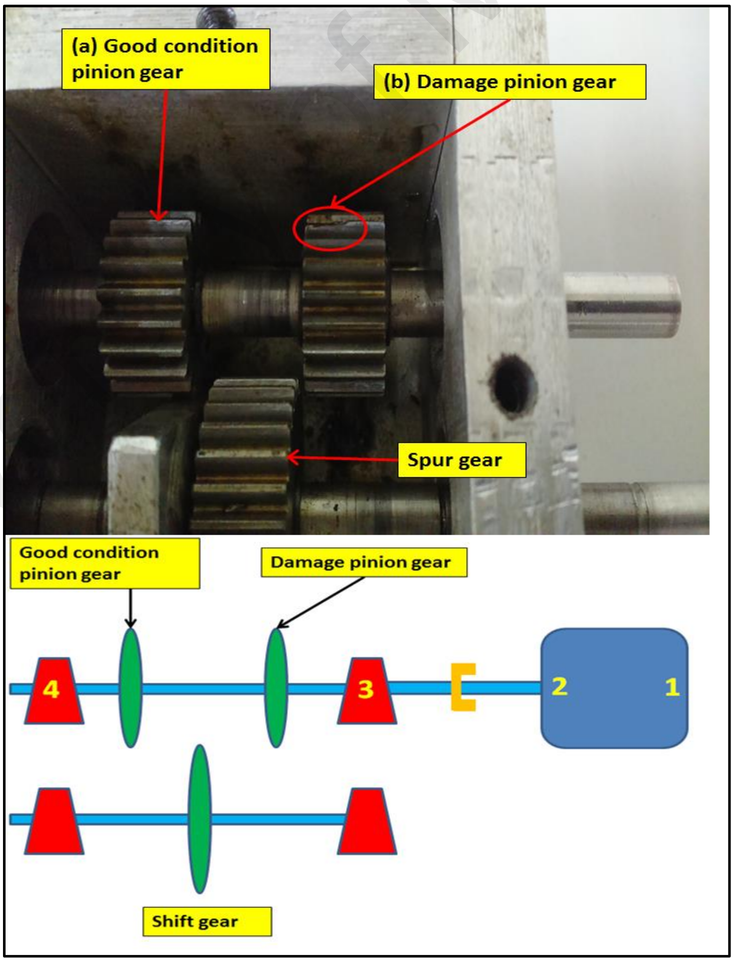

Figure 3.8: Gear fault testing with (a) Good condition pinion (b) Damaged pinion

3.3.2 Application on Industrial Machinery

The simplified ODS technique was then applied on industrial rotating equipment to show the effectiveness of this technique in the implementation in current CBM practice. There were four different types of machine which are suitable in demonstrating the machinery fault such as static imbalance, dynamic imbalance, parallel misalignment and angular misalignment. These machines in petrochemical plant located in east coast of Peninsular Malaysia are vertical centrifugal pump, horizontal centrifugal pump, horizontal centrifugal blower and belt driven centrifugal blower.

3.3.2.1 Industrial Example - Rotor Imbalance Problem

Figure 3.9 shows a vertical centrifugal pump. The pump only consists of one bearing which is represented by point 3. While measurement point 4 is located on the pump base. The pump is used to transport petrochemical substance. High vibration was detected after maintenance job on the pump was completed. It is crucial to perform the machinery fault detection without shutting down the machine. The result of detecting the static imbalance problem using the simplified ODS technique will further show the effectiveness of this technique.

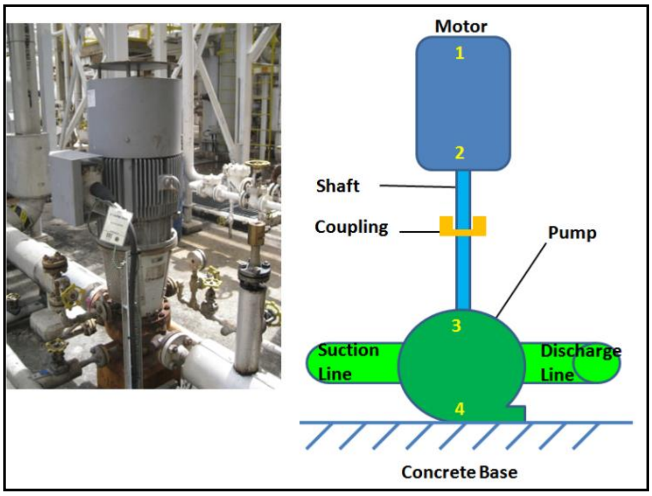

Figure 3.9: Vertical centrifugal pump having static imbalance problem

Figure 3.10 shows a horizontal centrifugal pump. The measurement point for this type of pump is similar as the laboratory rotor kit setup which consists of 4 measurement points. These 4 measurement points were identified at the closest point to the bearing location. The pump is used as a cooler water pump to transport the water to a cooling tower. It is crucial to perform the machinery fault detection without shutting down the machine. The result of detecting the dynamic imbalance problem using the simplified ODS technique will further show the effectiveness of this technique.

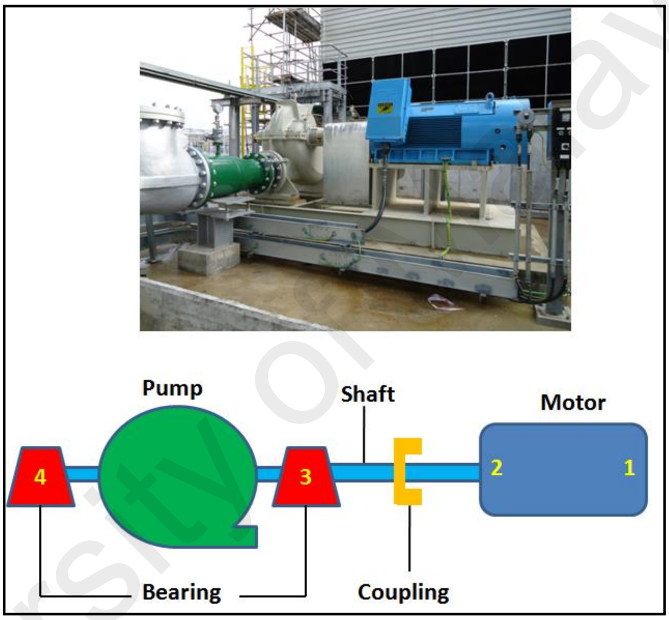

Figure 3.10: Horizontal centrifugal pump having dynamic imbalance problem

3.3.2.2 Industrial Example - Misalignment Problem

Figure 3.11 shows an ID fan. The measurement point for this type of fan is similar as the laboratory rotor kit setup which consists of 4 measurement points. These 4 measurement points were identified as the closest to the bearing location. This ID fan is used to evacuate flue gas from the furnace to atmosphere. It is crucial to perform the machinery fault detection without shutting down the machine. The result of detecting the parallel misalignment problem using the simplified ODS technique will further show the effectiveness of this technique.

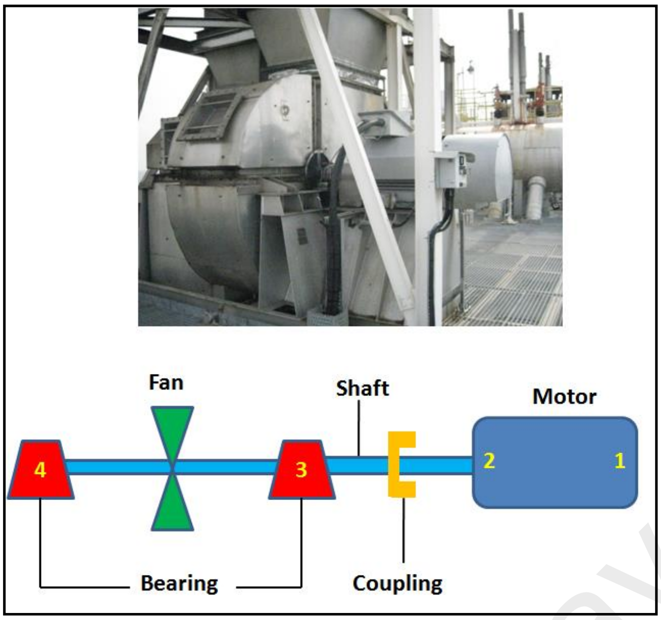

Figure 3.11: Induced draft (ID) fan having parallel misalignment problem

Figure 3.12 shows a horizontal belt driven blower. The arrangement for 4 points of measurement for this type of blower is different from the previous machine. 2 points were identified on the blower bearing and another 2 points on the motor. The 2 bearings of the blower are located on top of motor. Both the motor and the blower shaft are placed inside a cover for safety reason. To perform the vibration and relative phase data acquisition the cover has to be temporarily removed. High vibration was detected after maintenance job on the blower was completed. It is crucial to perform the machinery fault detection without shutting down the machine. The result of detecting the angular misalignment problem using the simplified ODS technique will further show the effectiveness of this technique.

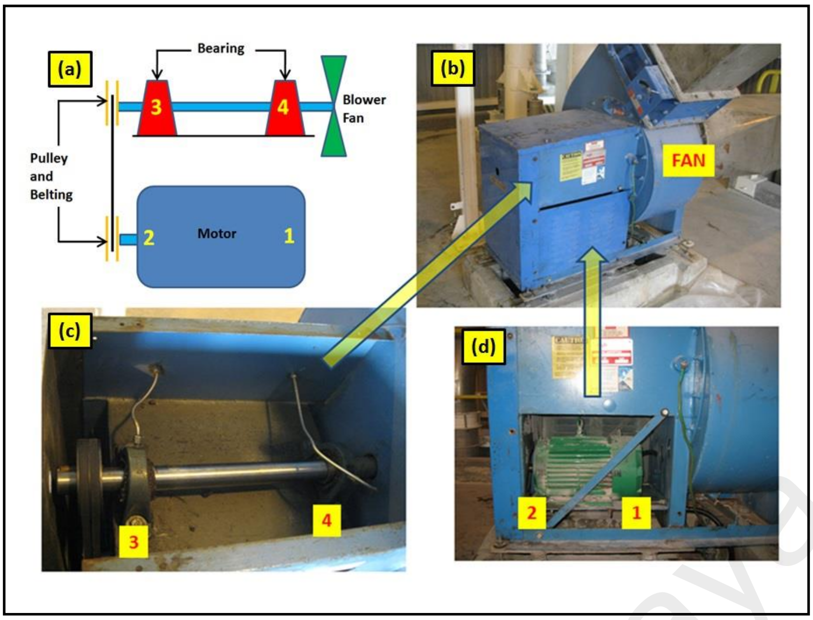

Figure 3.12: Horizontal belt driven blower having angular misalignment problem

3.4 Reciprocating Machinery Setup

The testing for reciprocating machinery was conducted on an air compressor in the lab. Using the simplified ODS technique the rotating motion of both the motor and air compressor can be visualised. Furthermore, the reciprocating motion was also able to be visualised. Based from this outcome, the next test was conducted on bio-fuel powered diesel engine to assess the vibration affected by the bio-fuel combustion. An advanced vibration analysis was also conducted to justify the effect on vibration was purely coming from the bio-fuel combustion.

3.4.1 Air Compressor

The reciprocating air compressor is operating at difference pressure of 1 bar, 2 bar, 3 bar and 4 bar. The motor shaft is running at 49Hz (2940rpm) meanwhile the crankshaft is running at 13.5Hz (810rpm). Vibration data was acquired to form the 8-point compressor ODS with 8 measurement points as shown in Figure 3.13. Points 1-4 were used to generate ODS to visualise the reciprocating motion of the piston. Points 5-8 were used to generate ODS to visualise the rotary motion of the crankshaft and motor shaft. Point 9-16 were used to generate a cubic ODS to visualise base plate motion. Points 9-12 were attached to the compressor whereas points 13-16 were attached on the base of compressor. Points 17-24 were also used to generate a cubic ODS to visualise base plate motion. Points 17-20 were attached to the motor meanwhile points 21-24 were attached on the base of motor.

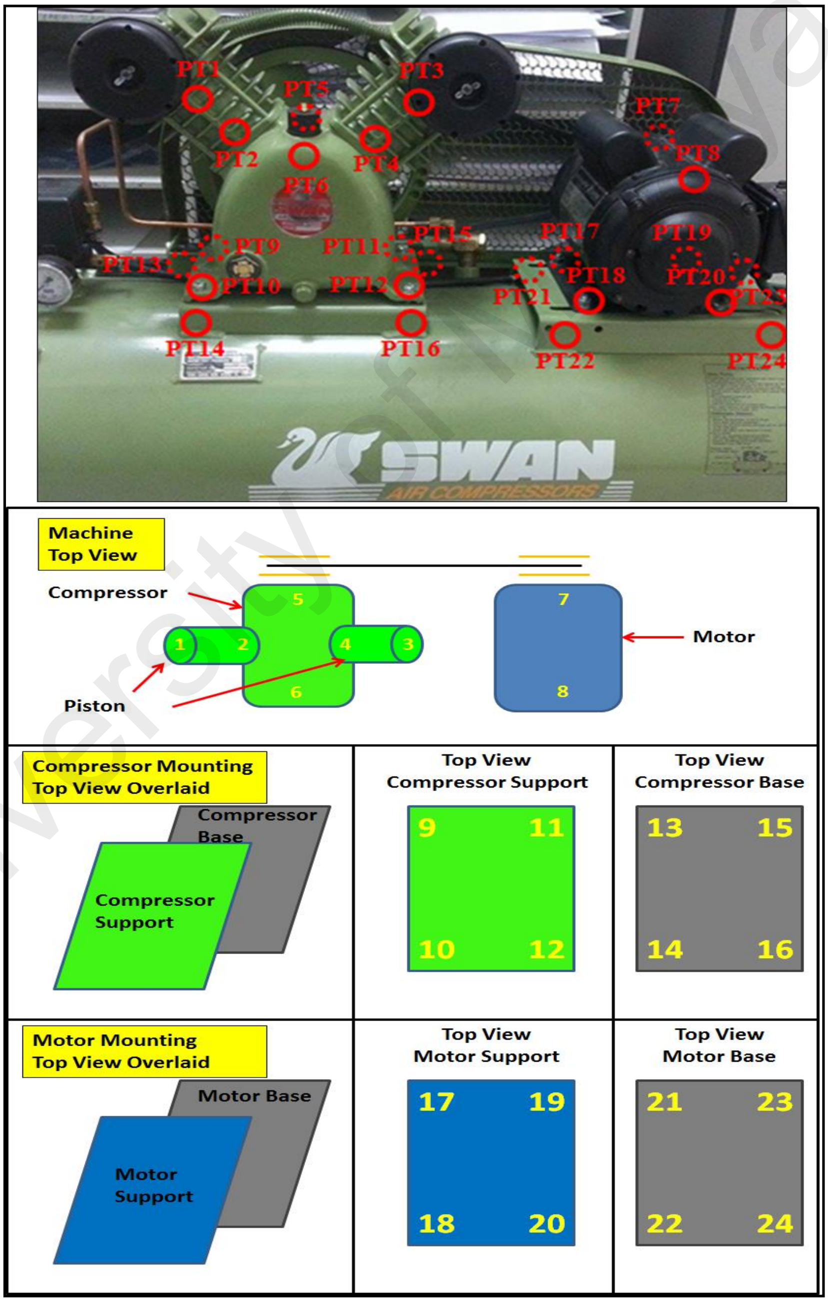

Figure 3.13: Measurement points on air compressor testing

3.4.2 Bio-Fuel Powered Diesel Engine

There are total of 12 measurement points for the bio-fuel diesel engine testing as shown in Figure 3.14. Four measurement points were identified on the top part of the engine body. Points 1 and 2 show the motion of the crankshaft, while Points 3 and 4 show the motion of the cylinder. Points 5 to 8 represents the engine support above the rubber mounting. Another four measurement points (Points 9 to 12) were identified on the engine base-plate, located at the bottom of the rubber mounting to observe any motion triggered by the rubber mounting. The accelerometer was mounted on Point 6 as the reference for relative phase data. The tri-axial accelerometer was used to capture vibration signals for all measurement points.

Acquisition of vibration data was repeated five times for every bio-fuel blend at two engine speeds to reduce measurement error and ensure reproducibility of the acquired data. Measurement errors caused by any unaccounted external vibration components were minimised using the RMS value rather than the peak value of the overall vibration. The effect of the sudden increase of vibration peak value due to these unaccounted vibrations could affect the validity of the results if the peak value of the overall vibration is being utilised. The effect of random noises in the vibration signal was further reduced by performing block averaging, i.e., 10 averages were performed at each measurement point in the axial, horizontal, and vertical directions. The averaging technique was successfully applied and discussed in a previous work (Mohd Mishani et al., 2015). The block averaging technique allowed for a more accurate representation of overall vibration in terms of RMS value, as the random noises were diminished over averages considering that the overall vibration signal was mainly from the engine. This approach also resulted in clearer vibration signals for both time-domain and frequency-domain analyses. Thus, the use of RMS in overall vibration and block averaging technique in vibration measurement could reduce or eliminate any errors during data acquisition. The aforementioned procedures could serve as the criteria to ensure the reproducibility of vibration data obtained.

The engine was tested at two running speeds using pure diesel (B0) and six fuel blends (i.e., B5, B10, B15, B20, B25, and B30). Vibration signals were captured for each fuel blend and compared with the engine vibration powered with pure diesel. A total 14 vibration data sets were recorded, i.e., 7 fuel blends × 2 engine speeds. Analysis of vibration data was performed statistically to study the performance of the bio-fuel and its blends. Vibration value and phase data were also analysed and compared for both time and frequency domains. The motion of the crankshaft, cylinder, engine base-plate, and support was processed and visualised through ODS analysis using DASYLab® software

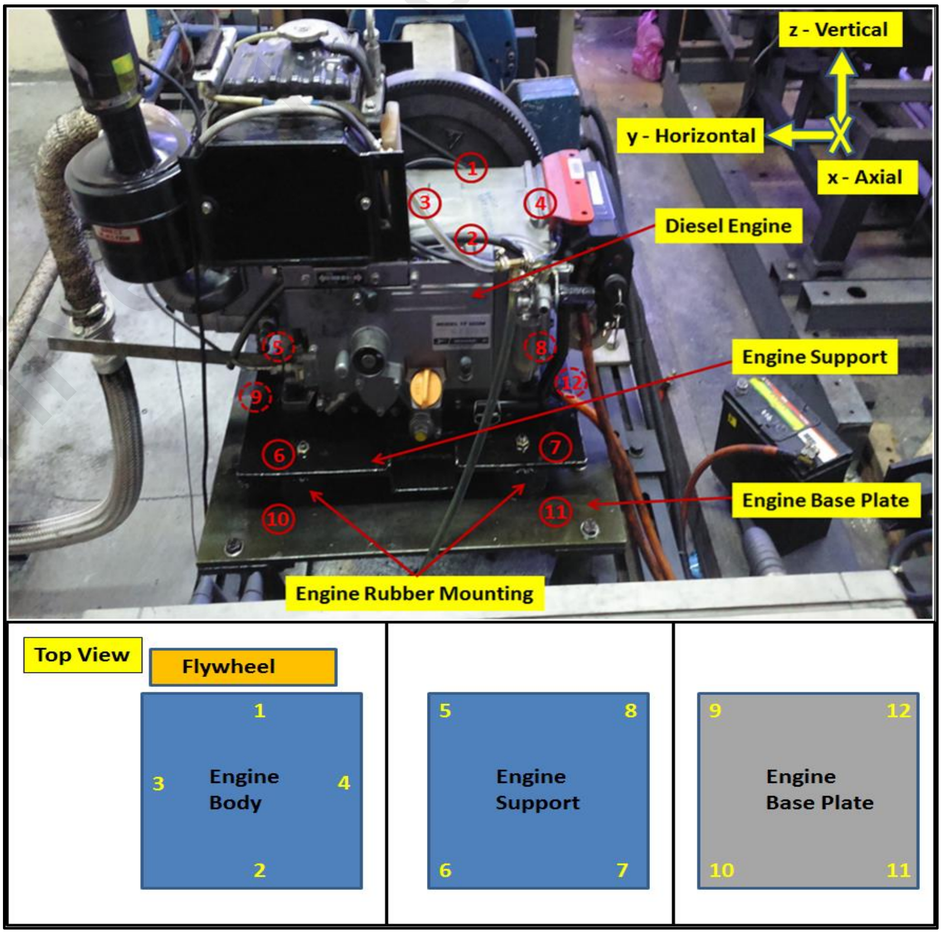

Figure 3.14: Measurement points on bio-fuel powered diesel engine testing

3.4.2.1 Bio-Fuel

Bio-fuel used in this research was produced from CI according to ASTM D6751 and EN 14214 standards. The production method used by Ong et al. was repeated to produce the CI bio-fuel. The bio-fuel was mixed with diesel before it was pumped to the diesel engine. In this research, six fuel blends were prepared according to ASTM D7467 standards (Hwai Chyuan Ong et al., 2014). These blends were B5, B10, B15, B20, B25, and B30. The numbers represented the percentage of bio-fuel for each fuel blend. Each fuel blend was tested at 1,500 rpm and 2,400 rpm. Vibration data were compared with those on the baseline pure diesel, B0. Table 3.1 shows the properties of the fuels.

Table 3.1: Properties of the Calophyllum Inophyllum bio-fuel(Ong et al., 2014)

Properties	Unit	ASTM D6751	B0 Diesel	B100 CI Bio-fuel	B20 Bio-fuel Blend
Density at 15ºC	kg/m^3	860-900	840.0	869.0	851.6
Cetane number	-	47 min	49.7	57.0	53.7
Viscosityat 40ºC	mm^2/s	1.9-6.0	2.95	4.00	3.22
Flash point	ºC	130 min	70.5	140.0	79.5
Cloud point	ºC	-3 to 12	-2.0	13.2	0
Calorific value	kJ/kg	-	45,825	41,397	41,523
Water content	wt%	0.03 max	0.0030	0.0050	0.0059
Acid value	mg KOH/g	0.8 max	0.051	1.620	0.180

3.4.2.2 Diesel Engine

For this testing, a single cylinder diesel engine manufactured by Yanmar (TF120M) was used. The single-cylinder engine is more preferable for testing the effectiveness of the proposed method, as the total vibration is merely contributed by single-reciprocating motion and is not as complex as the multi-cylinder engine in vibration signature. Furthermore, a single-cylinder engine can save more fuel as compared with multi-cylinder engines. Table 3.2 shows the technical specifications of the engine during conducting the experiments. The diesel engine was connected to a dynamometer to control the engine speed. The engine speed was set at two speeds, 1,500 rpm and 2,400 rpm. The engine was initially set at maximum speed. Dynamometer was used to achieve the desired engine speed. The engine speed of 1,500 rpm was the lowest speed that can be achieved. A high torque (brake force) was applied by the dynamometer to maintain engine speed at 1,500 rpm. A low brake force was required to maintain the engine speed at 2,400 rpm, thus achieving minimal torque. Torque is one of the external vibration sources that could contribute to the overall vibration of the engine. Therefore, these two speeds, i.e., maximum and minimum torque, were both used to investigate the effect of torque as the external factor in overall engine vibration. The causes of the external vibration source, such as torque, should be eliminated before determining the optimum bio-fuel blend in engine vibration, which is directly related to combustion.

Table 3.2: Technical specifications of a single cylinder Yanmar TF120M diesel engine

Brand	: Yanmar
Model	: TF 120M
Type	: Horizontal single-cylinder 4-stroke diesel engine
Compression ratio	: 17.7:1
Continuous rating output	: 10.5 HP / 2400 rpm
Maximum rating output	: 12.0 HP / 2400 rpm
Maximum power	: 7.7kW
Maximum engine speed	: 2400 rpm
Number of cylinders	: 1
Bore x stroke	: 92 x 96 mm
Displacement	: 0.638L
Combustion	: Direct injection
Injection timing	: 17.0 bTDC
Injection pressure	: 200 kg/cm^2
Cooling system	: Water-radiator
Fuel tank capacity	: 11 litre

CHAPTER 4: RESULTS AND DISCUSSIONS

4.0 Overview

Chapter 4 is divided into 3 main sections. Section 4.1 covers the development of the Simplified ODS Technique using DASYLab® Software which discussed the data acquisition and analysis procedures. Section 4.2 covers ODS analysis on rotating machinery vibration assessment. The application of this technique on rotating machinery is to identify machinery fault easily, within shorter time and more accurate. Section 4.3 covers ODS analysis on reciprocating machinery vibration assessment. The technique was first tested on laboratory air compressor to determine the effectiveness in visualising reciprocating motion. The technique was then used to assess bio-fuel powered diesel engine in determination of the optimum bio-fuel blend based on the engine vibration parameter. Furthermore, an advanced vibration analysis which covers time domain and frequency domain analysis were performed to justify the effect of bio-fuel combustion on engine vibration.

4.1 Development of Simplified ODS Technique using DASYLab® Software

The developed technique is linked to Microsoft Excel. All the measurement points and machines are set-up in the Microsoft Excel before it is imported to the DASYLab® software and displayed in the acquisition setup layout as shown in Figure 4.1. A total of 96 buttons are available to show all the measurement points that were set-up. Considering a common machine configuration with 4 measurement points, the acquisition setup layout covers up to 24 machines per day which is more than conventional vibration assessment covered for a day. The Block Size, Sampling Frequency (SFreq), Vector, Averaging and Date Column are set before data acquisition started. The Block Size determines the number of values that will be computed by the worksheet modules during a single processing cycle. The concept of computing the data in blocks increases the speed of the measuring process considerably; on the other hand, it strongly influences the real-time performance of the system. The sampling frequency specifies the rate of data transmitted by the DASYLab®. For example, if Block Size is 500 and Sampling Frequency is 1000, DASYLab® outputs a block for every 0.5 seconds. The vector specifies the direction of the measurement point. For a measurement point with opposite direction, the vector will be changed to negative sign. The averaging is used for a more accurate representation of overall vibration in terms of RMS value. Date column is set to avoid data overlapping with the previous saved data. It also allows the user to review the saved machine data and analyse the historical machine trending data based on different date columns.

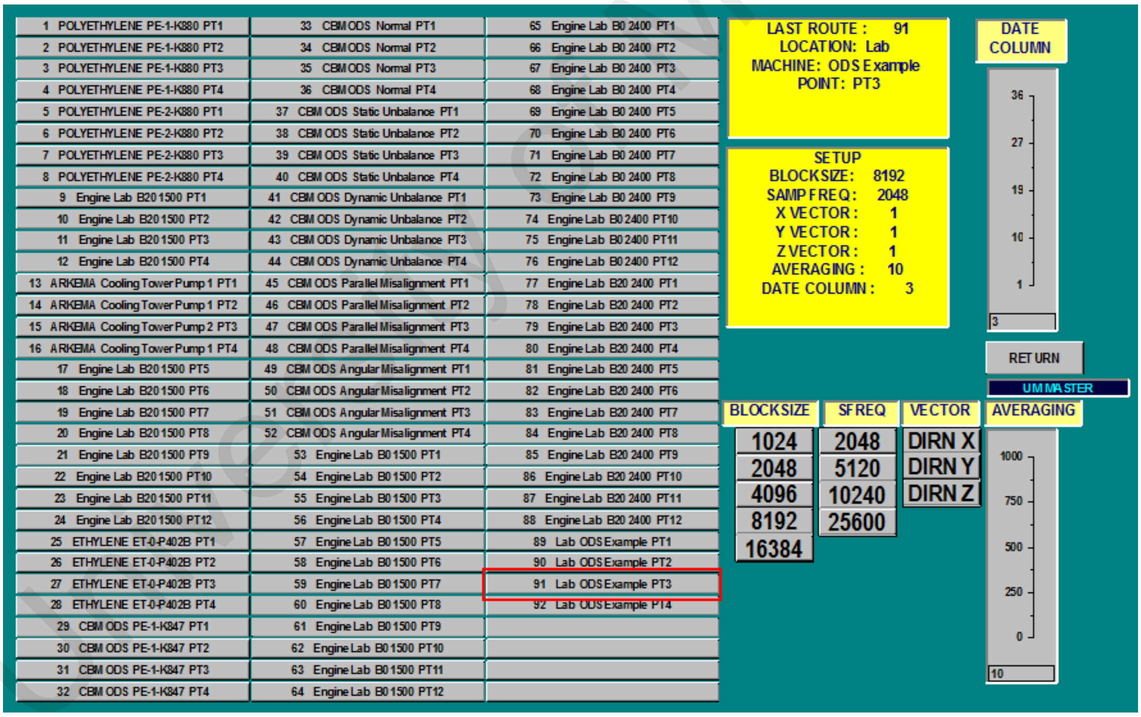

Figure 4.1: Layout of Acquisition Setup

During data acquisition process, user is presented with the Acquisition Spectra layout as shown in Figure 4.2. The layout consists of vibration spectra, time trace, and RMS tracking. Three vibration spectra at the top of the layout show the maximum frequency to screen if any higher frequency vibration components are recorded. Higher frequency vibration indicates a bearing or gear problem, while other machinery faults can be indicated from lower frequency vibration components. Conventionally, the spectra are zoomed-in to lower frequency as shown by three spectra at the bottom of layout to analyse the pattern for any machinery fault. The RMS tracking shows the trend of overall RMS value while the time trace is showing the signal from time domain.

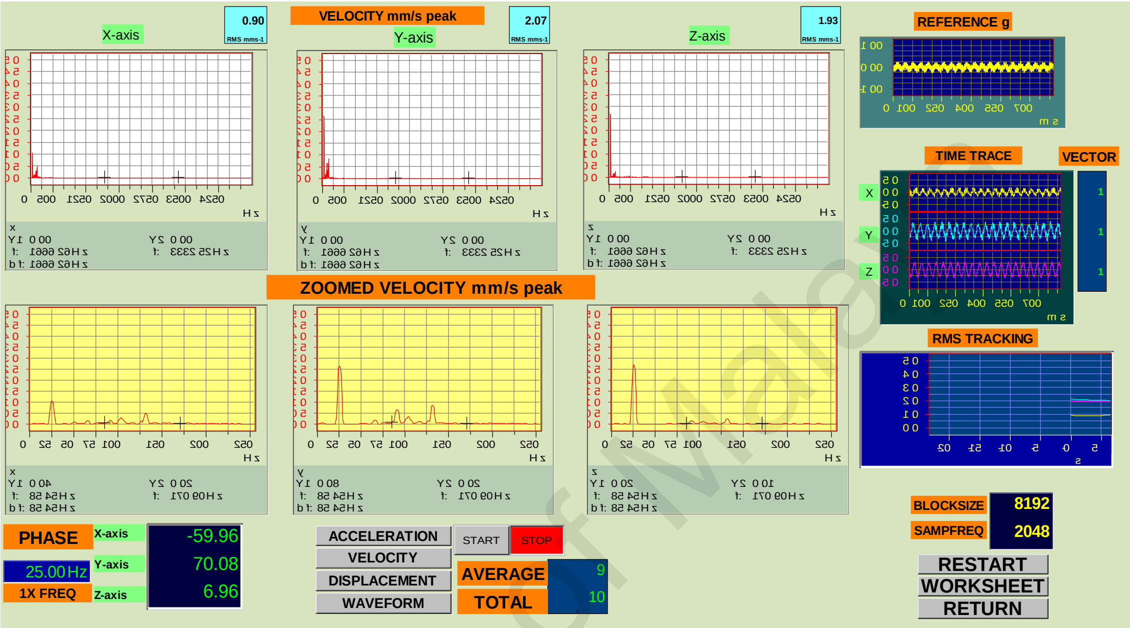

Figure 4.2: Layout of Acquisition Spectra

The layout of Analysis Setup is similar with the Acquisition Setup shown in Figure 4.3. However, all four measurement points are selected to show the overlaid vibration spectra in single display and analysed them concurrently. Error message will be shown if different machine measurement points are selected and the selection needs to be repeated. The column on the right shows the date of the acquired data.

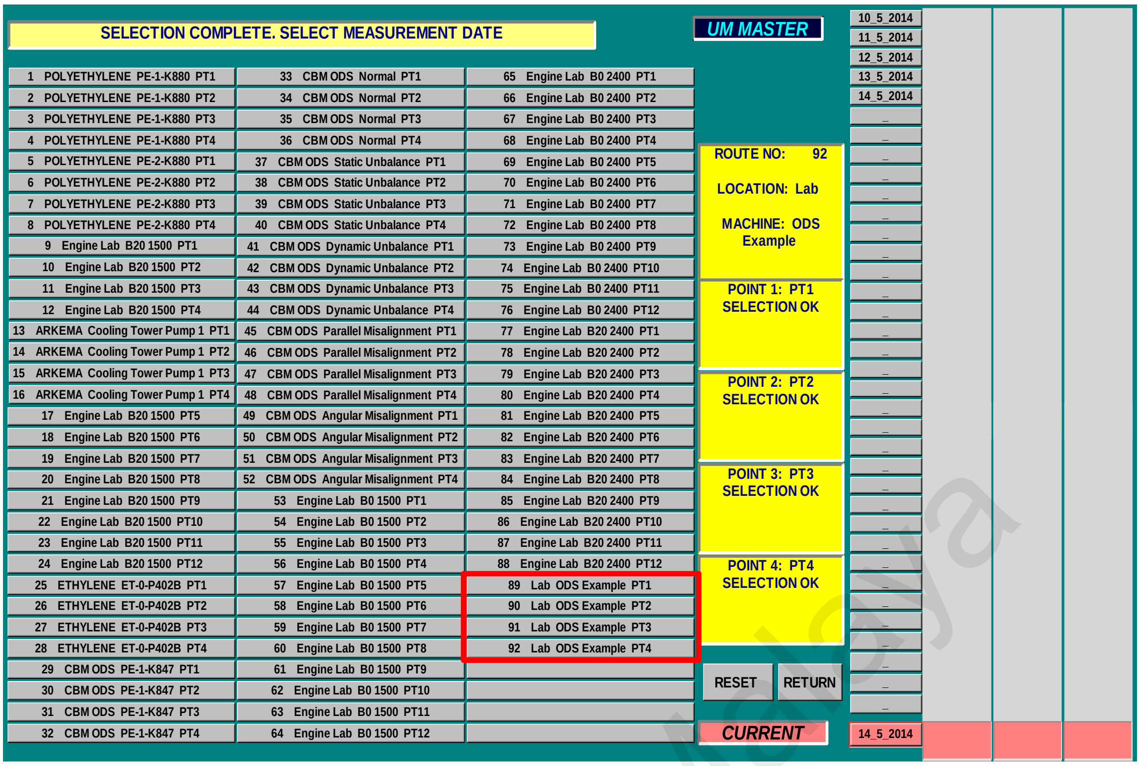

Figure 4.3: Layout of Analysis Setup

The Frequency Domain Analysis layout shows the overlaid vibration spectra in single plot. The DASYLab® read all the 24 data, i.e. amplitude and phase data of 4 measurement points in 3 principal directions from the saved global variables and displays them as shown in Figure 4.4. A separate vibration spectrum can be observed by selecting the separate button. The values of amplitude and phase are tabulated on the right of the layout. A specific frequency component from the spectra is selected to analyse the data through the simplified ODS analysis.

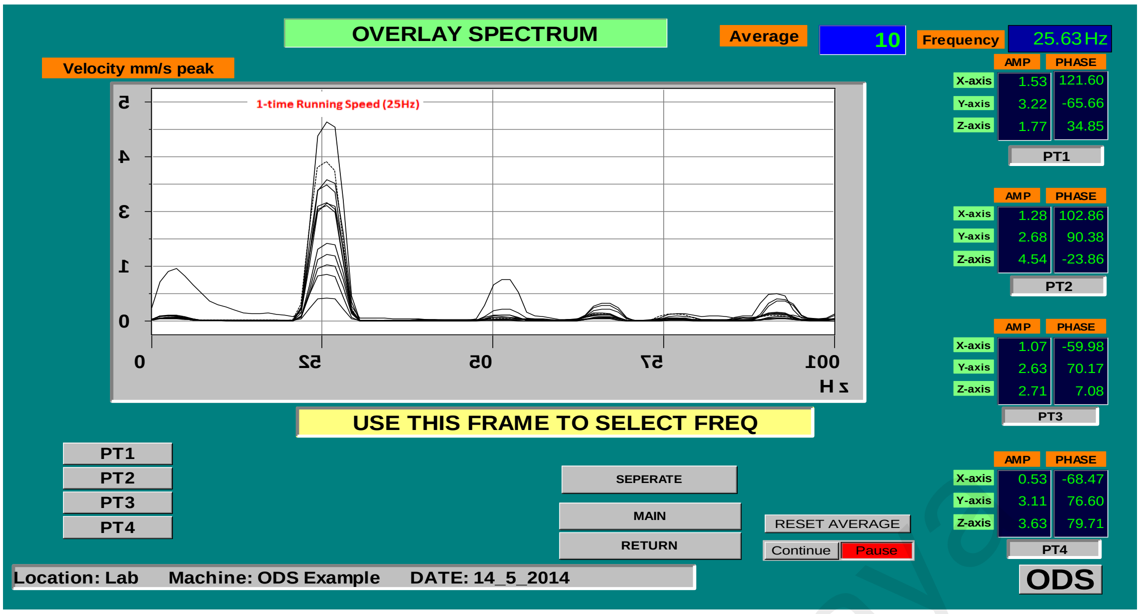

Figure 4.4: Layout of Frequency Domain Analysis

The saved data is read and run using a generator. The data is integrated through a sinusoidal signal to generate the harmonic motion of the simplified ODS as shown in Figure 4.5. The arrow shows the motion of the ODS. The indication of an in-phase relation is shown when two measurement points is moving in same direction, while the out-of-phase relation is shown when two measurement points is moving in opposite direction. The top view shows the motion from horizontal and axial direction. The motion from vertical and axial direction can be observed from the side view while the axial view shows the motion from vertical and horizontal direction. The velocity table shows the vibration amplitude in the unit of mm/s, while the phase table shows the position of the measurement point relative to the reference point in degrees.

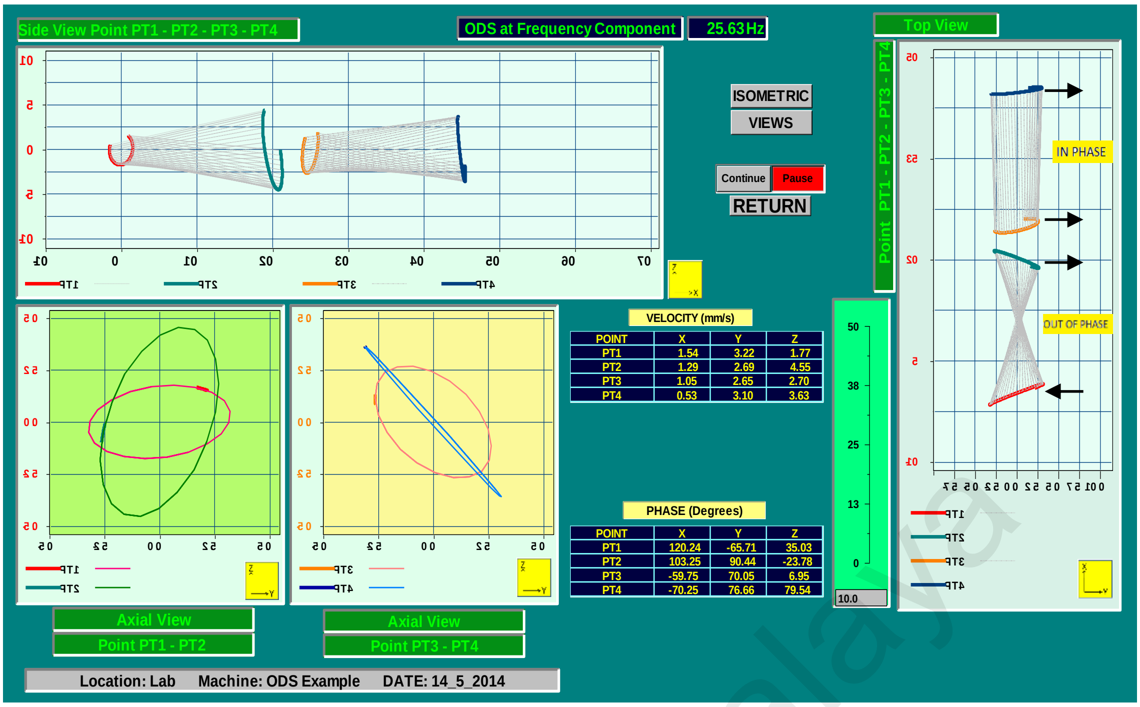

Figure 4.5: Layout of Simplified ODS Analysis

4.2 Vibration Assessment on Rotating Machinery

This section covers the application of ODS analysis on rotating machinery vibration assessment (fault diagnostic). The technique was tested in the laboratory before it was applied on industrial machinery to justify the effectiveness of this technique. In laboratory condition, machinery faults such as rotor imbalance, misalignment, support looseness, bearing fault and gear fault were effectively identified using the simplified ODS technique. Based on the previous research, rotor imbalance and misalignment were identified as primary machinery fault. The application of the simplified ODS technique on industrial machineries is able to identify both rotor imbalance and misalignment easier, within shorter time and more accurate compared to conventional machinery fault diagnostic technique.

4.2.1 Vibration Assessment of Laboratory Simulation Rig

Conventionally, CBM personnel using single axis accelerometer to acquire vibration data. More time is needed to acquire vibration data of 12 measurement points on a machine because of the usage of single axis accelerometer, while the usage of absolute phase using tachometer only needed on problematic machines with high vibration. Furthermore, the usage of absolute phase using tachometer requires the machine to be shut down. This practice also consumes longer time in machinery diagnostic as the user needs to screen through the entire measured vibration spectra one by one.

To improve this, a simplified ODS technique as shown in Figure 4.5 is proposed where tri-axis accelerometer, relative phase technique and visualisation of machine motion are integrated into current machinery fault diagnostic technique. At this stage, the performance of the proposed technique shows a more effective method where all the vibration and phase data of 12 measurement points on a machine can be presented concurrently as shown in Figure 4.4. Furthermore, vibration and phase data were acquired concurrently and reduced time spent for data acquisition.

The laboratory rotor kit was set to run at 25.5Hz (1530rpm). A normal vibration data was acquired by the simplified ODS as the baseline at all four measurement points. As a result, each set of measurement consisted of twelve spectra for all four measurement points in three different directions (axial, horizontal, and vertical). Figure 4.6 shows the vibration spectra of normal condition which is overlaid in single display. The animation of simplified ODS result for normal condition is shown in Figure 4.7 where the arrow points the direction of the movement. The simplified ODS was performed for every simulated fault conditions. The ODS for imbalance and misalignment only depends on the 1-time and 2-time running speed component (Hariharan & Srinivasan, 2011; Xu &

Marangoni, 1994). Therefore, other frequency components beside 1-time and 2-time running speed component will not be discussed further in this research.

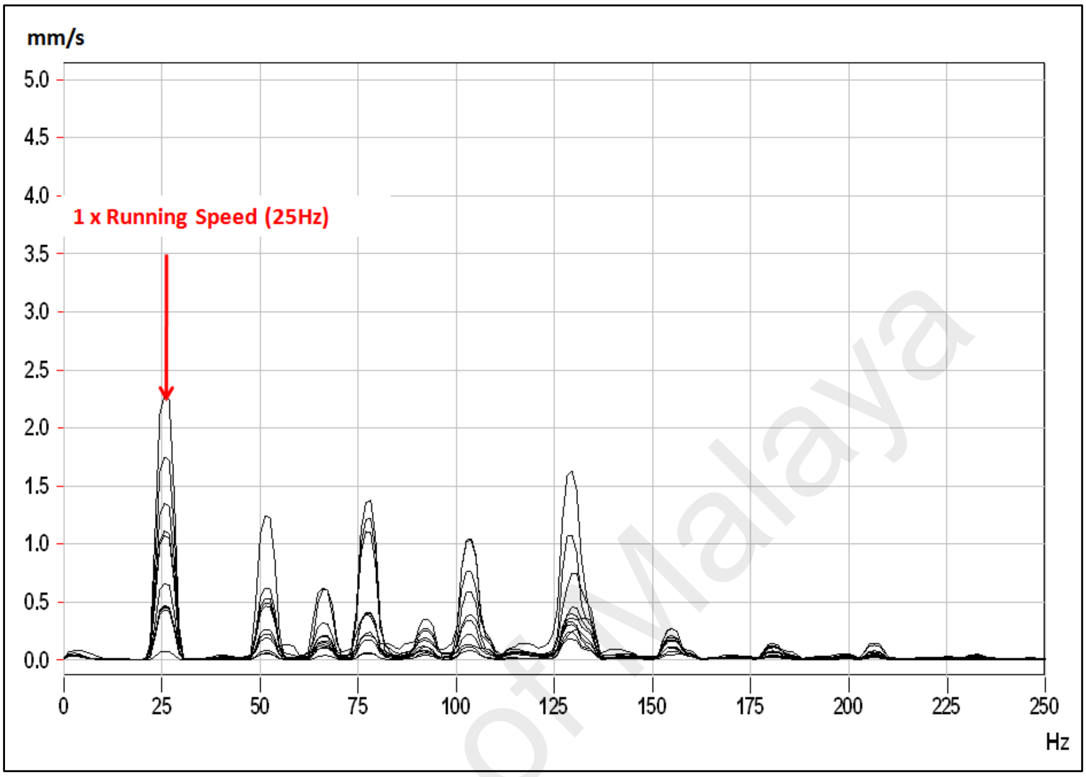

Figure 4.6: Normal Condition Spectra

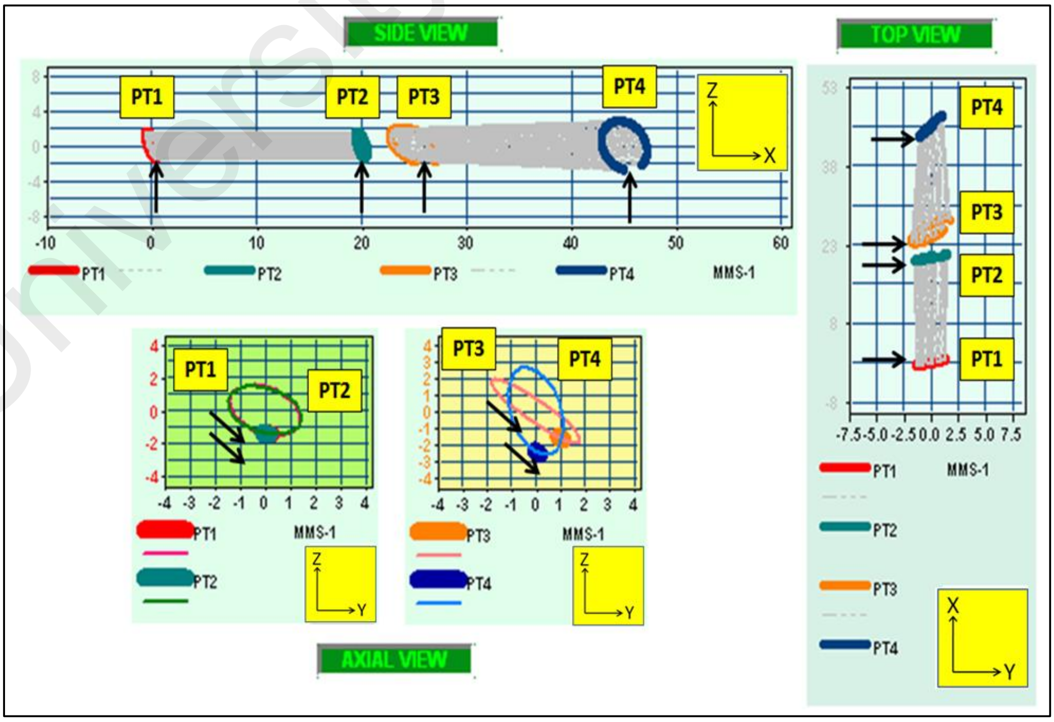

Figure 4.7: Normal Condition ODS

4.2.1.1 Vibration Assessment of Rotor Imbalance

The next testing was performed on the laboratory rotor kit to detect rotor imbalance. Figure 4.8 shows two examples of imbalance which are static imbalance and dynamic imbalance respectively. Conventionally, imbalance problem was characterised by dominant 1-time running speed component due to its high rotational force (Xu & Marangoni, 1994). However, it is difficult to differentiate static and dynamic imbalance based on vibration spectra only without the phase data. Conventional method requires the personnel to identify the problematic machines prior to measure the phase data for further analysis of the type of imbalance. With the proposed simplified ODS, the motion of static and dynamic imbalance can be visualised and differentiated by putting the cursor on 1-time running speed component. The simplified ODS as shown in Figure 4.9 enables personnel to visualise the motion of the machine. Figure 4.9(a) shows point 3 and point 4, i.e. points of driven load are moving in same direction which is in phase. This measurement is categorised as static imbalance. Meanwhile, Figure 4.9(b) shows point 3 and point 4 are moving in different direction which is out of phase. This is known as dynamic imbalance.

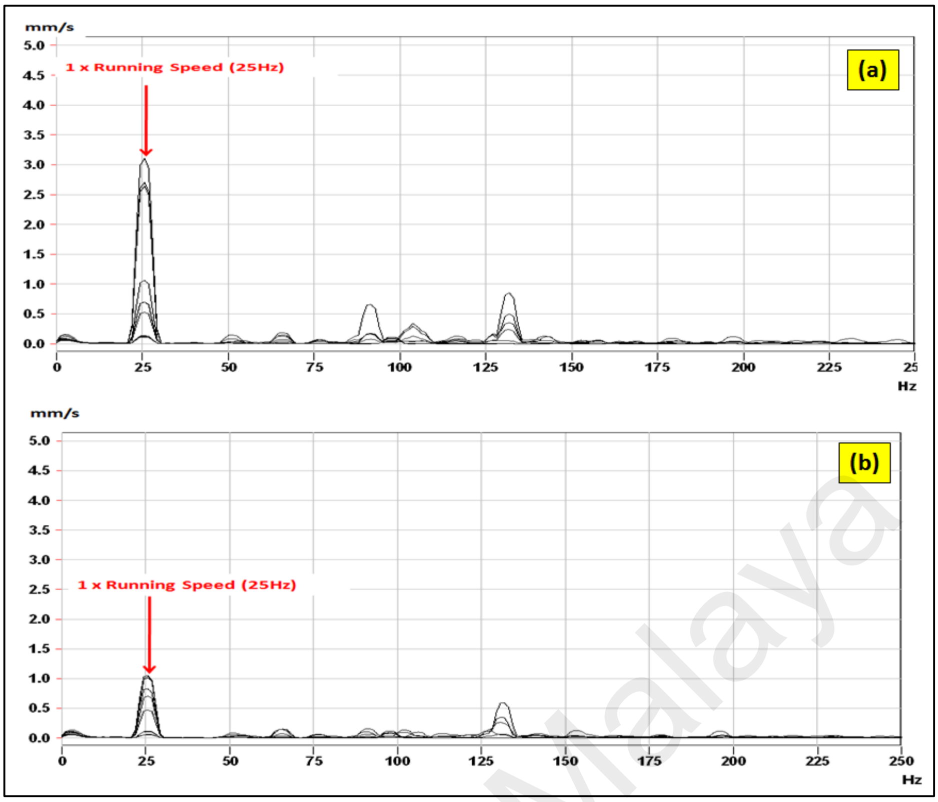

Figure 4.8: Vibration spectra of (a) Static imbalance (b) Dynamic imbalance

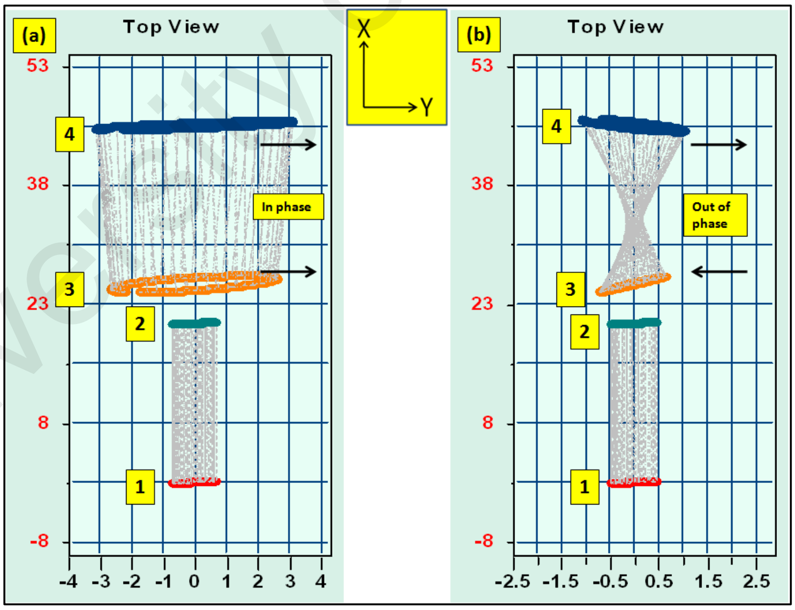

Figure 4.9: ODS of (a) Static imbalance (b) Dynamic imbalance

4.2.1.2 Vibration Assessment of Misalignment

In practice, there are two different type of misalignment faults, i.e. parallel and angular misalignment. Figure 4.10 shows the spectra obtained through conventional method consist of multiple harmonic of 1-time running speed component when the misalignment fault was simulated. Most of the time, multiple harmonic was associated with looseness problem where in this case it may lead to the wrong diagnosis. Similar to the previous case i.e. static and dynamic imbalance, spectrum data as shown in Figure 4.10(a) and 4.10(b) is not sufficient to identify and differentiate between parallel and angular misalignment. Furthermore, multiple harmonic appears in the spectrum may mislead to wrong diagnosis to indicate it as looseness problem. The competence of simplified ODS is examined in this case. The ODS for parallel and angular misalignment can be visualised by using magnitude and phase data at 2-time running speed component (Hariharan & Srinivasan, 2011). The result of simplified ODS is shown in Figure 4.11. Personnel can easily identify and differentiate the misalignment problem by visualising the motion of the machine. Figure 4.11(a) shows point 2 and point 3, i.e. points across flexible coupling are moving in different direction which is horizontally out of phase. This indicates the parallel misalignment problem. Meanwhile, Figure 4.11(b) shows point 2 and point 3 are moving in different direction which is axially out of phase. This is an indication of angular misalignment problem. The output results from all the laboratory condition testing shows that the vibration data acquisition using a tri-axis accelerometer is more efficient and time saving. Furthermore, relative phase of the two accelerometers and visualisation of the machine motion is more accurate, save more time and easier for analysing machine condition as compared to the conventional CBM assessment practice.

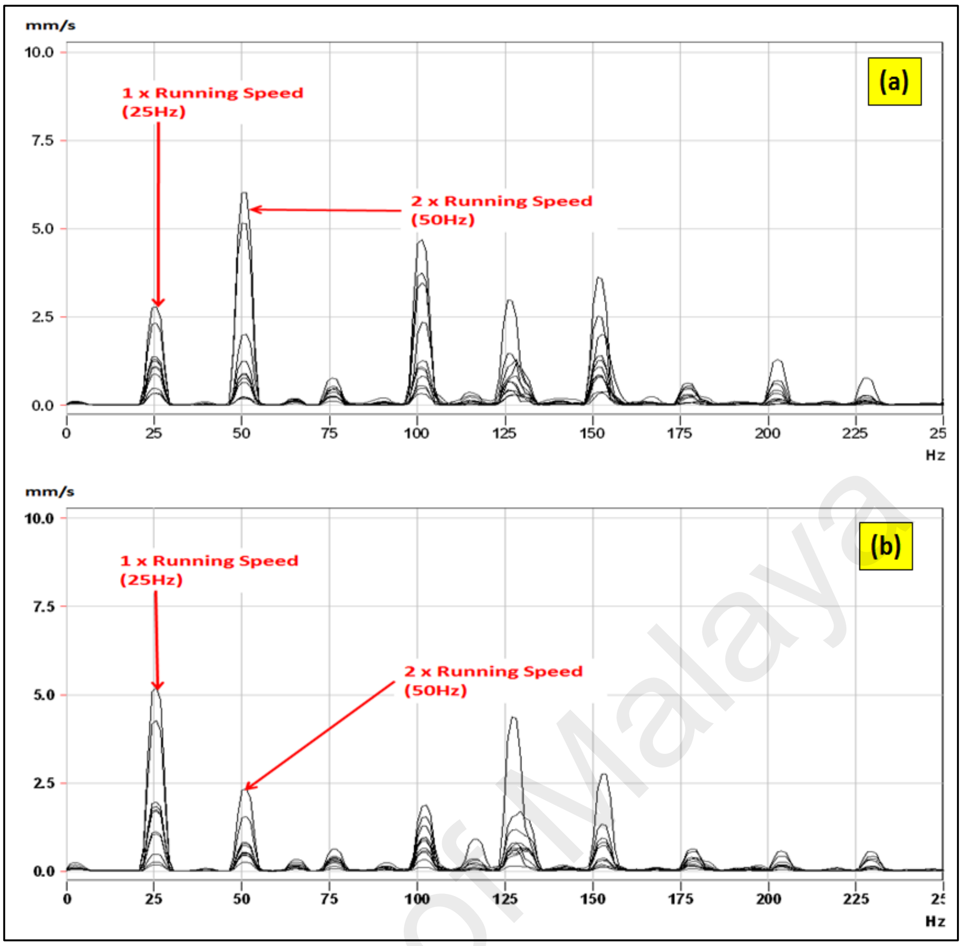

Figure 4.10: Vibration spectra of (a) Parallel misalignment (b) Angular misalignment

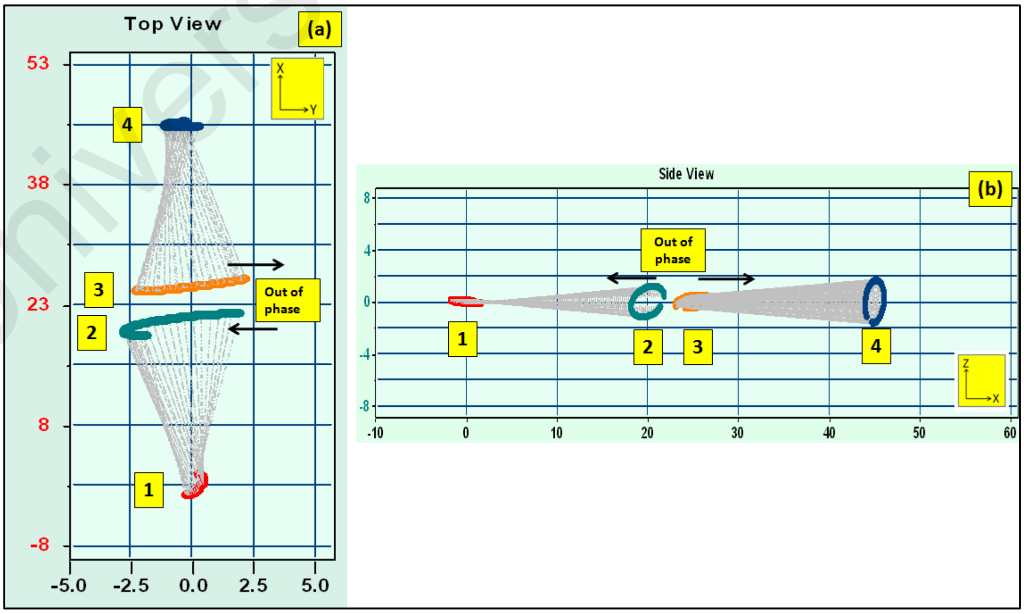

Figure 4.11: ODS of (a) Parallel misalignment (b) Angular misalignment

4.2.1.3 Vibration Assessment of Support Looseness

The laboratory motor is operating at 37Hz (2220rpm). Vibration and relative phase data is acquired to form the simplified ODS motion with 8 measurement points represents in cubic shape.

Figure 4.12(a) shows the overlaid spectrum of normal condition. The spectra are overlaid in single plot for each axis so that the specific frequency can be selected easily. The spectra show peaks at 37Hz, i.e., 1-time running speed and 74Hz, i.e., 2-time running speed. For the loose condition, the bolting of measurement point 4 was loosened. Figure 4.12(b) shows the overlaid spectra of loose condition. The peaks at 37Hz, i.e., 1-time running speed and 74Hz, i.e., 2-time running speed are same as normal condition. However, the spectra also show peaks at low frequency for loose condition.

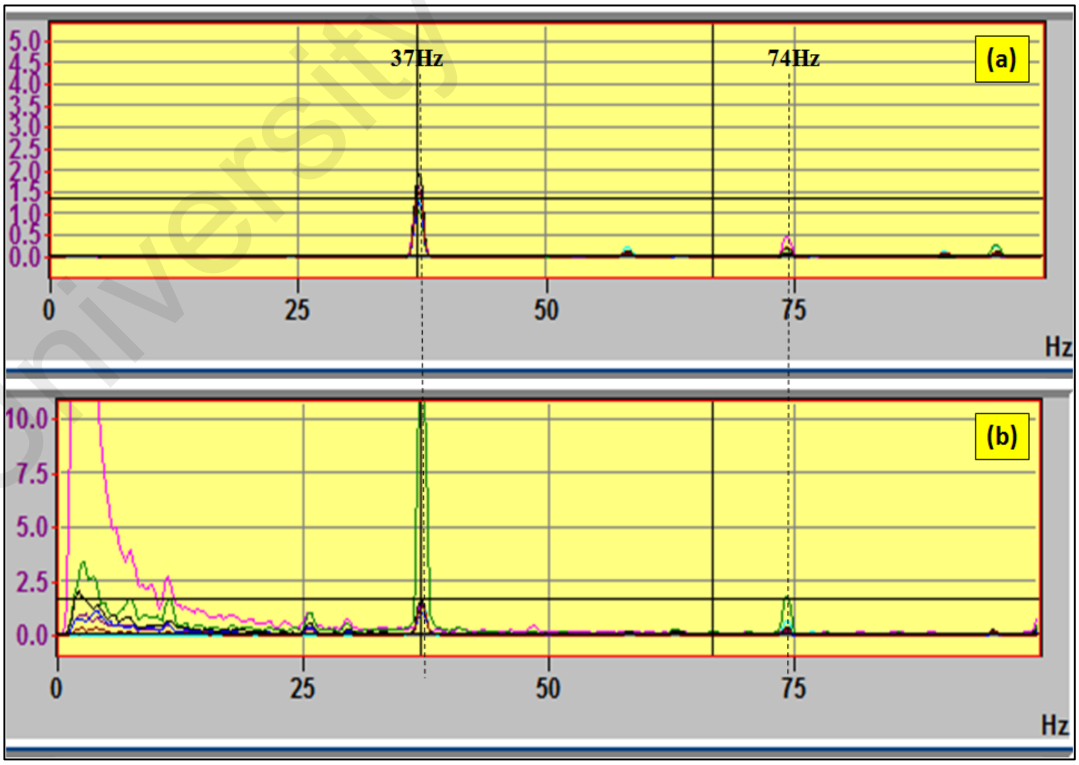

Figure 4.12: Vibration spectra of (a) Normal support condition (b) Loose motor support

The simplified ODS which is represented in 8-point cubic shape is shown in Figure 4.13. The ODS motion for normal condition at 37Hz is shown in the Figure 4.13(a). The arrows are showing the direction of the movement for each point. Points at upper layer which represent motor body are moving in same direction with the correspond points at bottom layer which represent base, thus it means the ODS is in phase which means it has no looseness problem. Meanwhile, the ODS motion for loose condition at 37Hz is shown in the Figure 4.13(b). Points 4 at upper layer is moving in opposite direction with the correspond point 8 at bottom layer which means out of phase. This shows the bolting between point 4 and point 8 is in loose condition. It proves that the simplified ODS technique can detect looseness problem easier, faster and more accurate compared to conventional method.

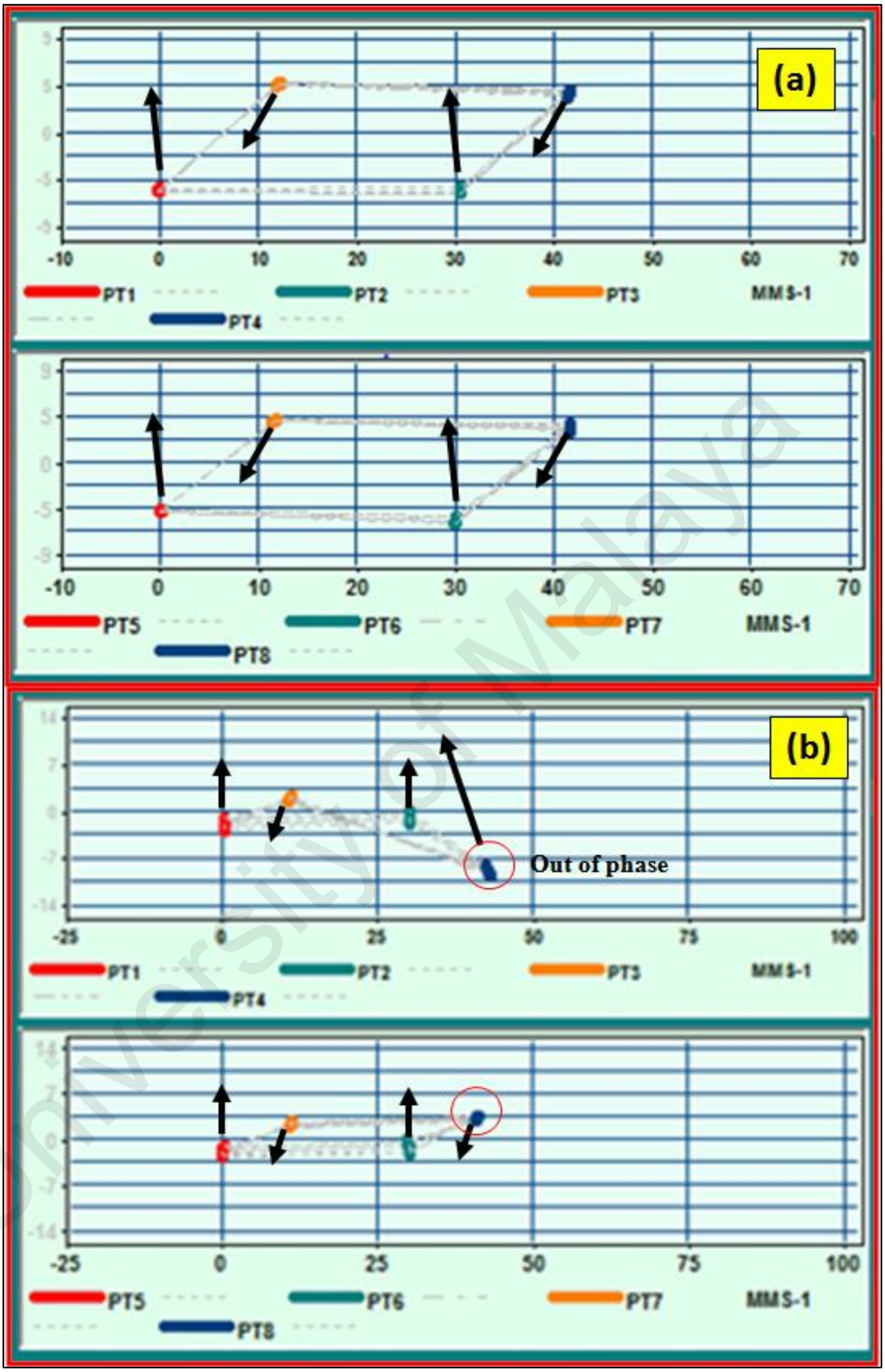

Figure 4.13: ODS of a) Normal condition (b) Loose motor support

4.2.1.4 Vibration Assessment of Bearing Fault

The test for bearing fault detection was performed with the 2 damage bearings, i.e., damage on the outer race and inner race installed on the same shaft and tested at the same time. Both bearing outer race and inner race damage generates bearing fault frequency component, i.e., BPFO and BPFI which can be observed in the frequency domain vibration spectrum. BPFO component can be observed from Figure 4.14(a) while BPFI component can be observed from Figure 4.14(b).

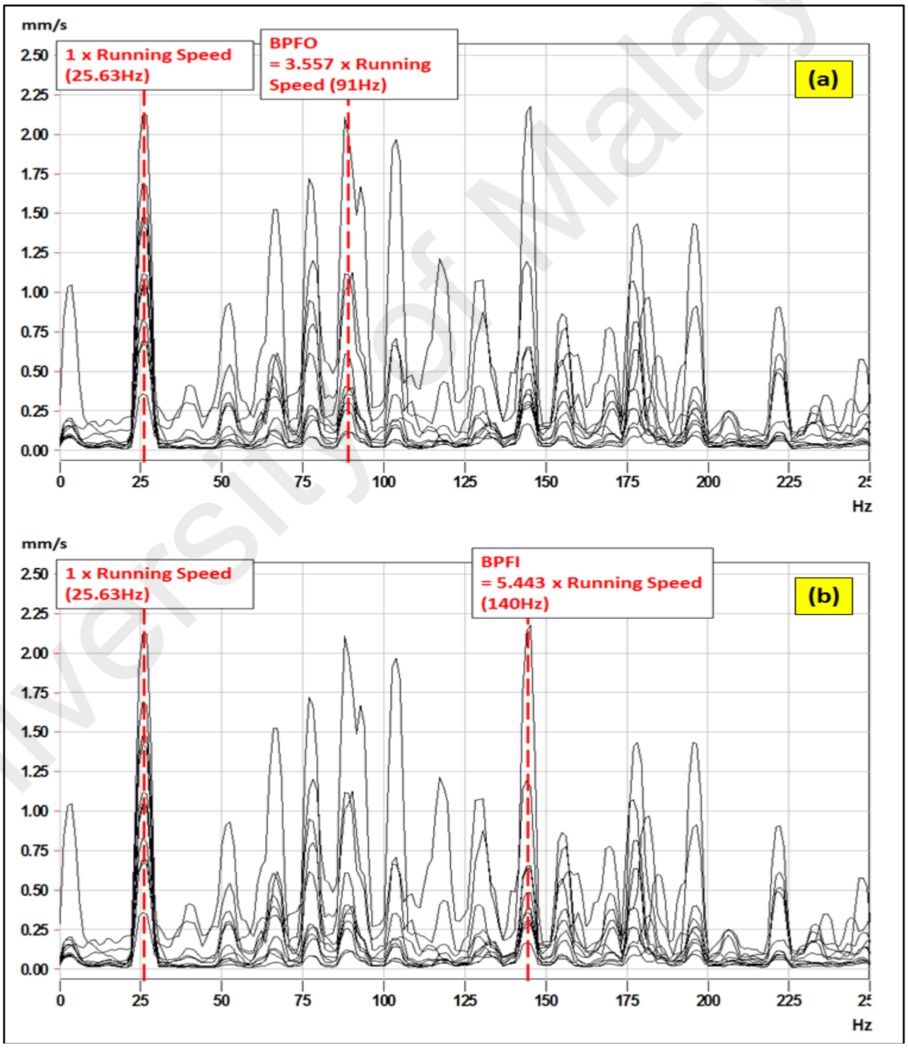

Figure 4.14: Overlaid vibration spectrum with (a) BPFO component (b) BPFI component

The BPFO and BPFI component are determined from the following equation;

$$BPFO = \frac{N_b}{2} \times RPM \times \left(1 + \frac{B_d}{P_d}\cos\theta\right) \tag{4.1}$$

$$BPFI = \frac{N_b}{2} \times RPM \times \left(1 - \frac{B_d}{P_d}\cos\theta\right) \tag{4.2}$$

where BPFO is the ball pass frequency of outer race and BPFI is the ball pass frequency of inner race

RPM is rotation per minute or the running speed of the machine

N_b is the number of ball of the bearing

B_d is the ball diameter

P_d is the pitch diameter

θ is the contact angle

All the parameters value for determination of BPFO and BPFI are obtained from the SKF bearing catalogue, with bearing number 1200 ETN9, where, N_b is equal to 7, B_d is equal to 4.75mm, and $P_d$is equal to 17.75mm. The ODS motion at BPFO component (91Hz) is presented in Figure 4.15(a) while ODS motion at BPFI (140Hz) is presented in Figure 4.15(b). Both ODS motion are showing almost identical motion with larger movement at measurement point 3 compared to measurement point 4. Measurement point 3 is where the bearing with inner race damage is located which is more severe compared to outer race damage. Furthermore, measurement point 3 is located near to the coupling which for this testing flexible coupling was used. The bearing used for this testing is a self-aligning ball bearing which is commonly used where severe misalignment occurs. Compared to other type of bearings, the self-aligning ball bearing is easier to be disassembled so that bearing fault can be created and easier to re-assemble it. The combination of impact from damage inner race bearing, bearing type and near to the flexible coupling possibly be the cause of larger ODS motion at measurement point 3 compared to measurement point 4.

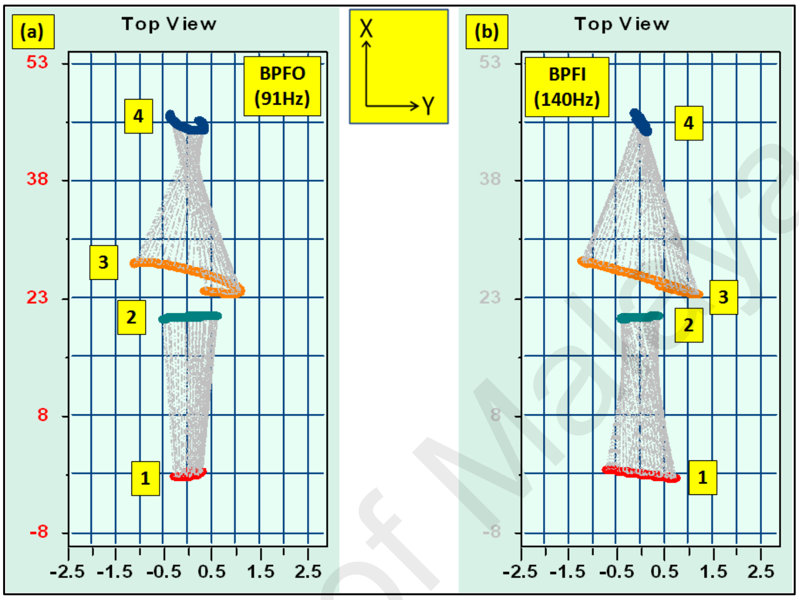

Figure 4.15: ODS of a) BPFO component (b) BPFI component

4.2.1.5 Vibration Assessment of Gear Fault

Both good condition gear and damage gear generates gear mesh frequency (GMF) component as shown in Figure 4.16. Figure 4.16(a) showing the result when the gear is in contact with the good condition pinion gear while Figure 4.16(b) showing the result when the gear is in contact with the damaged pinion gear. The vibration spectrum for this testing need to be zoomed because the GMF component is relatively too small compared to the running speed component. The GMF component can be determined from the following equation;

$$GMF = RPM \times N_T \tag{4.3}$$

where GMF is the gear mesh frequency, RPM is the running speed of the shaft and N_T is the number of gear teeth. The gear teeth for this testing are 20.

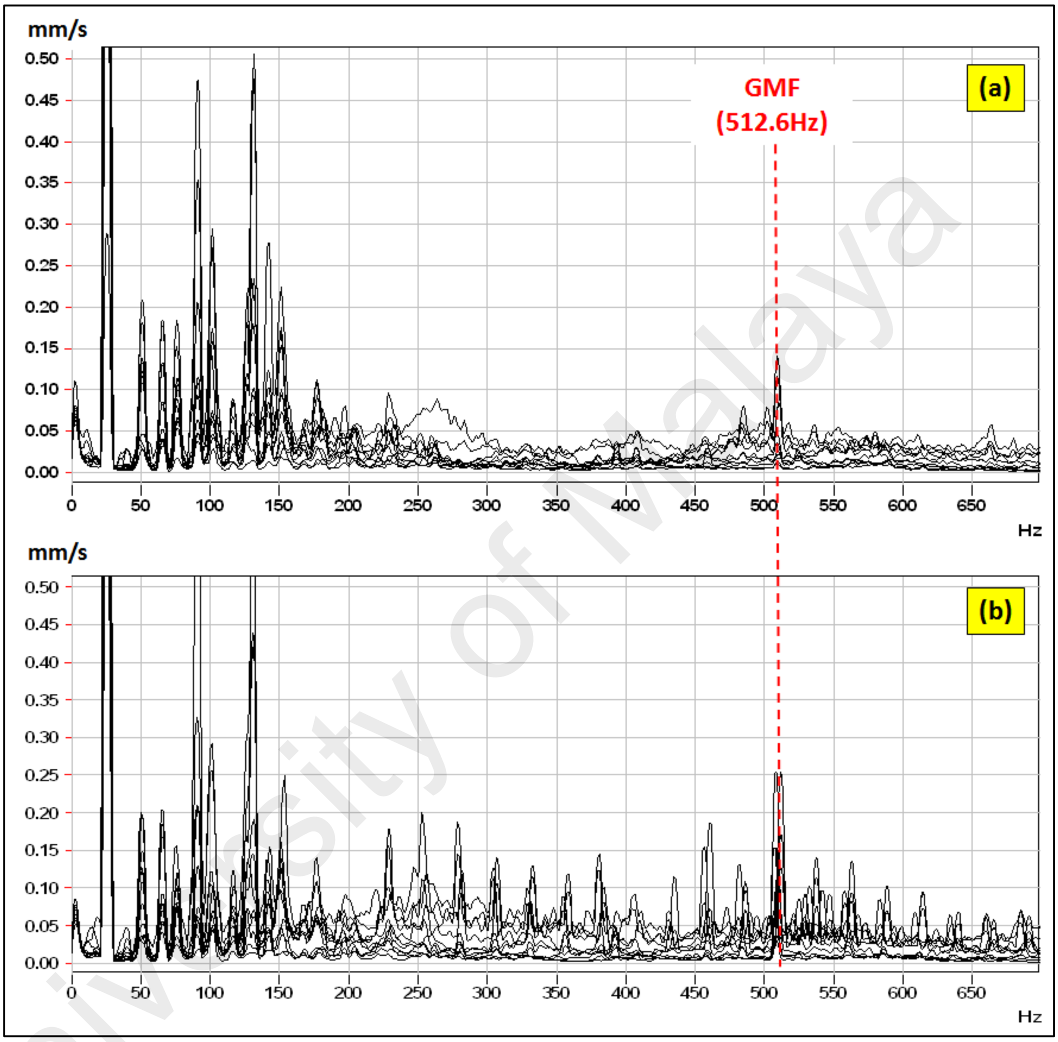

Figure 4.16: Vibration spectra of (a) Normal gear (b) Gear fault

The ODS for good condition gear is shown in Figure 4.17(a) while Figure 4.17(b) is showing the ODS for the damage gear. Both ODS is from the same GMF component which is 512.6Hz. The measurement point for both the good condition pinion gear and damaged pinion gear is located at measurement point 3 while measurement point 4 is located at the end of the shaft to complete the ODS motion. The damage gear is showing a larger ODS motion compared to good condition gear. This result shows that by using this simplified ODS technique, the location of a damage gear can also be determined easier, faster and more accurate.

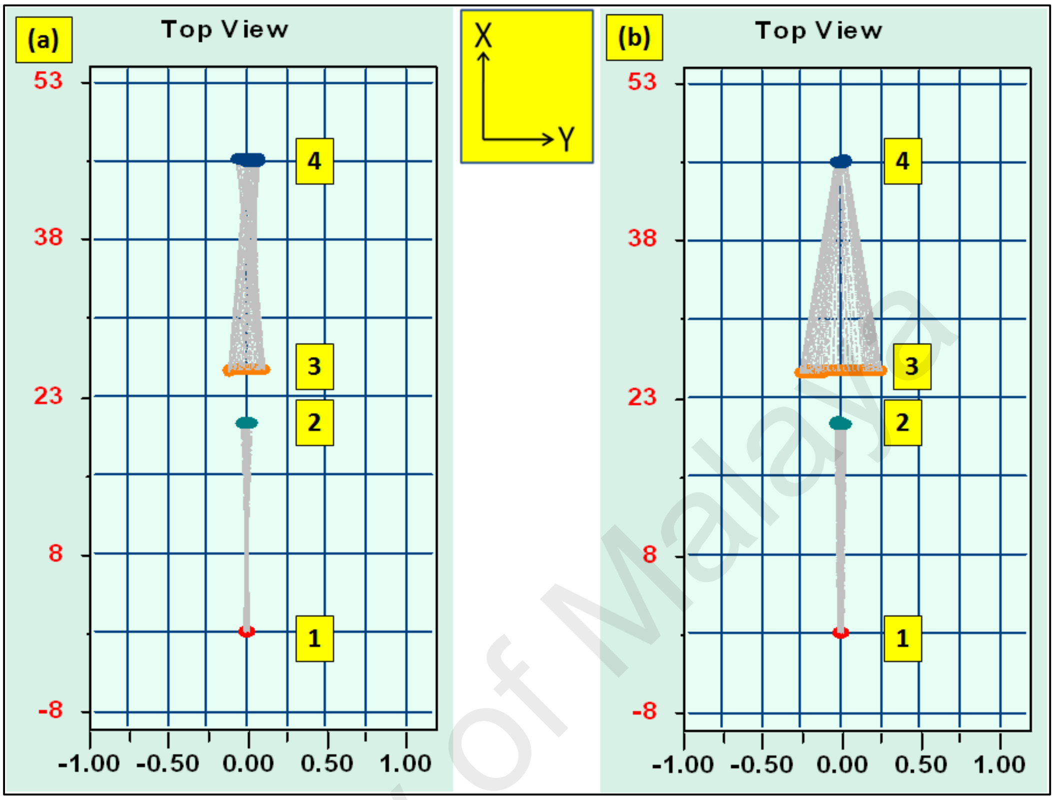

Figure 4.17: ODS of (a) Normal gear (b) Damage gear

The output results from the laboratory condition testing show that the vibration data acquisition using a tri-axis accelerometer is more efficient and time saving as compared to conventional method of machinery vibration assessment. Furthermore, relative phase of the 2 accelerometers and visualisation of the machine motion is more efficient and save more time for analysing machine condition as compared to the conventional vibration assessment practice.

4.2.2 Vibration Assessment of Industrial Machinery

Previously in section 4.2.1, the performance of simplified ODS has been successfully demonstrated and verified by using a laboratory kit. In this section, the performance of this technique is further examined. The testing on the real industrial machinery using the simplified ODS technique to identify the machinery fault easily and effectively as compared to the conventional practice is studied.

4.2.2.1 Vibration Assessment of Rotor Imbalance on Industrial Machinery

The effectiveness of ODS visualisation was first demonstrated from the industrial vertical centrifugal pump with static imbalance problem. The ODS as shown in Figure 4.18 shows point 1 and point 2 which are both at motor side are moving in relatively higher amplitude and in phase indicates a static imbalance problem. Conventionally, the vibration spectra as in Figure 4.19 were analysed. It shows a harmonic pattern where it may mislead to looseness problem. Further investigation found that the static imbalance problem occurs due to the pipe strain. It is crucial to ensure that both the suction and discharge of the pump are on the same level with the corresponding pipe line to avoid this problem.

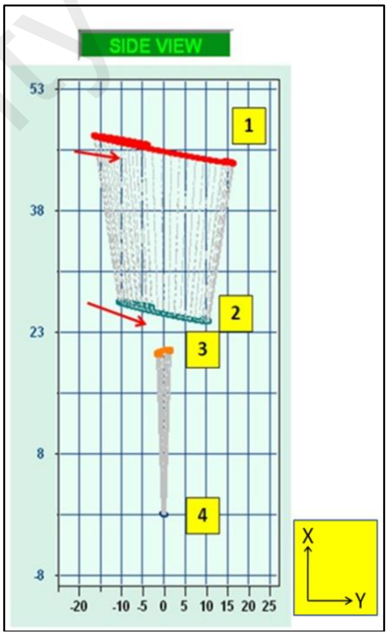

Figure 4.18: Industrial case ODS of Static imbalance

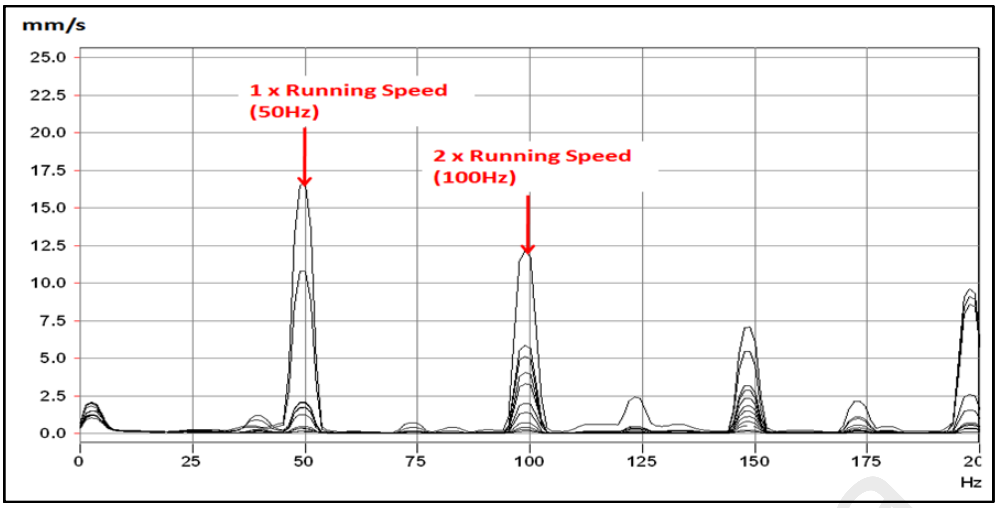

Figure 4.19: Industrial case overlaid vibration spectrum of Static imbalance

The proposed simplified ODS was then tested on an industrial horizontal centrifugal pump which undergoes dynamic imbalance problem. Figure 4.20 shows the ODS of Point 3 and point 4 which are both at pump side are moving in relatively higher amplitude and out of phase which indicates the dynamic imbalance problem Conventionally, the complex vibration spectra as shown in Figure 4.21 were analysed. It could not indicate the imbalance problem with the spectra only. It only shows a frequency component corresponding to the blade passing frequency (BPF). BPF with low vibration amplitude is considered as acceptable. However, due to low discharge pressure, further investigation was conducted. The problem occurred due to severe pump cavitation which causes the pump impeller to worn out. Furthermore, the pump cavitation problem was characterised by the raised noise floor which can be seen in the vibration spectra.

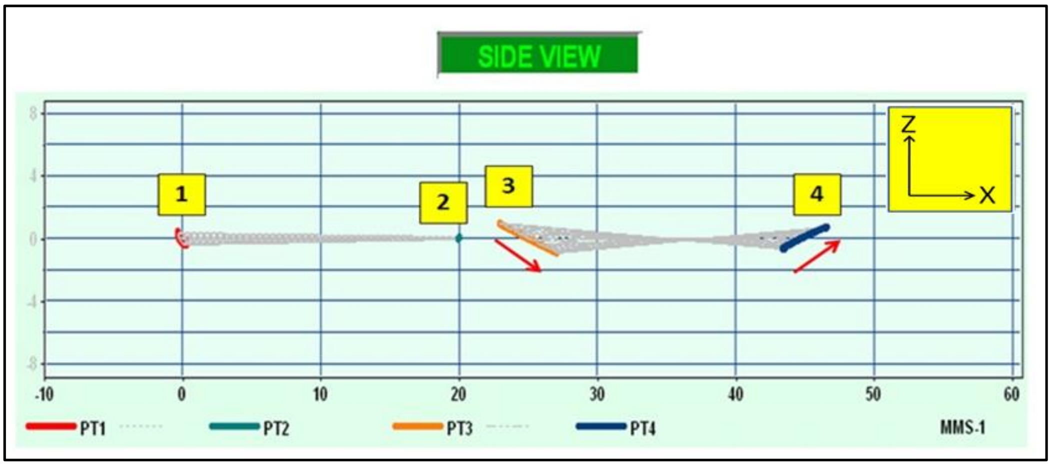

Figure 4.20: Industrial case ODS of Dynamic imbalance

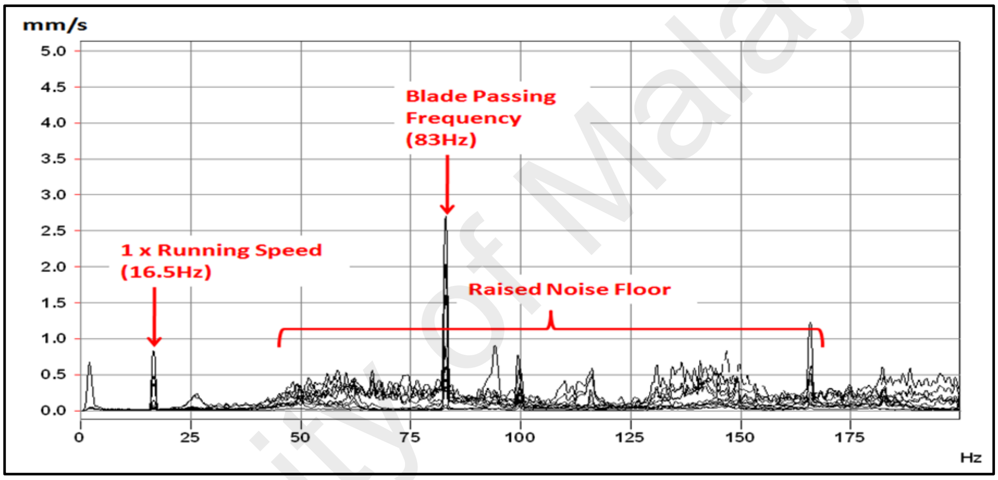

Figure 4.21: Industrial case overlaid vibration spectrum of Dynamic imbalance

4.2.2.2 Vibration Assessment of Misalignment on Industrial Machinery

The ODS visualisation of parallel misalignment was then demonstrated from the industrial horizontal centrifugal blower. The ODS is as shown in Figure 4.22 shows that point 2 and point 3, i.e. points across coupling are horizontally out of phase indicating parallel misalignment problem. Conventionally, vibration spectra as shown in Figure 4.23 were obtained where harmonic patterns can be observed in the spectra. Again, this finding may mislead the personnel to diagnose it as looseness problem. The investigation was conducted due to abnormal sound. Although the vibration spectra show relatively lower vibration amplitude, the simplified ODS is still able to show the motion of parallel misalignment. Further investigation found that the coupling shim was damaged.

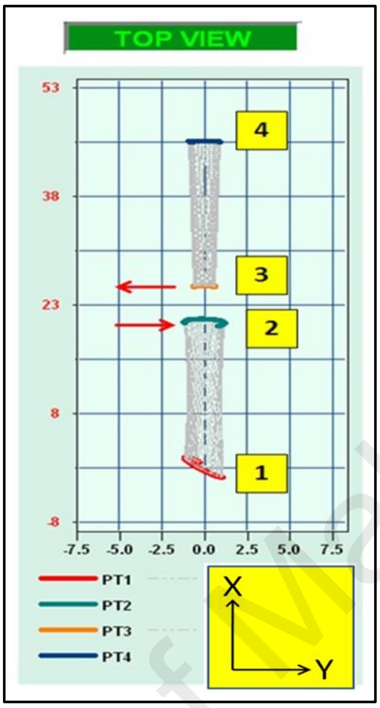

Figure 4.22: Industrial case ODS of Parallel misalignment

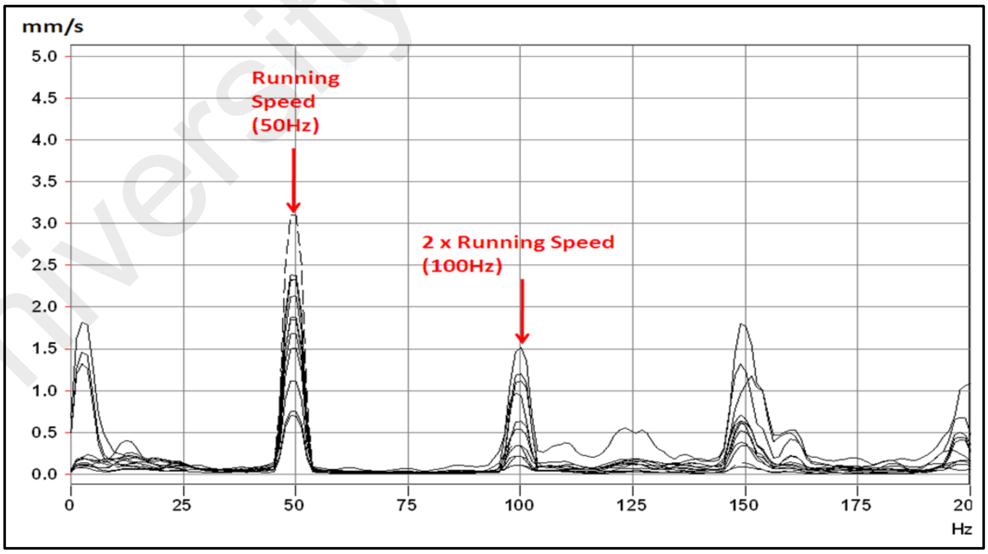

Figure 4.23: Industrial case overlaid vibration spectrum of Parallel misalignment

In addition, the simplified ODS was tested on a belt driven centrifugal blower with angular misalignment problem. Figure 4.24 shows the ODS that point 2 and point 3, i.e. points across pulley and belting are axially out of phase. Conventionally, vibration with the running speed, 2-time running speed components and multiple harmonic patterns spectra as shown in Figure 4.25 were observed and analysed. The harmonic pattern may mislead to belting looseness. Further investigation found that the vibration remain high after the spare motor was installed. The motor base plate was found flexible and was not properly aligned. Due to uneven level of the motor base plate, the pulley was axially misaligned. By using the simplified ODS, both parallel and angular misalignment can be detected earlier and easier.

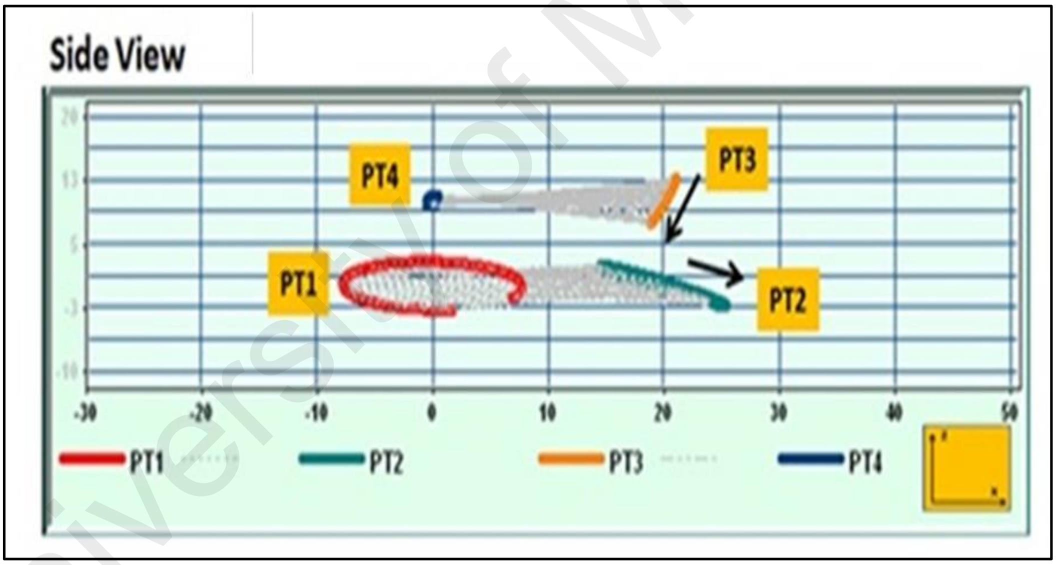

Figure 4.24: Industrial case ODS of Angular misalignment

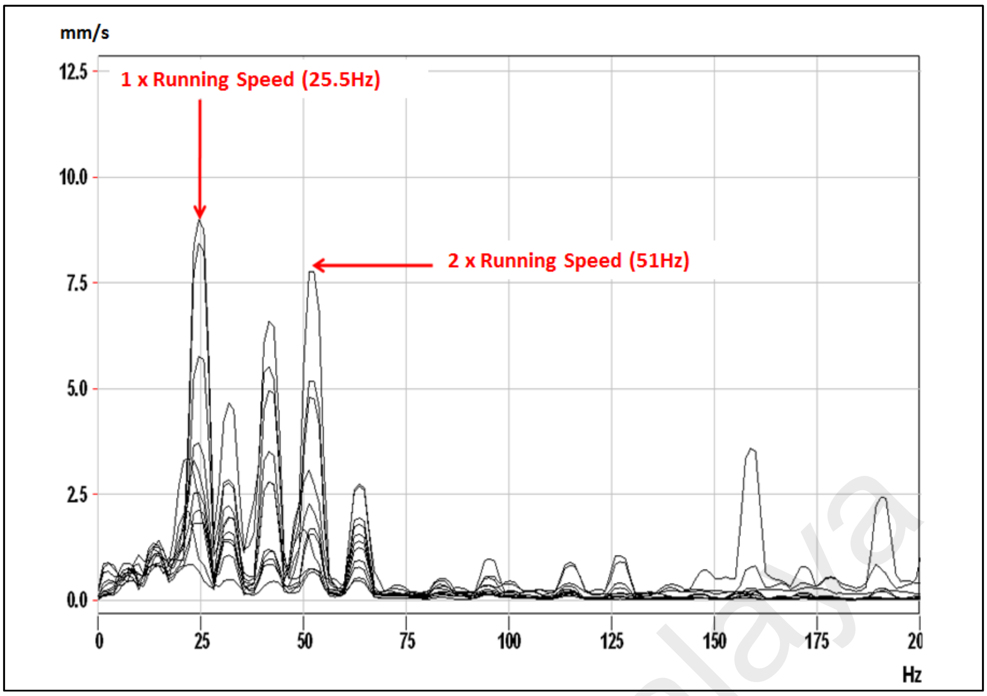

Figure 4.25: Industrial case overlaid vibration spectrum of Angular misalignment

4.3 Vibration Assessment on Reciprocating Machinery

In this section, the simplified ODS technique is able to show the motion of reciprocating machinery part. Motor fault of the air compressor is detected using this simplified ODS technique. While the reciprocating motion is showing that the vibration on the compressor is affected due to difference in operating pressure. The vibration increased as the operating pressure is increasing. The final test was performed on a bio-fuel powered diesel engine to determine the optimum bio-fuel blend based on the engine vibration parameter. The minimal engine vibration due to the bio-fuel combustion effect is the baseline in determining the optimum bio-fuel blend. Other external vibration source which is torque factor can be separated and determined by performing the frequency domain analysis. While by performing time domain analysis can identify the major component of vibration caused by the combustion of bio-fuel.

4.3.1 Vibration Assessment of Laboratory Air Compressor

The reciprocating air compressor is operating at difference pressure of 1 bar, 2 bar, 3 bar and 4 bar. The speed for both motor and crankshaft is determined using a tachometer. The motor shaft is running at 49Hz (2940 rpm) meanwhile the crankshaft is running at 13.5Hz (810 rpm). Vibration data is acquired using the simplified ODS technique with 8 measurement points.

Conventionally, the acceleration signals were obtained in the x-axis, y-axis and z-axis. The total acceleration of vibration was calculated from the RMS of the acceleration in all axes to compare the vibrations at different pressure.

$$a_{total} = \sqrt{a_x^2 + a_y^2 + a_z^2} \tag{4.4}$$

where a_{total} is the total acceleration of vibration

a_x is the RMS of acceleration in x-axis

a_y is the RMS of acceleration in y-axis

a_z is the RMS of acceleration in z-axis

From the calculated total acceleration of vibration for each point, a graph of total acceleration against pressure is plotted as shown in Figure 4.26. From the graph, generally it shows that pressure of 1 bar has the lowest vibration. However, the difference is not obvious as compare to the total acceleration of other pressure.

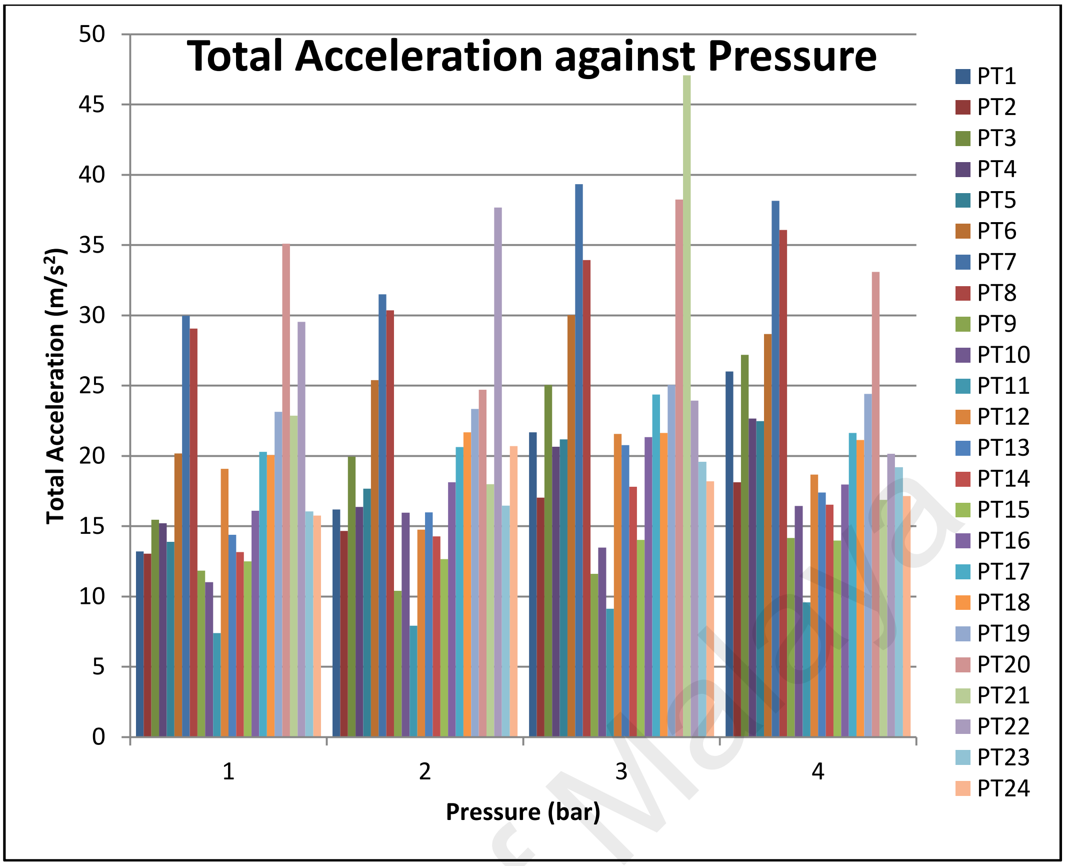

Figure 4.26: Total acceleration against pressure

The mean value of total acceleration for different pressure is calculated so that the vibration among different pressure can be compared easily. The calculated mean value of total acceleration is shown in Table 4.1. Then, the graph of calculated mean value of total acceleration is plotted as shown in Figure 4.27.

$$a_{mean} = \frac{\sum_{i=1}^{N} a_i}{N} = \frac{a_1+a_2+\cdots+a_{24}}{24} \quad (4.5)$$

where a_{mean} is the average of total acceleration

a_i is the total acceleration of point i

N is the total number of point

Table 4.1: Mean value of total acceleration for different pressure

Pressure (bar)	Mean of total acceleration, a_{mean}(m/s^2)
1	18.26
2	19.39
3	23.20
4	21.57

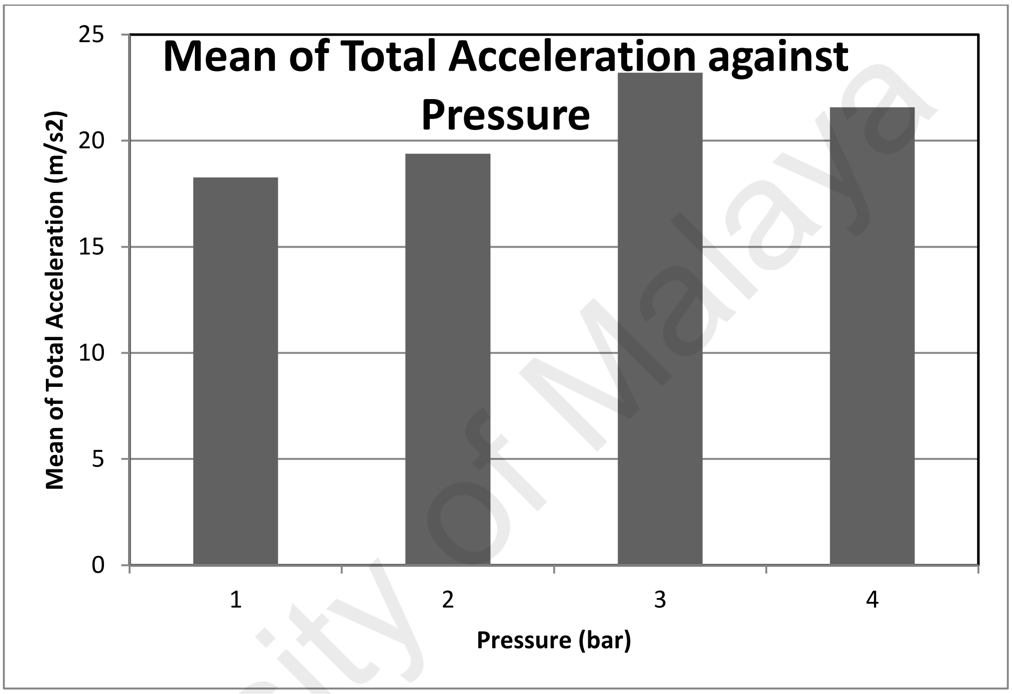

Figure 4.27: Mean of total acceleration for different pressure

From the Figure 4.27, it shows that the air compressor has the lowest vibration at pressure of 1 bar with 18.26m/s^2. The trending of graph also shows that the vibration increasing with the increasing pressure. The vibration data was further analysed using time domain and frequency domain analysis to identify and separate the vibration source.

Figure 4.28 shows a section of acceleration time domain signal of pressure 1 bar for air compressor in longitudinal axis (x), lateral axis (y) and vertical axis (z). Figure 4.28 shows that a complete cycle of is equal to 4.5Hz. It is 1/3 times of crankshaft running speed, 13.5Hz. It means the crankshaft rotates 3 times to complete 1 complete cycle of compressed air.

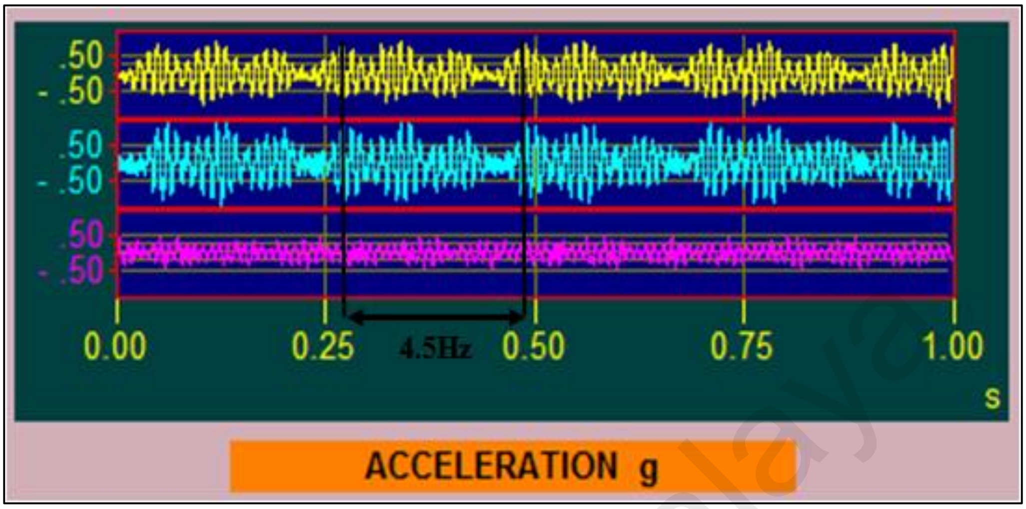

Figure 4.28: Time domain signal of pressure 1 bar for air compressor test

Figure 4.29 shows a vibration spectrum of frequency domain signal for air compressor at pressure of 1 bar. The spectra show peaks at 13.5Hz, i.e., 1-time running speed of crankshaft, 49Hz, i.e., 1-time running speed of motor shaft and 50Hz, i.e., 1-time line frequency. The spectra also show the harmonics of fundamental frequency of 4.5Hz. Other peaks are due to natural frequencies and pole pass side bands. Pole pass side bands are caused by eccentricity when the eccentric rotors produce rotating variable air gap between rotor and stator which induces a pulsating source of vibration which will cause a higher peak at 2-time line frequency. Pole pass sidebands are formed around 1-time running speed and 2-time line frequency.

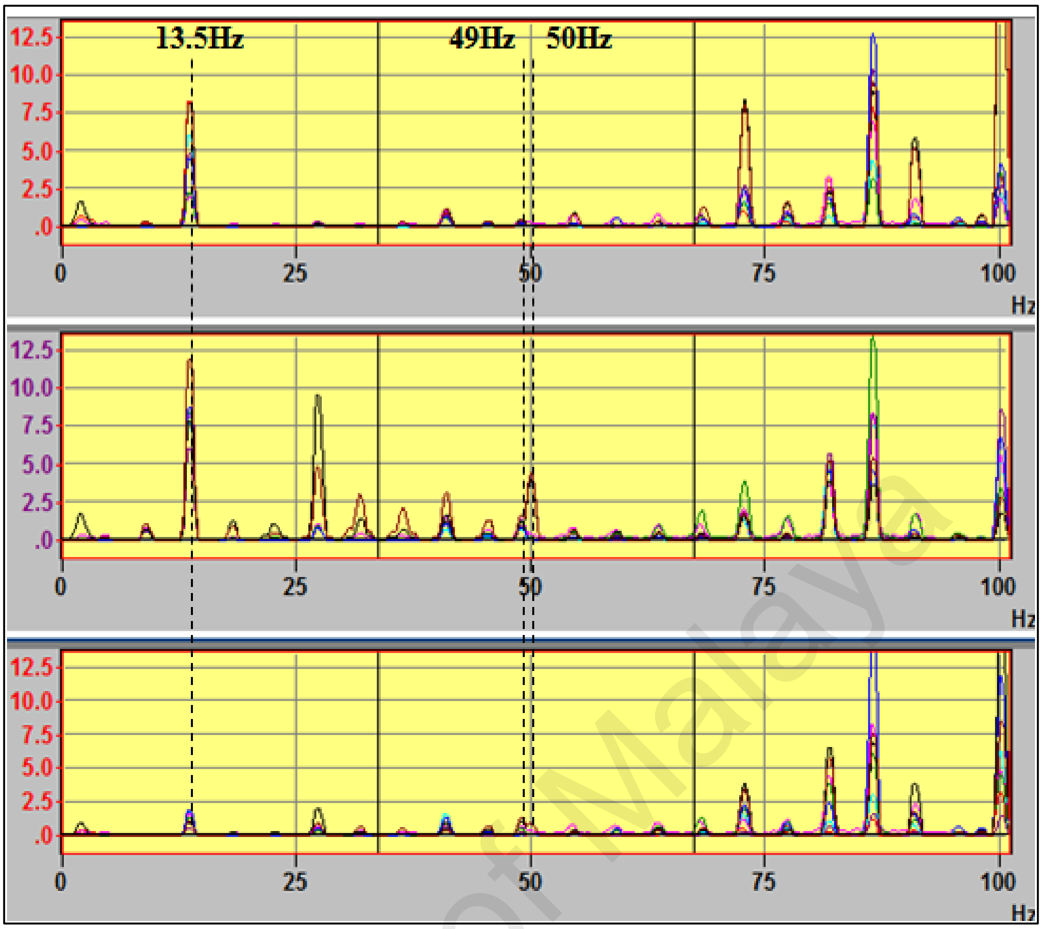

Figure 4.29: Frequency domain signal of pressure 1 bar for air compressor test

The developed simplified ODS technique was applied on the air compressor to investigate the effectiveness of showing the reciprocating ODS motion. The ODS motion of air compressor with pressure 1 bar at 13.5Hz is shown in the Figure 4.30. Points 1-4 at upper layer are rotating in same direction with the correspond point 5 and point 6 at bottom layer from compressor side. This shows that motion at 13.5Hz is dominated by the rotary motion of crankshaft. The motion at 13.5Hz is the same for other pressure as well.

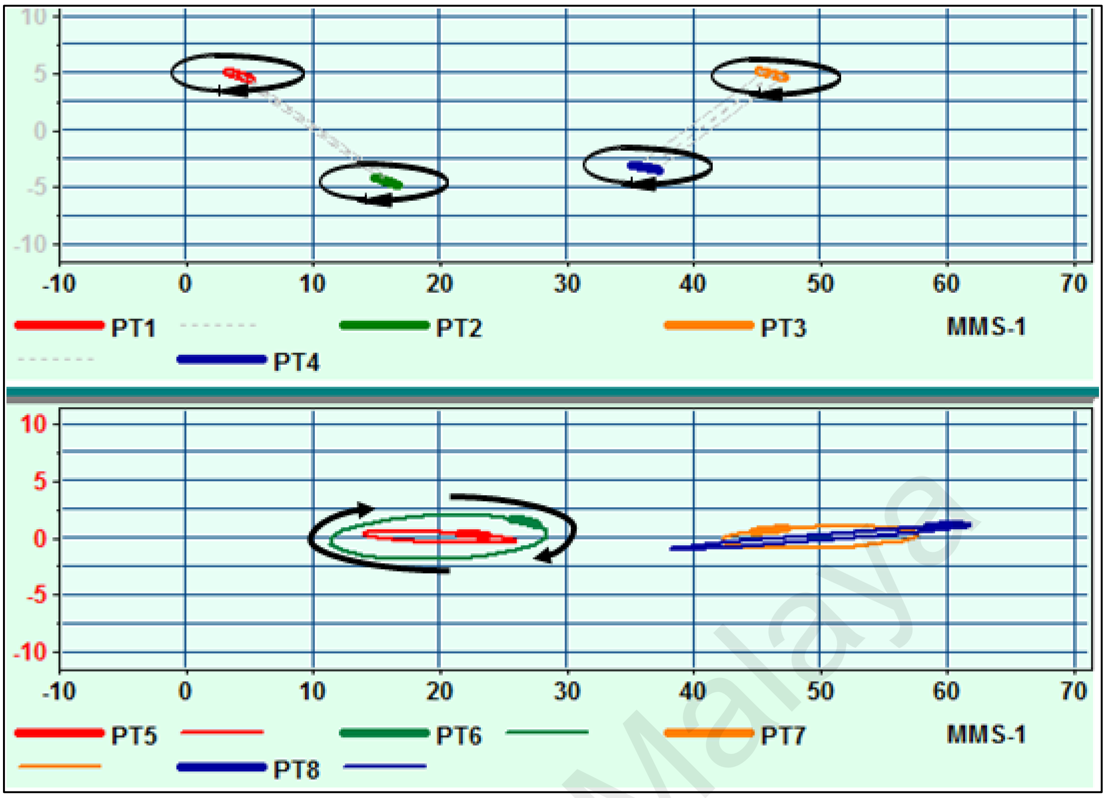

Figure 4.30: ODS of Air Compressor at 13.5Hz

The ODS motion of air compressor for pressure 1 bar at 49Hz is shown in the Figure 4.31. Point 1 and point 2 are moving in opposite direction with point 3 and point 4 which clearly show the reciprocating motion of both pistons. This shows that motion at 49Hz is dominated by the reciprocating motion of piston. The motion at 49Hz is the same for other pressure of reciprocating air compressor.

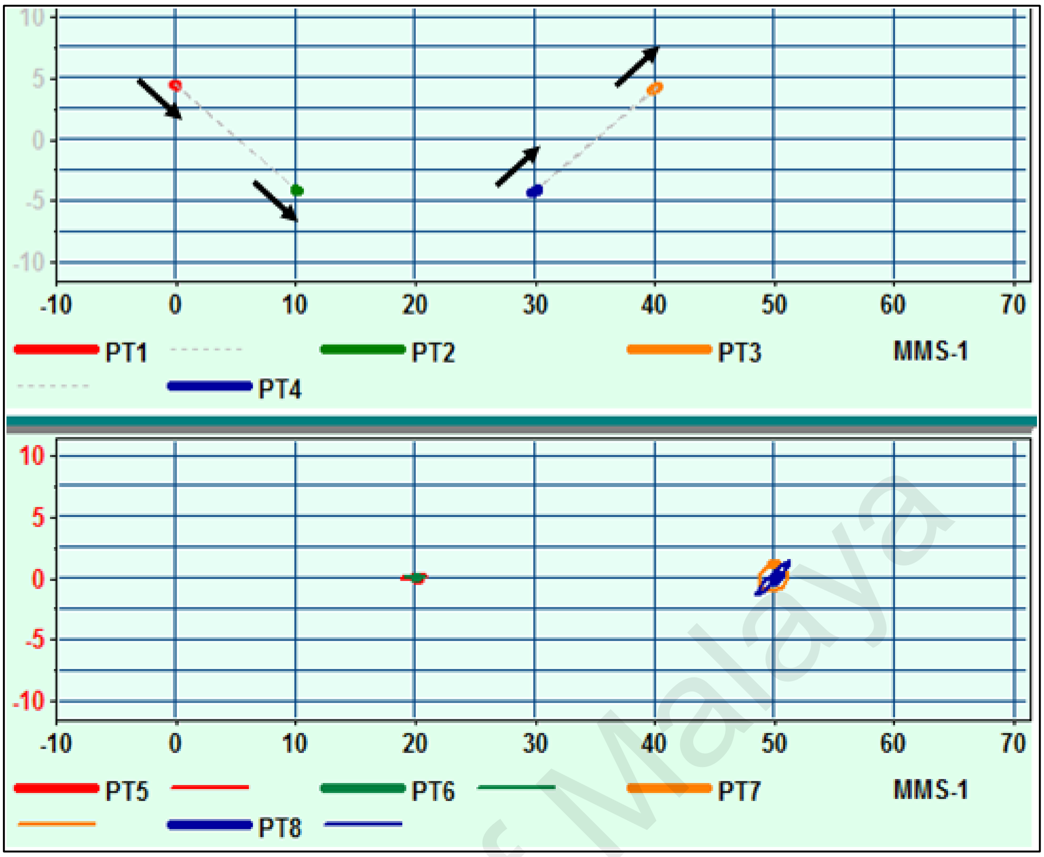

Figure 4.31: ODS of Air Compressor at 49Hz

The ODS motion of air compressor for pressure 1 bar at 50Hz is shown in the Figure 4.32. Point 7 and point 8 are moving in opposite direction with each other which means the motor shaft is out of phase. This shows the motor is under eccentricity problem. The motion at 50Hz is the same for other pressure too. The possible cause of this eccentricity problem is over tensioned belting. The over tensioned belting causes uneven gap between the rotor and stator inside the motor. This explains the difference in relative phase reading between 2 closed frequency component which is (49Hz and 50Hz).

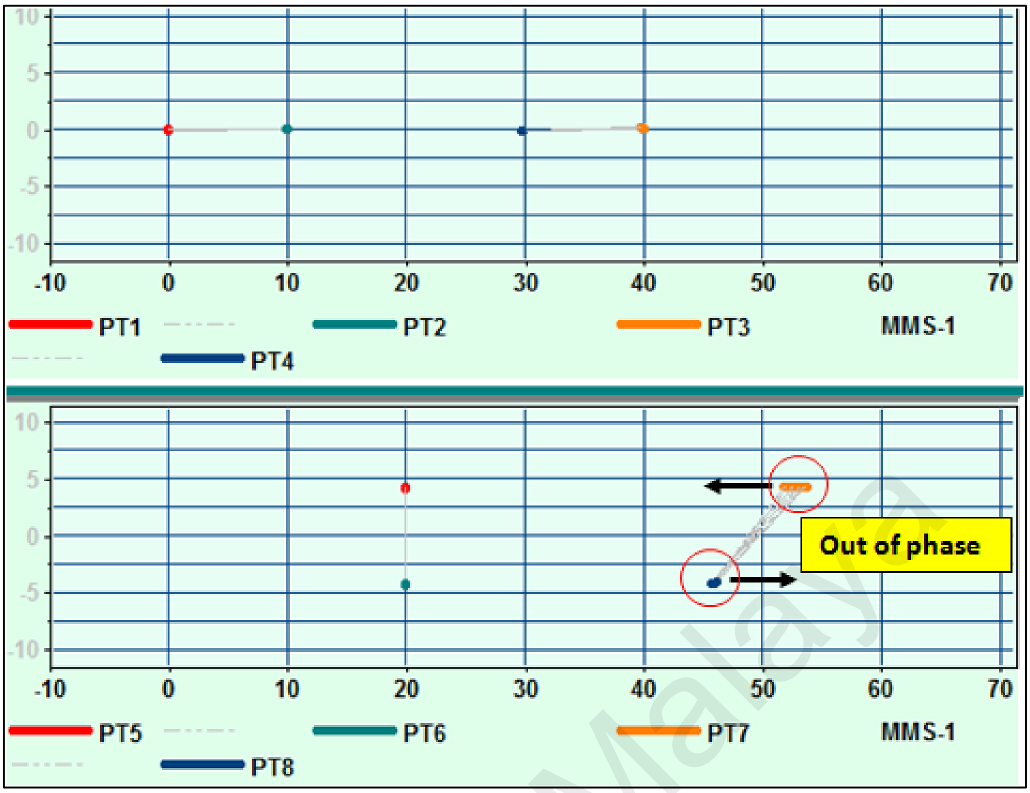

Figure 4.32: ODS of Air Compressor at 50Hz

The discussion for Figure 4.30 until Figure 4.32 proves that the reciprocating motion and rotary motion can be shown using this simplified ODS technique. Besides that, rotor eccentricity problem can be identified clearly through visualisation of the ODS motion.

4.3.2 Vibration Assessment of Bio-Fuel Powered Diesel Engine

Vibration data were acquired for the two running speeds, where the lowest speed was set to 1500 rpm and full speed at 2400 rpm. The engine ran at full-throttle position (i.e., 100% wide-open throttle during data acquisition). Dynomax-2000 software was used to control the engine running at 1500 rpm (maximum torque) and 2400 rpm (lowest torque).

The comparison of engine vibration used different bio-fuel blends at the lowest speed (i.e., 1500 rpm) and full speed (2400 rpm). Conventionally, the mean values of the total acceleration in RMS of the three measurement axes for each point were compared. The mean of the total acceleration in RMS is obtained using the following equation:

$$\bar{a}_{rms} = \frac{\sum_{i=1}^{N} a_{rms-i}}{N} = \frac{a_{rms-1}+a_{rms-2}+\cdots+a_{rms-12}}{12} \tag{4.6}$$

where $\bar{a}_{rms}$ is the mean of total acceleration in RMS of 12 measurement points; a_{rms-i} is the total acceleration in RMS from the x, y, and z axes at point i; and N is the total measurement point. The acquisition procedure is repeated to obtain five measurement data sets to ensure the reproducibility of acquired data.

The calculated mean value of total acceleration in RMS is plotted (Figure 4.33). The error of measurement during data acquisition at the engine speed of 1500 rpm was between 0.2 and 2.1. Error of measurement at the engine speed of 2400 rpm was in the range of 0.3 and 0.8. The small error values indicate that the result obtained from this experiment is reproducible.

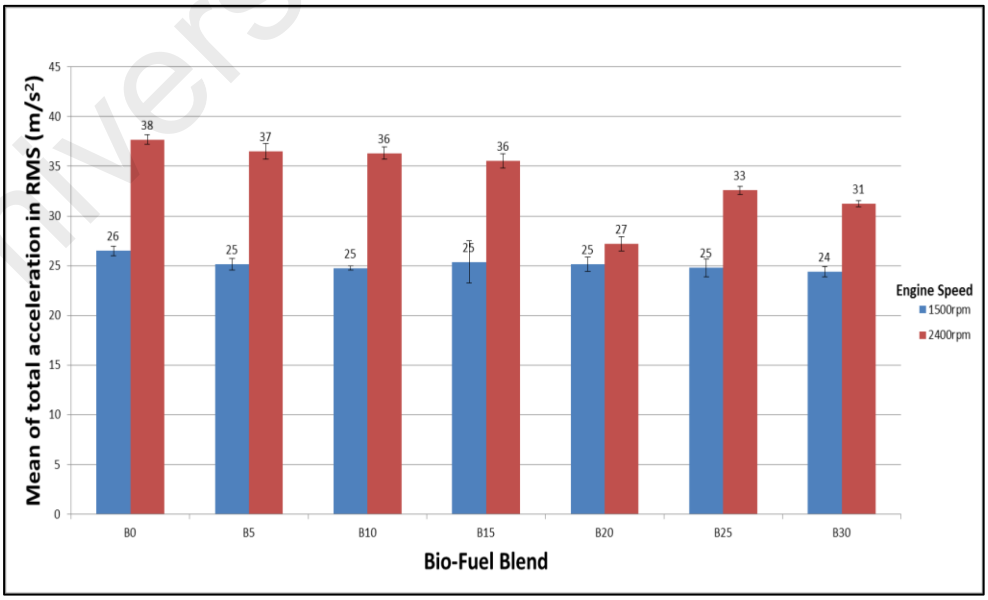

Figure 4.33: RMS Values of Vibration in terms of Acceleration for all Bio-fuel Blends

Figure 4.33 shows that the vibration level of the engine is almost the same for the lowest speed (1500 rpm). At full speed (2400 rpm), the bio-fuel blends significantly affected engine vibration. A significant change in vibration data was observed from engine vibration tested at the speed of 2400 rpm. For pure diesel B0, the engine showed higher vibration at full speed compared with the lowest speed. As the percentage of the bio-fuel increased, the engine showed lower vibration at full speed. Based on findings, B20 prominently showed lower vibration compared with pure diesel. A previous study (Hwai Chyuan Ong et al., 2014) on CI bio-fuel revealed that 20% fuel blend has less brake-specific fuel consumption (Bsfc) compared with diesel fuel. Biodiesel has a high oxygen content, which complements recent findings that B20 has more oxygen than pure diesel. The presence of rich oxygen in fuel-blend molecules triggers a combustion process. As a result, the brake thermal efficiency will increase, and the value of Bsfc will decrease. In vibration, a similar trend was observed. As shown in Figure 4.33, the overall vibration recorded in the pure diesel-powered engine is relatively higher than that of the bio-fuel-powered engine. Bio-fuel is oxygenated fuel, which contains higher oxygen content than pure diesel. Thus, it helps in increasing the efficiency of combustion in engine and producing relatively lower engine vibration. Trends for the 2400 rpm data showed that combustion efficiency directly affects engine vibration. However, the RMS value of vibration does not provide adequate justification to conclude that the high vibration is purely affected by the bio-fuel blend. Therefore, an advanced vibration analysis is needed to determine the causes of high vibration for the different bio-fuel blends.

The advanced vibration analysis involves time domain analysis and frequency domain analysis. Both analyses were performed to justify the engine vibration was purely affected due to bio-fuel combustion and to determine the exact value of the optimum bio-fuel blend based on the minimal engine vibration.

Combustion inside the IC engine is the major factor that creates the engine vibration. Combustion happens to create an impact, which leads to a high-amplitude transient vibration signal. The difference between the two highest vibration impacts observed from the time-domain analysis could determine the combustion factor. The vibration signal is further analysed in the time domain to determine the dominant vibration source. Figures 4.34 and 4.35 show sections of time-domain vibration signals for diesel engine run at 1500 rpm (lowest speed) and 2400 rpm (full speed) in the x, y, and z axes. Findings from Figure 4.34 show that the interval between the two highest impacts is equal to 12.5 Hz, which is half of that of the engine running at 1500 rpm (25 Hz). In Figure 4.35, the interval between the two highest impacts is 20 Hz, which is half of that of the engine running at 2400 rpm (40 Hz). Findings from the time-domain analysis is similar to the mechanisms of a single-cylinder four-stroke diesel engine. The crankshaft rotates twice every engine cycle. Combustion occurs every other rotation, which results in a strong peak at 0.5-time running speed (Tienhaara, 2004).

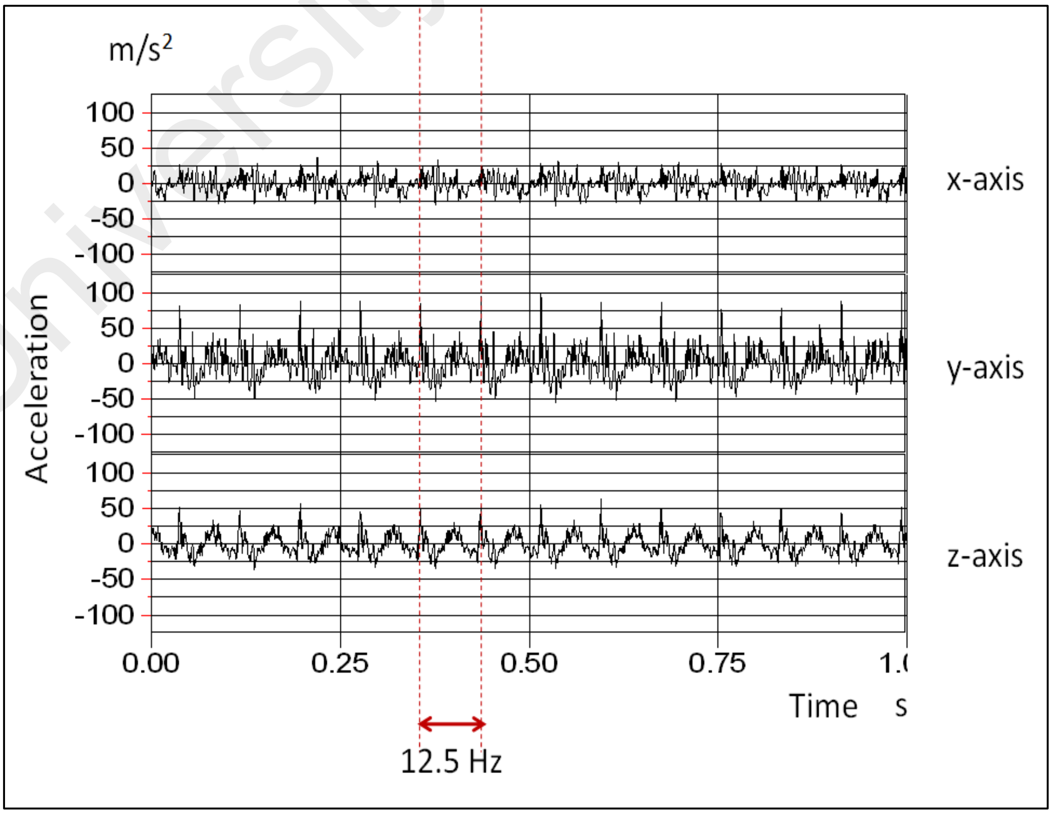

Figure 4.34: Time domain signal for engine speed 1500 rpm

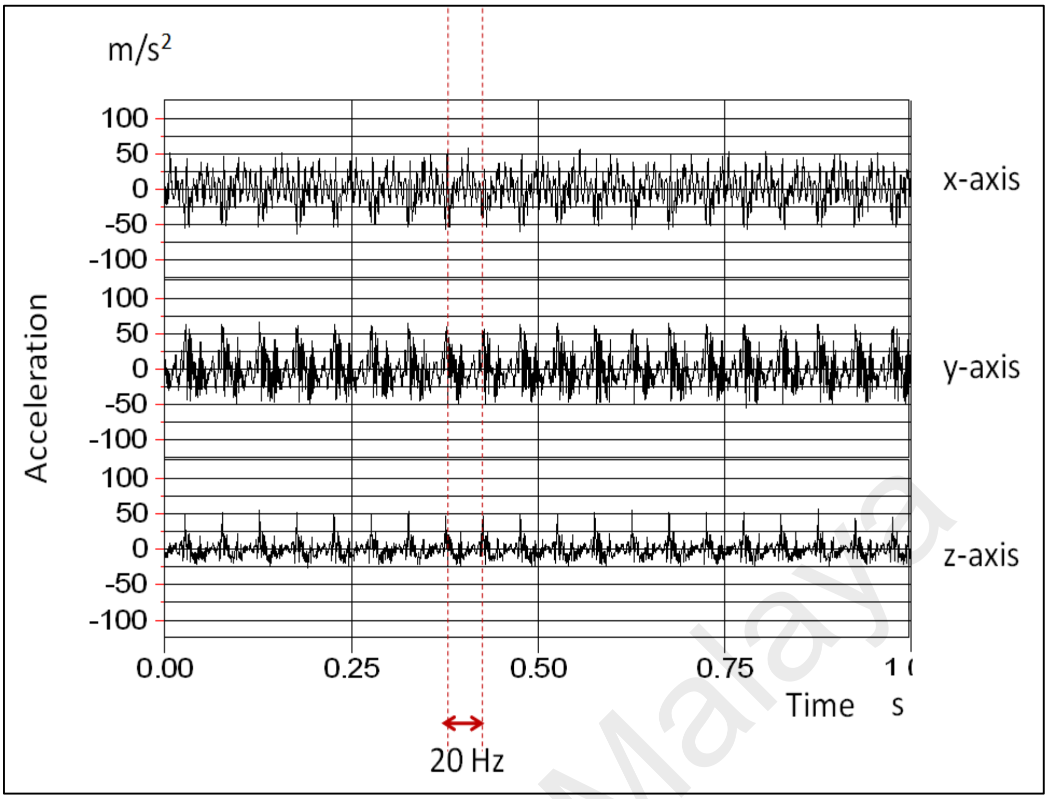

Figure 4.35: Time domain signal for engine speed 2400 rpm

The engine vibrations are mainly dominated by vibration due to combustion. The other lower vibration components are difficult to separate and identify using time-domain analysis. However, vibrations can be decomposed into frequency components through FFT for the ease of analysis. The frequency components are analysed in a spectrum plot.

After signal processing, the time-domain signal is decomposed through frequency-domain analysis. Frequency-domain analysis shows vibration and frequency components corresponding to the engine running speed and other vibration sources. As for this case, the other vibration source occurring at 0.5-time of the running speed comes from the engine combustion, which has been proven through time-domain analysis. Figure 4.36 shows the vibration spectra of the engine running at 1500 rpm. The spectra showed peaks at 12.5 Hz and 25 Hz for 0.5-time and 1-time running speeds, respectively. The spectra also showed the appearance of relatively less dominant harmonics, which are the positive integer multiples of the fundamental engine speed (25 Hz). The reciprocating motion of the piston due to the combustion in the cylinder also contributed to total vibration. The reciprocating motion effect caused the appearance of harmonics.

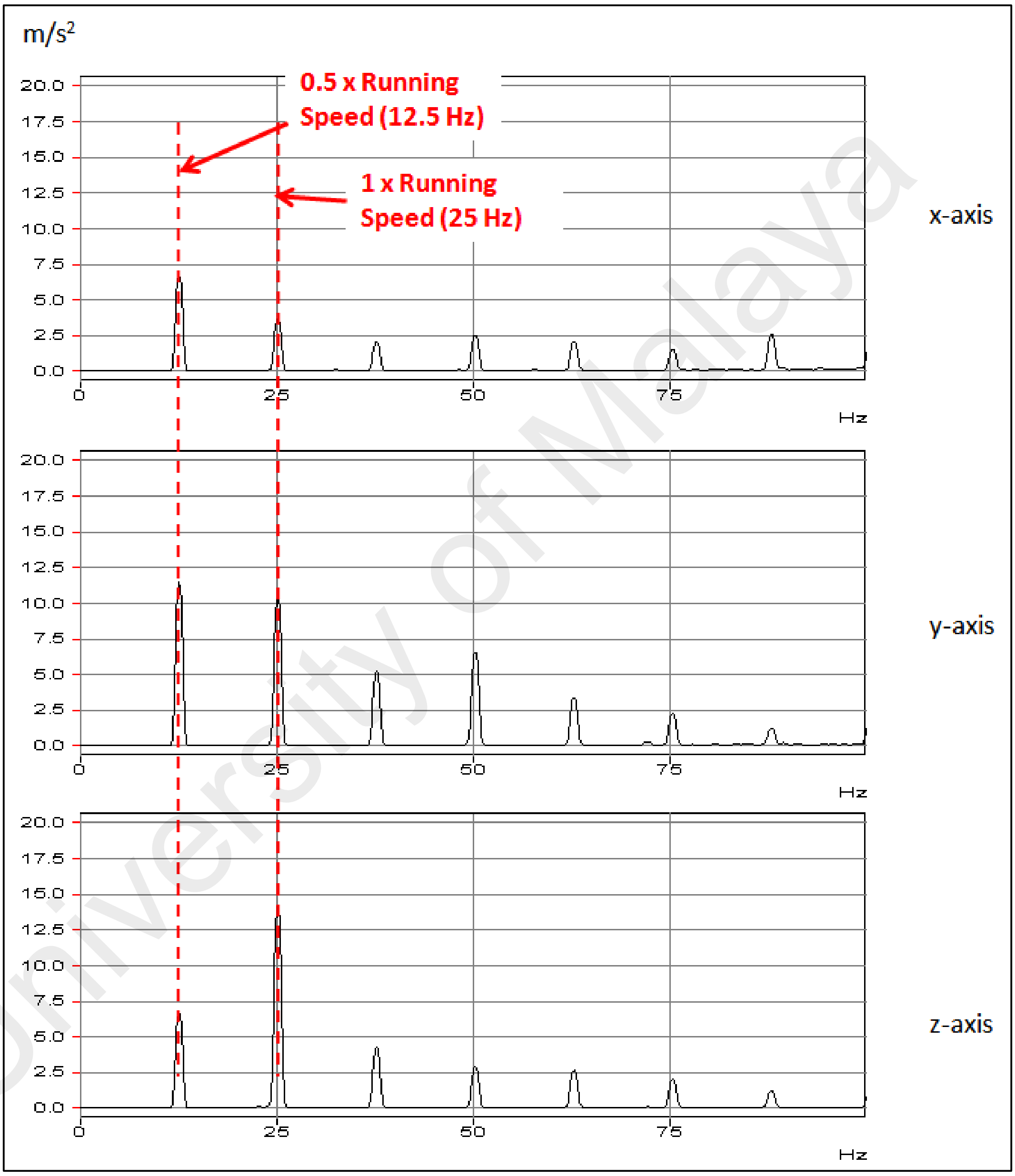

Figure 4.36: Vibration spectra for engine speed 1500 rpm

Figure 4.37 shows the vibration spectra of the engine running at 2400 rpm. The spectra showed peaks at 20 Hz and 40 Hz for the 0.5-time and 1-time running speeds, respectively. The spectra also show the harmonics of engine speed of 40 Hz due to the reciprocating motion effect from the piston.

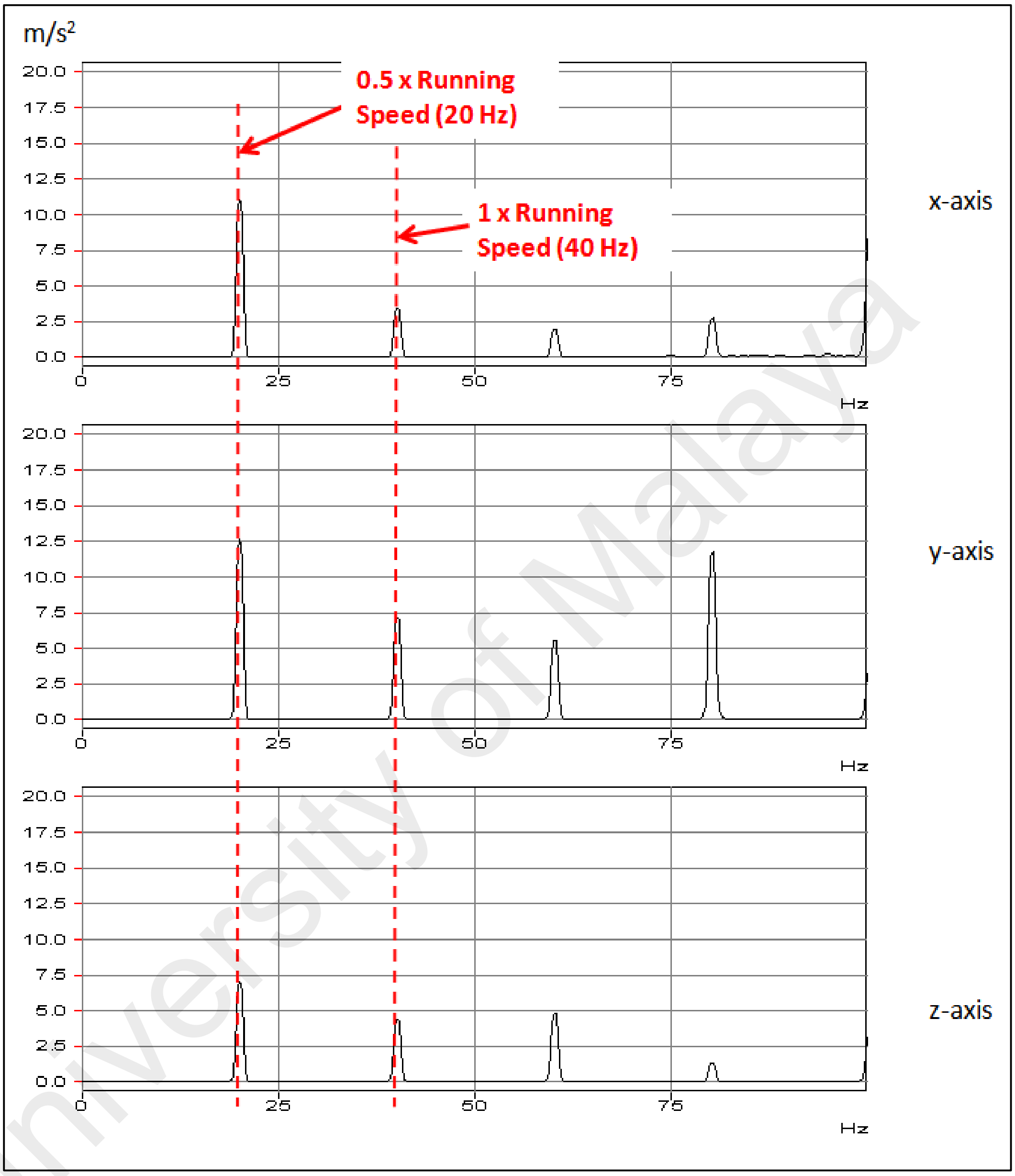

Figure 4.37: Vibration spectrum for engine speed 2400 rpm

Appendix A-D show the comparison of vibration spectra for all bio-fuel blends at both idle speed and full speed. The frequency domain analysis is able to separate the vibration into a specific frequency component. All vibration spectra show a dominant peak at 0.5-time running speed component followed by second dominant at 1-time running speed. For the test at engine speed 1500 rpm, the 0.5-time running speed component is equal to 12.5Hz with the running speed component equal to 25Hz. While engine test at speed 2400 rpm, the 0.5-time running speed component is equal to 20Hz with the running speed component equal to 40Hz.The comparison from all overlaid vibration spectrum shows significant change of bio-fuel blend B20 tested at engine speed 2400 rpm compared to the testing with engine speed 1500 rpm. Although the vibration is lower for the testing of engine speed 1500 rpm, it is hard to differentiate the optimum fuel blend of B20.

Figures 4.38 and 4.39 show the separated vibration component caused by the combustion and torque. As mentioned earlier, the combustion factor was identified as the 0.5-time running speed component. Torque was applied to control the engine speed, which directly affects the amplitude of the 1-time running speed component. All spectra showed a high peak at 0.5-time running speed, which is the frequency identified for the combustion. The amplitude of the 1-time running speed is relatively higher for the engine speed of 1500 rpm compared with the engine speed of 2400 rpm. The effect of engine torque is minimal at 2400 rpm, and the vibration is dominated by a 0.5-time running speed, which is related to fuel combustion. Therefore, the vibration level of different bio-fuel blends can be easily compared at full speed (2400 rpm). This setup explains the reason for the full speed 2400 rpm scenario with minimum torque is more suitable in identifying the optimum fuel blend in engine vibration as observed in Sub-section 4.2.2.1. Results show that other external vibration sources, which in this case is the torque, should be reduced or eliminated to determine the optimum bio-fuel blend based on the engine vibration. Therefore, the vibration caused by the torque is considered as an external source of error that must be reduced or eliminated.

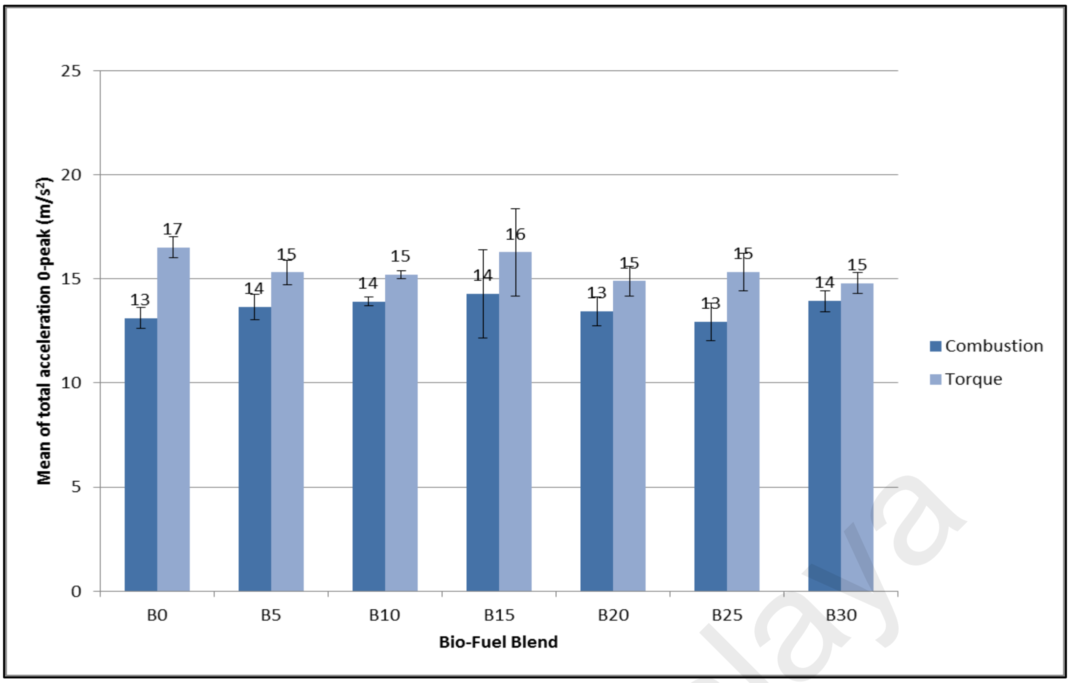

Figure 4.38: Comparison of Combustion and Torque at Engine Speed 1500 rpm

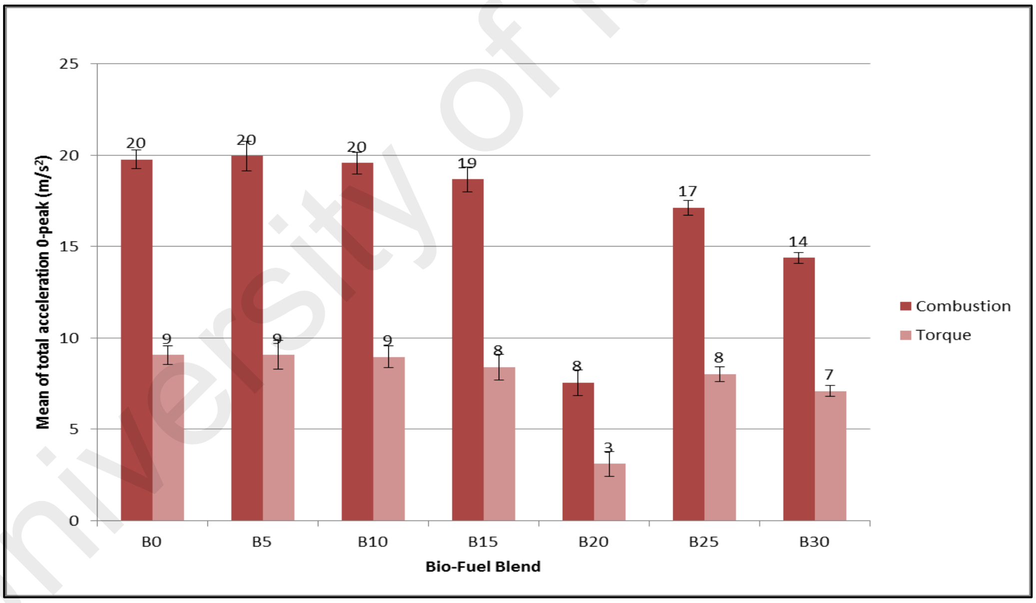

Figure 4.39: Comparison of Combustion and Torque at Engine Speed 2400 rpm

The vibrations at Points 3 and 4 of the engine were the dominant sources of high vibration. Both points are located at the engine cylinder, which was identified as the best location to represent the piston movement, which will be explored through ODS analysis. Hence, the comparison between combustion factor and torque factor focused on two measurement points. Furthermore, the vibration value acquired at the axial direction (x-axis) is too small as compared with the vibration value acquired from the horizontal (y-axis) and vertical directions (z-axis). The amplitude of the torque factor is determined using the following equation:

$$\text{Amplitude of torque factor } (1\times) = \frac{\sqrt{(Y_3^2 + Z_3^2)} + \sqrt{(Y_4^2 + Z_4^2)}}{2} \tag{4.7}$$

where Y_3 is the amplitude of the torque factor at the Point 3 y-axis, Z_3 is at the Point 3 z-axis, Y_4 is at the Point 4 y-axis, and Z_4 is at the Point 4 z-axis. The amplitude of the combustion factor can be determined using the following equation:

$$\text{Amplitude of combustion factor } (0.5\times) = \frac{\sqrt{(y_3^2 + z_3^2)} + \sqrt{(y_4^2 + z_4^2)}}{2} \tag{4.8}$$

where y_3 is the amplitude of the combustion factor at the Point 3 y-axis, z_3 is at the Point 3 z-axis, y_4 is at the Point 4 y-axis, and z_4 is at the Point 4 z-axis. The values obtained from Equations (4.7) and (4.8) are used to determine the error of the torque factor, which is the ratio of torque to the combustion amplitude as represented by:

$$\mathrm{e} = \frac{amplitude\ of\ torque\ factor\ (1x)}{amplitude\ of\ combustion\ factor\ (0.5x)} \tag{4.9}$$

The calculated error value of the torque factor is tabulated in Table 4.2. Engine vibration testing at a speed of 2,400 rpm shows relatively lower error in the torque factor (0.5) as compared with the low speed at 1,500 rpm (1.1). Performing the engine vibration testing at higher speed with lower torque shows that the error of the torque factor is reduced by 55%. Thus, the engine vibration purely caused by bio-fuel combustion can be evaluated and is more suitable for the identification of the optimum fuel blend.

Table 4.2: Error caused by the torque factor

Speed (RPM)	Impact of torque factor (Ratio)							
	B0	B5	B10	B15	B20	B25	B30	average
1500	1.3	1.1	1.1	1.1	1.1	1.2	1.1	1.1
2400	0.5	0.5	0.5	0.5	0.4	0.5	0.5	0.5

Relative phase measurement is another important data that should be considered for evaluating engine vibration. The combination of vibration and phase measurement produced an engine motion that can be visualised through ODS analysis. The ODS analysis at 0.5-time and 1-time running speeds can determine bio-fuel blends with minimal vibration through visualisation of the engine motion. The minimal vibration will show the motion with the smallest amplitude compared with other vibrations. The result of ODS analysis of different fuel blends at the engine speed of 1,500 rpm is difficult to visualise and compare through animation because the vibration amplitudes are almost identical due to high torque factor. A significant change of ODS motion can be observed between pure diesel B0 and fuel blend B20 for the test with engine speed 2400 rpm. ODS analysis results for B0 and B20 at 1,500 rpm and 2,400 rpm will be compared and discussed.

Figure 4.40 and 4.41 show the results of ODS analyses for B0 and B20 with engine speed 1500 rpm and 2400 rpm, respectively. Visualisations are compared side by side in a single frame. Points 1 and 2 represent the crankshaft, whereas Points 3 and 4 represent the cylinder piston. The ODS at 1-time corresponds to the engine speed while ODS at 0.5-time corresponds to the bio-fuel combustion. The arrows show how far each measurement point moves. The testing with engine speed 1500 rpm shows almost identical ODS motion for both B0 and B20 as shown in Figure 4.40 although the vibration reduces for bio-fuel B20 compared with pure diesel B0.

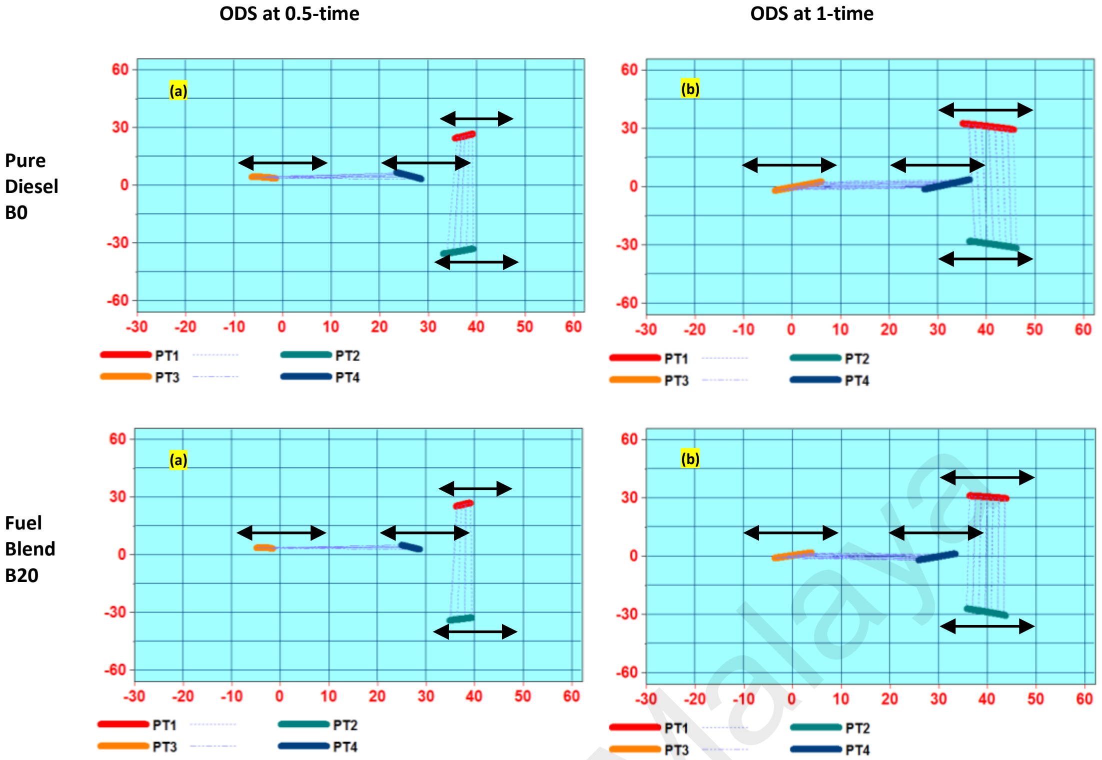

Figure 4.40: ODS of engine piston and crankshaft with engine speed 1500 rpm

Figure 4.41 shows the simplified ODS testing with engine speed 2400 rpm. ODS of 1-time engine speed could display the reciprocating motion of the piston and the rotating motion of the crankshaft. Both reciprocating and rotating motion can be observed clearly at this frequency. ODS of 0.5-time engine speed is more suitable for the comparison of vibration of diesel engine powered by different fuel blends because it is related to combustion factor. Better comparison between B0 and B20 can be visualised through ODS analysis with engine speed 2400 rpm, which purely affected by the ignition of combustion. The ODS motion shows that all of the engine components (i.e., crankshaft, cylinder piston) exhibit higher vibration with B0 as compared with B20.

Figure 4.42 shows the ODS motion of engine support and base plate. The rocking motion of the engine support can be observed from Points 5 to 8. Meanwhile, the engine support is observed to have a higher vibration compared with the engine base plate. Any motion at Points 9 to 12 is less visible due to the isolation of the base from the engine using rubber mounting. The same finding was observed for other test with different bio-fuel blends. Complete ODS results are displayed in Appendix E-J.

In summary, performing the engine vibration testing at higher speed with lower torque is more suitable for the identification of the optimum fuel blend. Findings from time-domain analysis show that combustion is the dominant source of vibration. By decomposing the vibration signal into frequency domain, 1-time engine speed ODS is able to display the reciprocating motion of the piston and the rotating motion of the crankshaft clearly. Combustion is identified as the frequency component of 0.5-time engine speed, although the reciprocating and rotating motion is less visible because the it is related to the combustion factor, a linear motion moving along the cylinder (y axis) was still observed. This linear motion can be related to the piston movement during combustion. In addition, better comparison of vibration between fuel blends can be visualised through ODS analysis at 0.5-time engine speed, which directly affects the ignition of combustion. Therefore, visualising engine motion through ODS motion can help untrained personnel in identifying the optimum fuel blend without analysing all of the vibration values and phase measurement data.

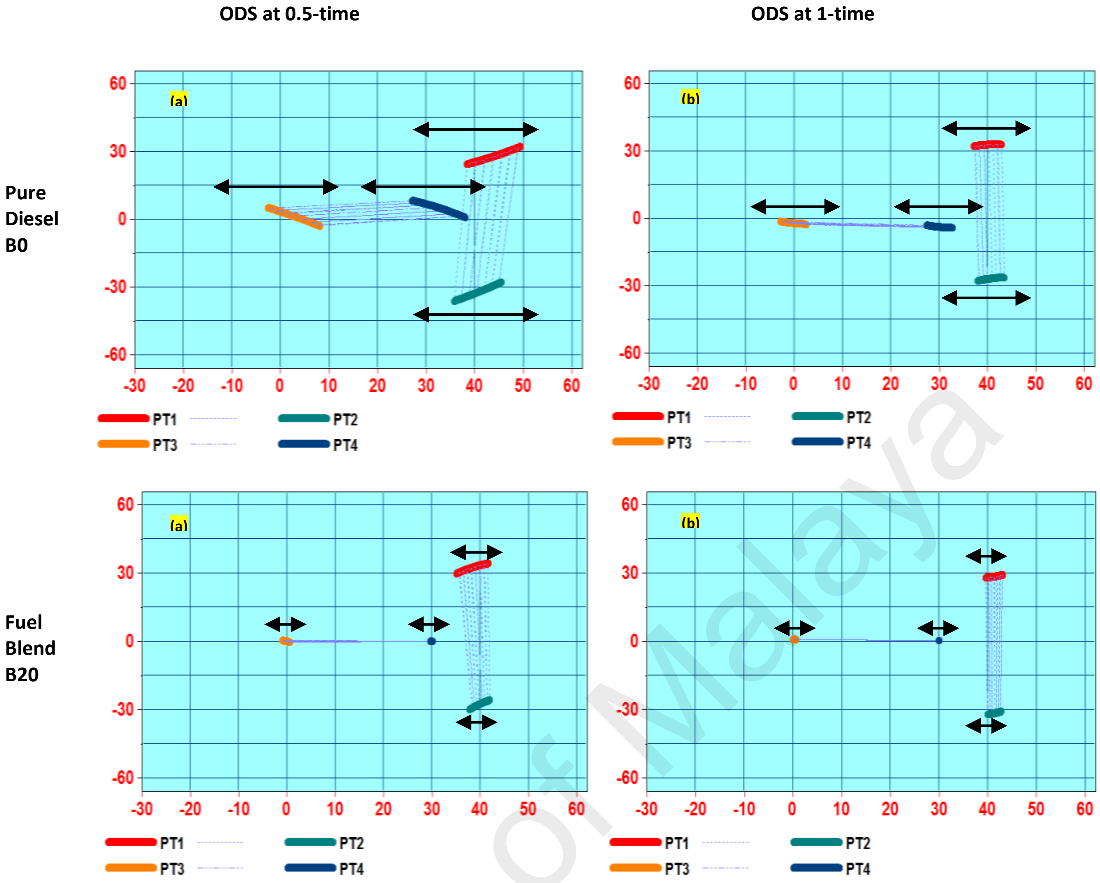

Figure 4.41: ODS of engine piston and crankshaft with engine speed 2400 rpm

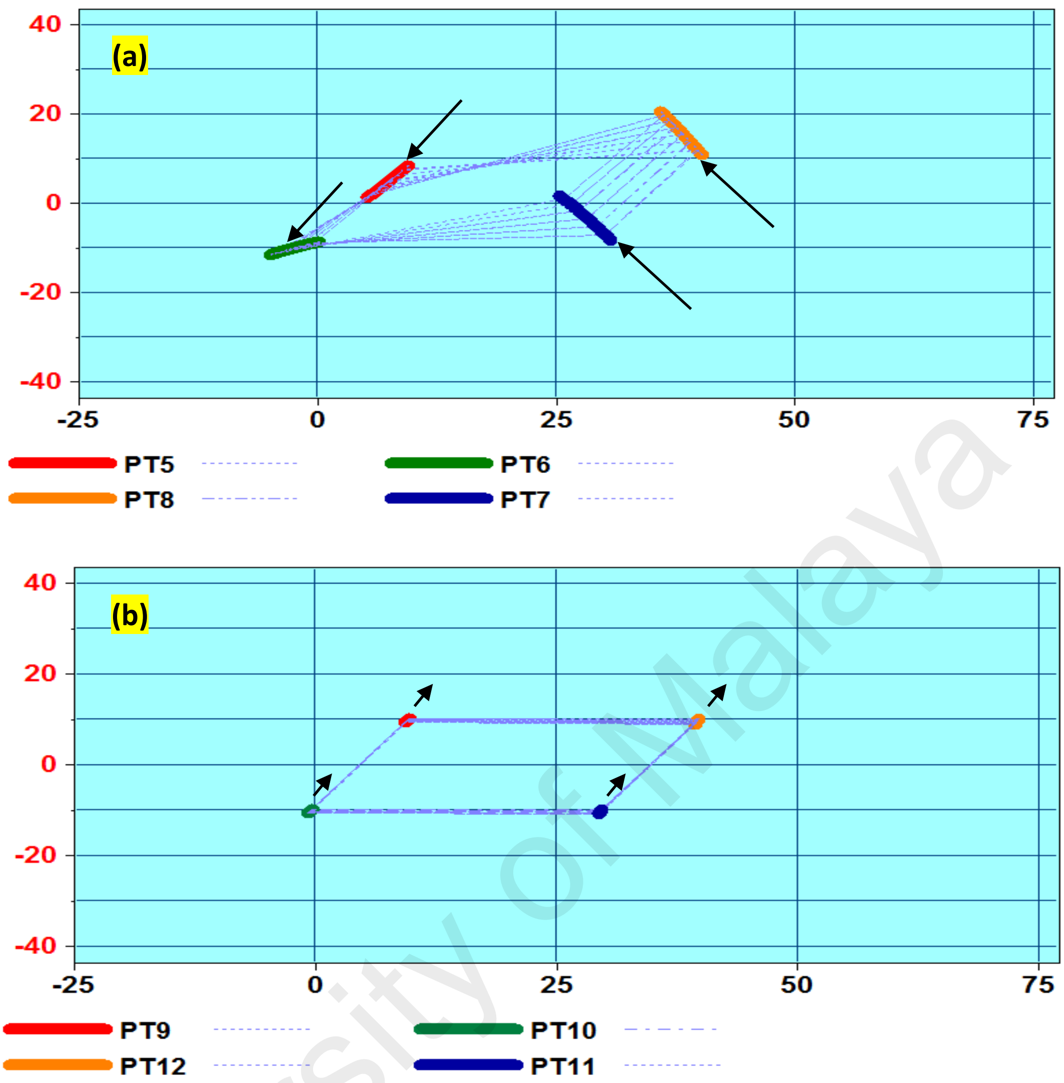

Figure 4.42: ODS of engine support and base plate

CHAPTER 5: CONCLUSION

In this research, a simplified ODS application in machinery vibration assessment shows a more effective approach as compared to current machinery vibration assessment practice. This simplified ODS technique consist of both frequency domain and time domain data. The simplified ODS technique was developed by identifying the suitable measurement point which is nearest to the bearing location. 4 measurement points is enough to show the ODS motion of a general rotating machinery arrangement instead of using a lot of measurement points to show the ODS motion. The study was divided into 2 main parts which is vibration assessment on rotating machinery and vibration assessment on reciprocating machinery. The simplified ODS technique was applied on rotating laboratory kit and real industrial case study to assess the vibration and detect rotating machinery fault. Furthermore, the simplified ODS technique was able to show the reciprocating motion. The second part is focusing on assessing the vibration caused by reciprocating motion with the aim of identification of bio-fuel blend. No machinery fault simulation was performed for the second part of this research.

In the first part, simplified ODS analysis approach was proven as more effective and should be integrated into current machinery vibration assessment practice which relies on vibration spectrum only. From the simplified ODS analysis, personnel can visualise the motion of the machine. Therefore, primary machine problem such as imbalance and misalignment can be detected earlier, easier and more accurate, hence avoiding any secondary failure such as (bearing damage, worn impeller, broken rotor bar, cracked gear teeth etc.) in shorter time without analysing every single spectrum. Furthermore, advanced or specialised knowledge is unnecessary for personnel to apply this technique into machinery vibration assessment program. The integration of this technique will eventually enhance the current practice of rotating machinery vibration assessment by reducing the time required for performing vibration data acquisition and analysis and may possibly reducing downtime cost with early and effective machine fault detection.

In the second part of this study, the simplified ODS analysis approach was used to assess the motion of reciprocating machinery. The application of simplified ODS analysis for rotating machinery is more to diagnosis of machinery fault. However, due to the complexity of reciprocating machinery which in this research is focusing on diesel engine, the application of simplified ODS analysis is more on determining the optimum bio-fuel blend based on the minimal engine vibration. Furthermore, advanced vibration analysis in term of time domain analysis, frequency domain analysis and vibration RMS trending was performed to justify the result obtained from the simplified ODS analysis. Performing time domain analysis can identify the major component of vibration caused by the combustion of bio-fuel. Other external vibration cause which is the torque factor can be separated and determined by performing the frequency domain analysis. Through the ODS motion, the optimum bio-fuel blend can be determined faster and easier. By visualising the reciprocating ODS motion, bio-fuel blend B20 shows the motion with the smallest amplitude among all tested bio-fuel blends. From the study, it is noticed that when the engine runs at full speed, it has a lower engine torque as compared to lowest speed with higher torque. Thus, bio-fuel powered engine at full speed is more suitable to be used in identifying optimum fuel blend. Bio-fuel blends B20 has the minimal vibration with the overall RMS acceleration of $27 m/s^2$ compared to other bio-fuel blends at full speed 2400rpm.

REFERENCES

Abdelrhman, a. M., Leong, M. S., Saeed, S. A. M., & Al Obiadi, S. M. A. A.-O. (2012). A review of vibration monitoring as a diagnostic tool for turbine blade faults. *Applied Mechanics and Materials*, *229–231*, 1459–1463.

Abdul Rahman, A. G., Noroozi, S., Dupac, M., Al-Attas, S. M. S. M., & Vinney, J. E. (2013). A hybrid approach for nondestructive assessment and design optimisation and testing of in-service machinery. *Nondestructive Testing and Evaluation*, *28*(1), 44–57.

Al-Badour, F., Sunar, M., & Cheded, L. (2011). Vibration analysis of rotating machinery using time-frequency analysis and wavelet techniques. *Mechanical Systems and Signal Processing*, *25*(6), 2083–2101.

Atabani, A. E., Silitonga, A. S., Ong, H. C., Mahlia, T. M. I., Masjuki, H. H., Badruddin, I. A., & Fayaz, H. (2013). Non-edible vegetable oils: A critical evaluation of oil extraction, fatty acid compositions, biodiesel production, characteristics, engine performance and emissions production. *Renewable and Sustainable Energy Reviews*, *18*, 211–245.

Bakar, A. H. A., Illias, H. A., Othman, M. K., & Mokhlis, H. (2013). Identification of failure root causes using condition based monitoring data on a 33 kV switchgear. *International Journal of Electrical Power and Energy Systems*, *47*(1), 305–312.

Bassyouni, M., Akhtar, F. H., Hussain, A., & Umer, A. (2012). Biodiesel production and investigations on the performance of diesel engine using jatropha oil. *Asian Transactions on Engineering*, *2*, 77–88.

Bhansali, S. S., & Shirgire, N. D. (2014). Analysis of vibration in diesel engine considering combustion gas forces: using grey cast iron material. *Recent and Innovation Trends in Computing and Communication*, *2*(3), 604–611.

Boyce, M. P. (2012). *Gas Turbine Engineering Handbook*. Butterworth-Heinemann.

Buscarello, R. T. (1985). *Practical Solutions to Machinery and Maintenance Vibration Problems*. Update International.

Carlucci, A. P., Chiara, F. F., & Laforgia, D. (2006). Analysis of the relation between injection parameter variation and block vibration of an internal combustion diesel engine. *Journal of Sound and Vibration*, *295*(1–2), 141–164.

Carnero, M. (2006). An evaluation system of the setting up of predictive maintenance programmes. *Reliability Engineering and System Safety*, *91*(8), 945–963.

Chen, Y. D., Du, R., & Qu, L. S. (1995). Fault features of large rotating machinery and diagnosis using sensor fusion. *Journal of Sound and Vibration*, *188*(2), 227–242.

Dweck, A. C., & Meadows, T. (2002). Tamanu (Calophyllum inophyllum) - The African, Asian, Polynesian and Pacific Panacea. *International Journal of Cosmetic Science*, *24*(6), 341–348.

Edwards, S., Lees, A. W., & Friswell, M. I. (1998). Fault diagnosis of rotating machinery. *Shock and Vibration Digest*, *30*(1), 4–13.

Elbhbah, K., & Sinha, J. K. (2013). Vibration-based condition monitoring of rotating machines using a machine composite spectrum. *Journal of Sound and Vibration*, *332*(11), 2831–2845.

Ettefagh, M. M., Sadeghi, M. H., Pirouzpanah, V., & Tash, H. A. (2008). Knock detection in spark ignition engines by vibration analysis of cylinder block: A parametric modeling approach. *Mechanical Systems and Signal Processing*, *22*(6), 1495–1514.

Fayyadh, M. M., Razak, H. A., & Ismail, Z. (2011). Combined modal parameters-based index for damage identification in a beamlike structure: theoretical development and verification. *Archives of Civil & Mechanical Engineering*, *11*(3), 587–609.

Fazal, M. A., Haseeb, A. S. M. A., & Masjuki, H. H. (2011). Biodiesel feasibility study: An evaluation of material compatibility; Performance; emission and engine durability. *Renewable and Sustainable Energy Reviews*, *15*(2), 1314–1324.

Ferrando Chacon, J. L., Artigao Andicoberry, E., Kappatos, V., Asfis, G., Gan, T. H., & Balachandran, W. (2014). Shaft angular misalignment detection using acoustic emission. *Applied Acoustics*, *85*, 12–22.

Fu, C., Ye, L., Liu, Y., Yu, R., Iung, B., Cheng, Y., & Zeng, Y. (2004). Predictive maintenance in intelligent-control-maintenance-management system for hydroelectric generating unit. *IEEE Transactions on Energy Conversion*, *19*(1), 179–186.

Ganeriwala.S, Patel.S, & Hartung.H.A. (1999). The truth behind misalignment vibration spectra of rotating machinery. In *Proceeding of International Modal Analysis Conference* (pp. 2077–2085). Kissimmee, FL.

Ganeriwala, S. N., Li, Z., & Richardson, M. H. (2008). Using operating deflection shapes to detect misalignment in rotating equipment. In *Proceeding of International Modal Analysis Conference* (Vol. 4, p. 7). Orlando, FL.

Ganeriwala, S. N., Schwarz, B., & Richardson, M. H. (2009). Operating deflection shapes detect unbalance in rotating equipment. *Sound and Vibration*, *43*(5), 11–13.

Geng, Z., & Chen, J. (2005). Investigation into piston-slap-induced vibration for engine condition simulation and monitoring. *Journal of Sound and Vibration*, *282*(3–5), 735–751.

Geng, Z., Chen, J., & Barry Hull, J. (2003). Analysis of engine vibration and design of an applicable diagnosing approach. *International Journal of Mechanical Sciences*, *45*(8), 1391–1410.

Ghobadian, B., Bhattacharya, M., Singh, N., & Jain, S. C. (1992). Structural attenuation characteristics of a small single cylinder DI diesel engine. In *National Conference on IC Engines and Combustion*. India.

Gong, X., & Qiao, W. (2012). Imbalance fault detection of direct-drive wind turbines using generator current signals. *IEEE Transactions on Energy Conversion*, *27*(2), 468–476.

Griffiths, W. J., & Skorecki, J. (1964). Some aspects of vibration of a single cylinder diesel engine: A. Effects of cooling water on cylinder pressure and surface vibration B. Mechanics of piston slap. *Journal of Sound and Vibration*, *1*(4).

Guzzomi, A. L., Hesterman, D. C., & Stone, B. J. (2007). The effect of piston friction on the torsional natural frequency of a reciprocating engine. *Mechanical Systems and Signal Processing*, *21*(7), 2833–2837.

Hameed, Z., Hong, Y. S., Cho, Y. M., Ahn, S. H., & Song, C. K. (2009). Condition monitoring and fault detection of wind turbines and related algorithms: A review. *Renewable and Sustainable Energy Reviews*, *13*(1), 1–39.

Hariharan, V., & Srinivasan, P. S. S. (2011). Vibration analysis of misaligned shaft with ball bearing system. *Songklanakarin Journal of Science and Technology*, *33*(1), 61–68.

Hashemian, H. M. (2011). Wireless sensors for predictive maintenance of rotating equipment in research reactors. *Annals of Nuclear Energy*, *38*(2–3), 665–680.

Heaton, R., & Hewitt, S. (2006). *The use of Operating Deflection Shapes (ODS) to model the vibration of sanders and polishers*. Derbyshire.

Hermans, L., & Van Der Auweraer, H. (1999). Modal testing and analysis of structures under operational conditions: industrial applications. *Mechanical Systems and Signal Processing*, *13*(2), 193–216.

How, H. G., Masjuki, H. H., Kalam, M. A., & Teoh, Y. H. (2014). Engine performance, emission and combustion characteristics of a common-rail diesel engine fuelled with bioethanol as a fuel additive in coconut oil biodiesel blends. *Energy Procedia*, *61*, 1655–1659.

Huang, R., Xi, L., Lee, J., & Liu, C. R. (2005). The framework, impact and commercial prospects of a new predictive maintenance system: intelligent maintenance system. *Production Planning & Control*, *16*(7), 652–664.

Ismail, Z. (2012). Application of residuals from regression of experimental mode shapes to locate multiple crack damage in a simply supported reinforced concrete beam. *Measurement*, *45*, 1455.

Ismail, Z. (2012). Finite element model updating of reinforced concrete beams with honeycomb damage. *Archives of Civil Engineering*, *58*, 135.

Ismail, Z., Abdul Razak, H., & Abdul Rahman, A. G. (2006). Determination of damage location in RC beams using mode shape derivatives. *Engineering Structures*, *28*(11), 1566–1573.

Ismail, Z., Doostdar, S., & Harun, Z. (2012). Factors influencing the implementation of a safety management system for construction sites. *Safety Science*, *50*(3), 418–423.

Ismail, Z., Ibrahim, Z., Ong, A. Z. C., & Rahman, A. G. A. (2012). Approach to reduce the limitations of modal identification in damage detection using limited field data for nondestructive structural health monitoring of a cable-stayed concrete bridge. *Journal of Bridge Engineering*, *17*(6), 867–875.

Ismail, Z., & Karim, R. (2013). Some technical aspects of spills in the transportation of petroleum materials by tankers. *Safety Science*, *51*(1), 202–208.

Ismail, Z., Kong, K. K., Othman, S. Z., Law, K. H., Khoo, S. Y., Ong, Z. C., & Shirazi, S. M. (2014). Evaluating accidents in the offshore drilling of petroleum: Regional picture and reducing impact. *Measurement*, *51*(1), 18–33.

Ismail, Z., Kuan, K. K., Yee, K. S., & Chao, O. Z. (2014). Examining the trend in loss of flexural stiffness of simply supported RC beams with various crack severity using model updating. *Measurement*, *50*(1), 43–49.

Ismail, Z., Lee, E. H., Sinti, L., Ibrahim, Z., & Razak, H. A. (2008). Application of local stiffness indicator on finite element RC beam model with multiple cracks. In *International Conference on Noise and Vibration Engineering* (Vol. 6). Leuven, Belgium.

Ismail, Z., Ong, A. Z. C., & Rahman, A. G. A. (2011). Crack damage detection of reinforced concrete beams using local stiffness indicator. *Scientific Research and Essays*, *6*(34), 6798–6803.

Ismail, Z., & Ong, Z. C. (2012). Honeycomb damage detection in a reinforced concrete beam using frequency mode shape regression. *Measurement*, *45*(5), 950–959.

Ismail, Z., Ramli, A. H., & Somarin, S. D. (2012). Lessons learned from accidents in downstream petroleum product processing and handling. *Oil Gas-European Magazine*, *38*(3), 157–162.

Ismail, Z., Razak, H. A., Ibrahim, Z., Rahman, A. G. A., & Hin, P. A. (2001). Detection of defects in reinforced concrete beams using modal data. In *Proceeding of International Modal Analysis Conference* (Vol. 2, pp. 1358–1362). Kissimmee, FL.

Ismail, Z., Tai, J. C., Kong, K. K., Law, K. H., Shirazi, S. M., & Karim, R. (2013). Using data envelopment analysis in comparing the environmental performance and technical efficiency of selected companies in their global petroleum operations. *Measurement*, *46*(9), 3401–3413.

Ismail, Z., Tan, P. L., & Abdul Razak, H. (2006). Detection of corrosion damage in RC beams using modal testing. In *International Conference on Noise and Vibration Engineering* (Vol. 2). Leuven, Belgium.

Jardine, A. K. S., Joseph, T., & Banjevic, D. (1999). Optimizing condition-based maintenance decisions for equipment subject to vibration monitoring. *Journal of Quality in Maintenance Engineering*, *5*(3), 192–202.

Jardine, A. K. S., Lin, D., & Banjevic, D. (2006). A review on machinery diagnostics and prognostics implementing condition-based maintenance. *Mechanical Systems and Signal Processing*, *20*(7), 1483–1510.

Khoo, S. Y., Ismail, Z., Kong, K. K., Ong, Z. C., Noroozi, S., Chong, W. T., & Rahman, A. G. A. (2014). Impact force identification with pseudo-inverse method on a lightweight structure for under-determined, even-determined and over-determined cases. *International Journal of Impact Engineering*, *63*, 52–62.

Kiran Sastry, G. R., Kumar, I. N. N., Prasad, S. C., Rao, B. V. A., & Asme. (2005). Comparative performance study of Jatropha methyl ester as diesel fuel substitute on DI diesel engine with emphasis on vibration & noise as potential engine parameters. In *Power and Energy Systems* (pp. 195–203). Benalmadena, Spain.

Liu, Z., & Kleiner, Y. (2013). State of the art review of inspection technologies for condition assessment of water pipes. *Measurement*, *46*(1), 1–15.

Maleki, E., Aroua, M. K., & Sulaiman, N. M. N. (2013). Castor oil - A more suitable feedstock for enzymatic production of methyl esters. *Fuel Processing Technology*, *112*, 129–132.

Mazinani, I., Jumaat, M. Z., Ismail, Z., & Chao, O. Z. (2014). Comparison of shear lag in structural steel building with framed tube and braced tube. *Structural Engineering and Mechanics*, *49*(3), 0.

McHargue, P. L., & Richardson, M. H. (1993). Operating Deflection Shapes from time versus frequency domain measurements. In *Proceeding of International Modal Analysis Conference* (pp. 1–8). Orlando, FL.

Mobley, R. K. (1999). *Root Cause Failure Analysis* (Vol. 52). Newnes.

Mobley, R. K. (2002). *An Introduction to Predictive Maintenance*. Butterworth-Heinemann.

Mohd Mishani, M. B., Ong, Z. C., Chong, W. T., Khoo, S. Y., & Abdul Rahman, A. G. (2015). A simplified technique to distinguish unbalance and misalignment using frequency domain Operating Deflection Shape. *Jurnal Teknologi*, *76*(8), 1–4.

Monajemi, H., Abdul Razak, H., & Ismail, Z. (2012). Reliability of dynamically measured flexibility matrix on damage detection of frame structures. In *Proceeding of International Modal Analysis Conference* (Vol. 6, pp. 369–376). Jacksonville, FL.

Monajemi, H., Razak, H. A., & Ismail, Z. (2013). Damage detection in frame structures using damage locating vectors. *Measurement*, *46*(9), 3541–3548.

Ong, H. C., Mahlia, T. M. I., Masjuki, H. H., & Norhasyima, R. S. (2011). Comparison of palm oil, Jatropha curcas and Calophyllum inophyllum for biodiesel: A review. *Renewable and Sustainable Energy Reviews*, *15*(8), 3501–3515.

Ong, H. C., Masjuki, H. H., Mahlia, T. M. I., Silitonga, A. S., Chong, W. T., & Leong, K. Y. (2014). Optimization of biodiesel production and engine performance from high free fatty acid Calophyllum inophyllum oil in CI diesel engine. *Energy Conversion and Management*, *81*, 30–40.

Ong, H. C., Silitonga, A. S., Masjuki, H. H., Mahlia, T. M. I., Chong, W. T., & Boosroh, M. H. (2013). Production and comparative fuel properties of biodiesel from non-edible oils: Jatropha curcas, Sterculia foetida and Ceiba pentandra. *Energy Conversion and Management*, *73*, 245–255.

Pan, E., Liao, W., & Xi, L. (2012). A joint model of production scheduling and predictive maintenance for minimizing job tardiness. *The International Journal of Advanced Manufacturing Technology*, *60*(9), 1049–1061.

Pascual, R., Golinval, J.-C., & Razeto, M. (1999). On-line damage assessment using operating deflection shapes. In *Proceeding of International Modal Analysis Conference* (pp. 1225–1231). San Antonio, Texas.

Pennacchi, P., Vania, A., & Chatterton, S. (2012). Nonlinear effects caused by coupling misalignment in rotors equipped with journal bearings. *Mechanical Systems and Signal Processing*, *30*, 306–322.

Rahman, A. G. A., Chao, O. Z., & Ismail, Z. (2011). Effectiveness of Impact-Synchronous Time Averaging in determination of dynamic characteristics of a rotor dynamic system. *Measurement*, *44*(1), 34–45.

Rahman, A. G. A., Ong, Z. C., & Ismail, Z. (2011). Enhancement of coherence functions using time signals in Modal Analysis. *Measurement*, *44*(10), 2112–2123.

Razak, H. A., Teng, S. L., Ismail, Z., & Abdul Rahman, A. G. (2001). Crack detection in a simply supported RC beam using simplified Laplacian. In *Proceeding of International Modal Analysis Conference* (Vol. 2, pp. 1344–1350). Kissimmee, FL.

Reddy, Y. A. K., & Rao, B. V. A. (n.d.). Combustion and vibration analysis of IDI-diesel engine fuelled with neat preheated Jatropha Methyl Ester. *Int. Journal of Engineering Research and Applications*, *22*, 780–790.

Reilly, T. (2011). A review of signal processing and analysis tools for comprehensive rotating machinery diagnostics. *Rotating Machinery, Structural Health Monitoring, Shock and Vibration*, *5*(x), 463–479.

Sadeghinezhad, E., Kazi, S. N., Badarudin, A., Oon, C. S., Zubir, M. N. M., & Mehrali, M. (2013). A comprehensive review of bio-diesel as alternative fuel for compression ignition engines. *Renewable and Sustainable Energy Reviews*, *28*, 410–424.

Sadeghinezhad, E., Kazi, S. N., Sadeghinejad, F., Badarudin, A., Mehrali, M., Sadri, R., & Reza Safaei, M. (2014). A comprehensive literature review of bio-fuel performance in internal combustion engine and relevant costs involvement. *Renewable and Sustainable Energy Reviews*, *30*, 29–44.

Saghafinia, A., Kahourzade, S., Mahmoudi, A., Hew, W. P., & Nasir Uddin, M. (2012). Broken rotor bar fault detection of 3-phase induction motor using online adaptive continuous wavelet transform and fuzzy logic. *International Review of Electrical Engineering*, *7*(3), 4383–4394.

Salaheldeen, M., Aroua, M. K., Mariod, A. A., Cheng, S. F., & Abdelrahman, M. A. (2014). An evaluation of Moringa peregrina seeds as a source for bio-fuel. *Industrial Crops and Products*, *61*, 49–61.

Saleem, M. A., & Diwakar, G. (2012). Detection of unbalance in rotating machines using shaft deflection measurement during its operation. *Journal of Mechanical and Civil Engineering*, *3*(3), 8–20.

Sastry, G. R. K., Venkateswarlu, K., Yousufuddin, S., & Murthy, B. S. R. (2012). Performance, vibration and emission analysis of diesel engine fuelled with fish oil bio diesel blends. *International Journal of Advanced Engineering Technology*, *3*(1), 116–120.

Scheffer, C., & Girdhar, P. (2004). *Practical Machinery Vibration Analysis and Predictive Maintenance*. Newnes.

Schwarz, B. J., & Richardson, M. H. (1999). *Introduction to operating deflection shapes*. *CSI Reliability Week*.

Schwarz, B., & Richardson, M. H. (2004). Measurements required for displaying Operating Deflection Shapes. In *Proceeding of International Modal Analysis Conference* (pp. 1–6). Dearborn, MI.

Selim, M. Y. . (2001). Pressure–time characteristics in diesel engine fueled with natural gas. *Renewable Energy*, *22*(4), 473–489.

Sheng, C., Li, Z., Qin, L., Guo, Z., & Zhang, Y. (2011). Recent progress on mechanical condition monitoring and fault diagnosis. *Procedia Engineering*, *15*, 142–146.

Silitonga, A. S., Masjuki, H. H., Mahlia, T. M. I., Ong, H. C., & Chong, W. T. (2013). Experimental study on performance and exhaust emissions of a diesel engine fuelled with Ceiba Pentandra biodiesel blends. *Energy Conversion and Management*, *76*, 828–836.

Taghizadeh-Alisaraei, A., Ghobadian, B., Tavakoli-Hashjin, T., & Mohtasebi, S. S. (2012). Vibration analysis of a diesel engine using biodiesel and petrodiesel fuel blends. *Fuel*, *102*, 414–422.

Taghizadeh, A. A., Tavakoli, H. T., & Ghobadian, B. (2010). An analysis and evaluation of vibrations of power tiller in the stationary conditions. *Iranian Journal of Biosystems Engineering*, *41*(1), 27–35.

Tandon, N., & Choudhury, A. (1999). A review of vibration and acoustic measurement methods for the detection of defects in rolling element bearings. *Tribology International*, *32*(8), 469–480.

Tienhaara, H. (2004). Guidelines to engine dynamics and vibration. *Marine News*, 20–25.

Tsang, A. H. C. (1995). Condition-based maintenance: tools and decision making. *Journal of Quality in Maintenance Engineering*, *1*(3), 3–17.

Velarde-Suárez, S., Ballesteros-Tajadura, R., & Hurtado-Cruz, J. P. (2006). A predictive maintenance procedure using pressure and acceleration signals from a centrifugal fan. *Applied Acoustics*, *67*(1), 49–61.

Verma, A. K., Sarangi, S., & Kolekar, M. H. (2013). Shaft misalignment detection using stator current monitoring. *International Journal of Advanced Computer Research*, *3*(8).

Wang, C., Zhang, Y., & Zhong, Z. (2008). Fault diagnosis for diesel valve trains based on time-frequency images. *Mechanical Systems and Signal Processing*, *22*(8), 1981–1993.

Wang, J., & Hu, H. (2006). Vibration-based fault diagnosis of pump using fuzzy technique. *Measurement*, *39*(2), 176–185.

Xu, M., & Marangoni, R. D. (1994). Vibration analysis of a motor-flexible coupling-rotor system subject to misalignment and unbalance, part II: experimental validation. *Journal of Sound and Vibration*, *176*(5), 681–691.

Zloto, T., Ptak, P., & Prauzner, T. (2012). Analysis of signals from inductive sensors by means of the DasyLab software. *Annales UMCS Informatica*, *12*(1), 31–37.

LIST OF PUBLICATIONS AND PAPERS PRESENTED

Ong, Z.C., Mishani, M.B.M., Chong, W.T., Soon, R.S., Ong, H.C., Ismail, Z. (2017). Identification of Optimum Calophyllum Inophyllum Bio-fuel Blend in Diesel Engine using Advanced Vibration Analysis Technique. *Renewable Energy*. 109: p. 295-304. (PUBLISHED. ISI Paper. Q2)

Mishani, M.B.M., Ong, Z.C., Chong, W.T., Khoo, S.Y., Rahman, A.G.A. (2015). A Simplified Technique to Distinguish Unbalance and Misalignment Using Frequency Domain Operating Deflection Shape. *Jurnal Teknologi*. 76:8 p.1-4 (PUBLISHED. Scopus Index Paper)

Mishani, M.B.M., Ong, Z.C., Chong, W.T., Khoo, S.Y., Rahman, A.G.A. Enhancement of Condition-Based Monitoring Assessment Program through Simplified Machine Vibration Motion Visualization. *Journal of Mechanical Science and Technology*. (Under Review – MEST-D-16-02418, ISI Paper. Q3).